การดัดแปรพื้นผิวของเม็ดแป้งด้วยการดูดซับกรดสเตียริก โดยใช้เทคโนโลยีของไหลเหนือวิกฤต

นายธนากร เกริงกำจรกิจ

วิทยานิพนธ์นี้เป็นส่วนหนึ่งของการศึกษาตามหลักสูตรปริญญาเภสัชศาสตรมหาบัณฑิต
สาขาวิชาเภสัชอุตสาหกรรม ภาควิชาวิทยาการเภสัชกรรมและเภสัชอุตสาหกรรม
คณะเภสัชศาสตร์ จุฬาลงกรณ์มหาวิทยาลัย
ปีการศึกษา 2552

SURFACE MODIFICATION OF STARCH GRAINS BY ADSORPTION OF STEARIC ACID USING SUPERCRITICAL FLUID TECHNOLOGY

Mr. Thanakorn Khroengkhamjornkit

A Thesis Submitted in Partial Fulfillment of the Requirements
for the Degree of Master of Science in Pharmacy Program in Industrial Pharmacy
Department of Pharmaceutics and Industrial Pharmacy
Faculty of Pharmaceutical Sciences
Chulalongkorn University
Academic Year 2009

Thesis Title	SURFACE MODIFICATION OF STARCH GRAINS BY ADSORPTION OF STEARIC ACID USING SUPERCRITICAL FLUID TECHNOLOGY
By	Mr. Thanakorn Khroengkhamjornkit
Field of Study	Industrial Pharmacy
Thesis Advisor	Associate Professor Poj Kulvanich, Ph.D.
Thesis Co-Advisor	Jittima Chatchawalsaisin, Ph.D.

Accepted by the Faculty of Pharmaceutical Sciences, Chulalongkorn University in Partial Fulfillment of the Requirements for the Master's Degree

……..… Dean of the Faculty of Pharmaceutical Sciences
(Associate Professor Pintip Pongpech, Ph.D.)

THESIS COMMITTEE

……..… Chairman
(Professor Garnpimol C. Ritthidej, Ph.D.)

……..… Thesis Advisor
(Associate Professor Poj Kulvanich, Ph.D.)

……..… Thesis Co-Advisor
(Jittima Chatchawalsaisin, Ph.D.)

……..… Examiner
(Narueporn Sutanthavibul, Ph.D.)

……..… External Examiner
(Assistant Professor Sujimon Tunvichien, Ph.D.)

ธนากร เกริงกำจรกิจ: การดัดแปรพื้นผิวของเม็ดแป้งด้วยการดูดซับกรดสเตียริกโดยใช้เทคโนโลยีของไหลเหนือวิกฤต. (SURFACE MODIFICATION OF STARCH GRAINS BY ADSORPTION OF STEARIC ACID USING SUPERCRITICAL FLUID TECHNOLOGY) อ.ที่ปรึกษาวิทยานิพนธ์หลัก: รศ.ดร.พจน์ กุลวานิช, อ.ที่ปรึกษาวิทยานิพนธ์ร่วม: ดร.จิตติมา ชัชวาลย์สายสินธ์, 121 หน้า.

การใช้กระบวนการขยายตัวอย่างรวดเร็วของสารละลายสภาวะเหนือวิกฤตโดยไม่ใช้ตัวทำละลายเพื่อดัดแปรพื้นผิวของเม็ดแป้งข้าวโพดโดยการเคลือบด้วยกรดสเตียริก และศึกษาผลของอุณหภูมิและความดันของคาร์บอนไดออกไซด์สภาวะเหนือวิกฤต และอัตราส่วนของแป้งและกรดสเตียริกที่มีต่อการดัดแปรพื้นผิวของเม็ดแป้ง วิเคราะห์ลักษณะของแป้งเคลือบด้วยกล้องจุลทรรศน์อิเล็กตรอนแบบส่องกราด วัดขนาดอนุภาคโดยอาศัยหลักการกระจายของแสง ประเมินคุณสมบัติในการดูดซับไอความชื้นโดยน้ำหนัก คุณสมบัติในการไหลและความหนาแน่นต่างๆ เทคนิคดิฟเฟอเรนเชียลสแกนนิงแคลอรีเมทรี เทคนิคเทอร์โมกราวิเมตริกอนาลิซิส เทคนิคการเลี้ยวเบนของรังสีเอ็กซ์และเทคนิคฟูเรียทรานสฟอร์มอินฟราเรดสเป็กโตรสโกปี และนำแป้งเคลือบมาประยุกต์ใช้เป็นสารช่วยหล่อลื่นในการตอกอัดยาเม็ดเทียบกับกรดสเตียริกและแมกเนเซียมสเตียเรท จากการศึกษาพบว่าความดันของคาร์บอนไดออกไซด์สภาวะเหนือวิกฤตไม่มีผลต่อการดัดแปรพื้นผิวของเม็ดแป้ง แต่อุณหภูมิของคาร์บอนไดออกไซด์สภาวะเหนือวิกฤตและอัตราส่วนของแป้งและกรดสเตียริกเป็นปัจจัยที่มีผลต่อการดัดแปรพื้นผิวของเม็ดแป้ง ภาพจากกล้องจุลทรรศน์อิเล็กตรอนแบบส่องกราดแสดงให้เห็นว่ากรดสเตียริกสามารถเคลือบเป็นแผ่นฟิล์มบางและสม่ำเสมอเมื่อลดปริมาณของกรดสเตียริกให้อยู่ในระดับต่ำโดยใช้ความดัน 3000 ปอนด์ต่อตารางนิ้วและอุณหภูมิ 60 องศาเซลเซียส และยืนยันโดยการวัดขนาดอนุภาคพบว่า อนุภาคของแป้งเคลือบมีขนาดใหญ่ขึ้นเมื่อเทียบกับอนุภาคของแป้งข้าวโพดที่ไม่ได้เคลือบ การประเมินคุณสมบัติในการดูดซับไอความชื้นโดยน้ำหนักพบว่าแป้งเคลือบมีเปอร์เซ็นต์การเปลี่ยนแปลงโดยน้ำหนักต่ำกว่าแป้งข้าวโพดที่ไม่ได้เคลือบแสดงให้เห็นว่าแป้งเคลือบด้วยกรดสเตียริกมีการดูดความชื้นน้อยกว่า การประเมินความหนาแน่นต่างๆของแป้งข้าวโพดที่ไม่ได้เคลือบและแป้งเคลือบพบว่ามีความแตกต่างกัน แป้งเคลือบด้วยกรดสเตียริกไม่มีการเปลี่ยนแปลงและ/หรือการเกิดอันตรกิริยาระหว่างแป้งและกรดสเตียริก ทั้งนี้แป้งเคลือบสามารถนำมาใช้เป็นสารช่วยหล่อลื่นในกระบวนการตอกยาเม็ดได้

ภาควิชา วิทยาการเภสัชกรรมและเภสัชอุตสาหกรรม ลายมือชื่อนิสิต…….....…….

สาขาวิชา…….เภสัชอุตสาหกรรม……...…ลายมือชื่อ อ.ที่ปรึกษาวิทยานิพนธ์หลัก…...….....

ปีการศึกษา…….……2552…….……ลายมือชื่อ อ.ที่ปรึกษาวิทยานิพนธ์ร่วม……...…...…

4976569333: MAJOR INDUSTRIAL PHARMACY
KEYWORDS: FINE PARTICLE COATING / SURFACE MODIFICATION / STARCH GRAINS / STEARIC ACID / SUPERCRITICAL FLUID TECHNOLOGY

THANAKORN KHROENGKHAMJORNKIT: SURFACE MODIFICATION OF STARCH GRAINS BY ADSORPTION OF STEARIC ACID USING SUPERCRITICAL FLUID TECHNOLOGY. THESIS ADVISOR: ASSOC. PROF. POJ KULVANICH, Ph.D., THESIS CO-ADVISOR: JITTIMA CHATCHAWALSAISIN, Ph.D., 121 pp.

The rapid expansion of supercritical solution with a nonsolvent (RESS-N) was applied to modify the surface of corn starch grains by coating with stearic acid. The effects of temperature and pressure of $scCO_2$, and ratio of starch and stearic acid on the surface modification of starch grains were investigated. Coated starches were characterized using scanning electron microscopy (SEM), laser light scattering particle size analysis, moisture absorption, powder flowability and density measurement, differential scanning calorimetry (DSC), thermogravimetric analysis (TGA), X-ray powder diffraction (XRPD) and Fourier transform infrared (FT-IR) spectroscopy and was applied as lubricant in tabletting process in comparison with stearic acid and magnesium stearate. The pressure of $scCO_2$ did not affect but temperature of $scCO_2$ and ratio of corn starch and stearic acid were found to be the influential factors on surface modification of starch grains. SEM images showed that stearic acid deposited onto the surface of starch grains forming a thin, uniform and smooth film when reducing the content of stearic acid using pressure of 3000 psi and temperature of 60 °C. This result was supported by an increase in particle size of coated starch which corresponding with the amount of stearic acid used in the mixture. The gravimetric vapour sorption analysis of coated starches showed the percentage of mass change lower than uncoated corn starch, this result corresponding with the result obtained from the determination of moisture absorption property using Karl Fischer method. It indicated that coated starches were coated with stearic acid, a hydrophobic material, almost did not absorb moisture. The bulk and tapped density, compressibility index and apparent density showed different between uncoated corn starch and coated starch. Physicochemical characterizations of coated starches indicated that no change and/or evidence of interaction between starch and stearic acid. The stearic acid coated starches could be applied as a lubricant in tablet formulations.

Department : Pharmaceutics and Industrial Pharmacy	Student's Signature……..…..
Field of Study : .....Industrial Pharmacy.....	Advisor's Signature…….….....
Academic Year : ……..……2009…….……	Co-Advisor's Signature……..……...

ACKNOWLEDGEMENTS

Firstly, I would like to express my sincere gratitude to my thesis advisor, Associate Professor Poj Kulvanich, Ph.D., Department of Pharmaceutics and Industrial Pharmacy, Faculty of Pharmaceutical Sciences, Chulalongkorn University, for his very excellent meaningful advice, invaluable guidance, supervision, interests and encouragement throughout my investigation.

My express also goes to my co-advisor, Jittima Chatchawalsaisin, Ph.D., Department of Pharmaceutics and Industrial Pharmacy, Faculty of Pharmaceutical Sciences, Chulalongkorn University, for her invaluable advice, comments and helpful suggestions for correction of this thesis.

I wish to express my appreciation to Narueporn Sutanthavibul, Ph.D., Department of Pharmaceutics and Industrial Pharmacy, Faculty of Pharmaceutical Sciences, Chulalongkorn University and Assistant Professor Sujimon Tunvichien, Ph.D., Department of Pharmaceutical Technology, Faculty of Pharmacy, Srinakharinwirot University, as examiners for their valuable advice, comments and helpful suggestions for correction of this thesis.

I wish to express my appreciation for suggestion of using Supercritical Fluid Extractor-400 (SFE-400) instrument to Associate Professor Rapepol Bavovada, Ph.D., Department of Pharmacognosy and Pharmaceutical Botany, Faculty of Pharmaceutical Sciences, Chulalongkorn University.

I am sincerely thankful to Siam Medicare Co., Ltd. for supplying the corn starch of pharmaceutical grade.

The acknowledgement is also given to all staff of the Faculty of Pharmaceutical Sciences, Chulalongkorn University, especially the staff in the Department of Pharmaceutics and Industrial Pharmacy for their assistance and support. I am really thankful to my seniors, especially Vipaluk Patomchaiviwat, Ph.D. for their consultation, guidance, suggestion and help.

The financial assistance from the Graduate School Chulalongkorn University is gratefully acknowledged.

Ultimately, I would like to express my heartfelt thanks to my parents, my brother, my sister, and my friends for their care, endless love, encouragement, understanding, and cheerfulness throughout my graduate study.

CONTENTS

Page

Page

LIST OF TABLES

LIST OF FIGURES

Figure **Page**

LIST OF ABBREVIATIONS

ASES	=	Aerosol Solvent Extraction System
α	=	Angle of repose
Å	=	Angstrom
atm	=	Atmosphere
2θ	=	Bragg angle
ρ_b	=	Bulk density
Carr's CI	=	Carr's Compressibility Index
°C	=	Degree celcius
$°Cmin^{-1}$	=	Degree celcius per minute
CO_2	=	Carbon Dioxide
DSC	=	Differential Scanning Calorimetry
DVS	=	Dynamic Vapour Sorption
FT-IR	=	Fourier Transform Infrared
g	=	Gram
GAS	=	Gas Antisolvent
g/cm^3	=	Gram per cubic centimeter
g/sec	=	Gram per second
h	=	Height of powder sample
K	=	Kelvin
kPa	=	Kilopascal
kp	=	Kilopound
kV	=	Kilovolt
LOD	=	Loss on Drying
mL	=	Milliliter
$mLmin^{-1}$	=	Milliliter per minute
mm	=	Millimeter
min	=	Minute
MPa	=	Megapascal
N	=	Newton
N/A	=	not available
P_c	=	Critical pressure

PCA	=	Precipitation with a Compressed Fluid Antisolvent
PGSS	=	Precipitation from Gas Saturated Solutions
psi	=	Pounds per square inch
r	=	Radius of shallow petri dish
RESS	=	Rapid Expansion of Supercritical Solutions
RESS-N	=	Rapid Expansion of Supercritical Solutions with a Nonsolvent
RH	=	Relative humidity
rpm	=	Round per minute
sec	=	Second
sec/step	=	Second per step
SAS	=	Supercritical Antisolvent
SCT	=	Supercritical Fluid Technology
scCO$_2$	=	Supercritical Carbon Dioxide
SCF	=	Supercritical Fluid
SCFs	=	Supercritical Fluids
SFE	=	Supercritical Fluid Extractor
SEDS	=	Solution Enhanced Dispersion by Supercritical Fluids
SEM	=	Scanning Electron Microscope
ρ_t	=	Tapped density
T_c	=	Critical temperature
TGA	=	Thermogravimetric Analysis
µl	=	Microliter
µm	=	Micrometer
% (wt/vol)	=	Percent weight by volume
% (wt/wt)	=	Percent weight by weight
XRPD	=	X-ray Powder Diffractometry

CHAPTER I

INTRODUCTION

Solid dosage forms like tablets and capsules are the most popular and preferred drug delivery systems because they have high patient compliance, relatively easy to produce, easy to market, accurate dosing, good physical and chemical stability (Marshall and Rudnic, 1990; Joshi and Duriez, 2004). Tablet dosage form is mainly composed of the drug and excipients such as diluent, binder, lubricant, disintegrant and glidant. Lubricant is an important excipient to improve the quality and manufacturing efficiency of tabletting process. It helps in reducing the friction at the interface between a tablet surface and the die wall during ejection and reduces wear on punches and dies, prevent sticking to punch faces, improve the fluidity and filling properties, and manufacturing efficiency of solid preparations. Insufficient fluidity of the bulk powder in the tabletting process causes problems such as an increase in the variability of the tablet weight, impairment of content uniformity and deterioration of the product quality. Also, inadequate plasticity due to friction and adhesion among powder particles lead to troubles in the manufacturing process and deterioration of productivity (Aoshima *et al*., 2005). Friction can also damage the machine and tablets during ejection. Moreover, high temperature generated during compression can affect drug stability (Kara *et al*., 2004).

Some of the commonly used tablet lubricants are stearic acid, magnesium stearate, glycerol esters of fatty acids, DL-leucine and sodium benzoate (Turkoglu *et al*., 2005). Stearic acid, a wax-like material, is one common used as a lubricant in solid pharmaceutical formulations. It is a hard, white or faintly yellow-colored, some what glossy, crystalline solid or a white or yellowish white powder. It has a slight odor and taste suggesting tallow. It is practically insoluble in water but freely soluble in benzene, carbon tetrachloride, chloroform and ether, and soluble in ethanol, hexane and propylene glycol. The melting point of stearic acid is about 60 °C (Allen, 1994). Therefore, particle size reduction of stearic acid can be somewhat difficult. However, particle size reduction methods have become less desirable because of environmental

concerns and possible volatile organic compound emissions. Strict pollution control have forced industries to move away from the use of conventional organic solvent as a medium for particle size reduction towards alternative particle size reduction technologies i.e. hot melt coating systems. However, some significant drawbacks including high cost of instruments and difficulty in formulation of hot melt coating are experienced.

About two thirds of the products used in the pharmaceutical industry are in the form of particulate solids. Consequently, a lot of effort has been put into research in particle generation processes. Conventional well-known processes for particle size reduction of solid materials are crushing and grinding (which for some compounds are carried out at cryogenic temperatures), air micronization, sublimation and recrystallization/precipitation from solution. There are several practical problems associated with the above-mentioned processes. Some substances are unstable under conventional milling conditions, and in recrystallization processes the product is contaminated with solvent, and waste solvent streams are produced. Applying supercritical fluid technology (SCT) may overcome the drawbacks of conventional processes and several processes for formation of solid particles using dense gases for micronization have been studied intensively.

Since the mid-1980s, a new method of powder generation has appeared involving crystallization with supercritical fluids (SCFs). Carbon dioxide (CO_2) is the most widely used solvent and its innocuity and ‘‘green’’ characteristics make it the best candidate for the pharmaceutical industry. Supercritical carbon dioxide ($scCO_2$) is an ideal medium to be used in place of volatile organic solvent in a pharmaceutical process due to being non-toxic, nonflammable, environmental-friendly and having relatively low critical temperature (T_c = 31.1 °C) and mild critical pressure (P_c = 73.8 bars). Moreover, CO_2 is gaseous at ambient conditions, which simplifies the problem of solvent residues (Fages *et al*., 2004). Supercritical processes, e.g. rapid expansion of supercritical solutions (RESS), supercritical anti solvent (SAS) and particles from gas saturated solutions (PGSS), give micro- or even nanoparticles with narrow size distribution. The unique thermo-dynamic and fluid-dynamic properties of supercritical fluids can be used also for particle coating and/or surface modification, for formation of composite particles, for impregnation of solids, for formation of solid

emulsions. The RESS process is an attractive technology for the production of small, uniform and solvent-free particles. The RESS containing a non-volatile solute leads to loss of solvent power by the fast expansion of the supercritical solution through an adequate nozzle, which can cause solute precipitation. The process is used to produce fine particles as very rapid nucleation of the solubilized material occurs during depressurization. Its application for coating may be possible when the coating material is dissolved while the core is insoluble in the supercritical fluid.

For the above reasons, it is interesting to study the surface modification of starch grains by coating with stearic acid using SCT by application of RESS with a nonsolvent (RESS-N) process. This coated starch can be applied as a lubricant in tablet formulations. Corn starch was chosen because it is one of the most common types of starch used as excipients in the manufacture of solid dosage form as diluent, binder and disintegrant. Stearic acid was considered in this study because it is well known from literature reviews that can be dissolved in $scCO_2$ (Kramer and Thodos, 1989).

The objectives of this study

1. To modify the surface of starch grains by coating with stearic acid using supercritical fluid technology with RESS-N process.

2. To investigate the effects of temperature, pressure, and ratio of starch and stearic acid on the surface modification of starch grains.

3. To apply stearic acid coated starch grains as lubricant in tabletting process in comparison with stearic acid and magnesium stearate.

CHAPTER II

LITERATURE REVIEW

Supercritical Fluid Technology (SCT)

SCT is a unique concept that exploits the solvent properties of SCFs above their critical temperature and pressure conditions. Near the critical point, SCFs possess liquid-like densities and gas-like transport properties. The solubilizing power of SCFs is sensitive to small changes in the operating conditions, and it is possible to fine-tune the pressure and the temperature to tailor the solvent capacity of SCFs for a particular process. SCT offers tremendous potential, as it is safe, environmentally friendly and economical. It has applications in the food industry, separations, chemical processing, pharmaceuticals, polymers and the environmental, textile and forest product industries, and in the cleaning of precision parts.

The low operating conditions (temperature and pressure) make SCFs attractive for pharmaceutical development. Their use is a relative new approach in pharmaceutical research. They provide viable alternatives to conventional size-reduction methods and are advantageous in the preparation of ultrafine powders of thermolabile drugs. They offer novel solventless techniques for the preparation of drug-loaded microspheres compared to traditional microencapsulation techniques which use large amounts of organic solvents. For pharmaceutical scientists, SCT offers innovative and economical methods to achieve solvent-free particulate delivery systems in an environmental- and regulatory-friendly manner.

Fundamentals

For every solvent, there exists a critical temperature (T_c) and a critical pressure (P_c), beyond which no applied pressure can force the solvent into its liquid phase. A solvent is stated to be supercritical when its pressure and temperature are higher than its T_c and P_c. As the critical point of a solvent is approached (i.e. the T_c and P_c), its isothermal compressibility tends to infinity, causing dramatic changes in its molar volume or density. In the critical region, a substance that is gas at normal conditions

exhibits liquid-like density and an extremely high solvent capacity which depends on the pressure. The variable solvent capacity can be exploited for a number of applications. Figure 2-1 provides a typical phase diagram for a pure compound as a function of temperature and pressure. The three lines divide the diagram into three regions: solid, liquid and gas. Along these lines, two phases are in equilibrium, whereas at the triple point the three states of aggregation coexist. The discontinuous transition from liquid to gas ends at the critical point. Beyond this point, a low density gas can be compressed continuously into a dense fluid. In this region, the thermophysical properties exhibit very high rates of change with respect to temperature and pressure. Along a near critical isotherm (between T_c and $1.2T_c$), the density and transport properties such as viscosity and diffusity, as well as other physical properties such as dielectrics such as dielectric constant and solvent strength can be varied continuously from gas-like to liquid-like with relatively small changes around the critical pressure (0.9-2.0 P_c). SCFs possess high solvent density and very high compressibility, and solubility parameters intermediate to those of liquids and gases. Solutes display exponential solubility enhancements in SCFs. The solubility values can be in the range of 10^3-10^8 and even higher than would expected in an ideal gas. SCFs have solute molecular diffusities much higher than those of liquids but low viscosities which are similar to those of gases. SCFs can be easily controlled between liquid-like and gas-like extremes by changing the pressure. Thus, supercritical solvents are ideal fluids for enhancing mass transfers from one region to another.

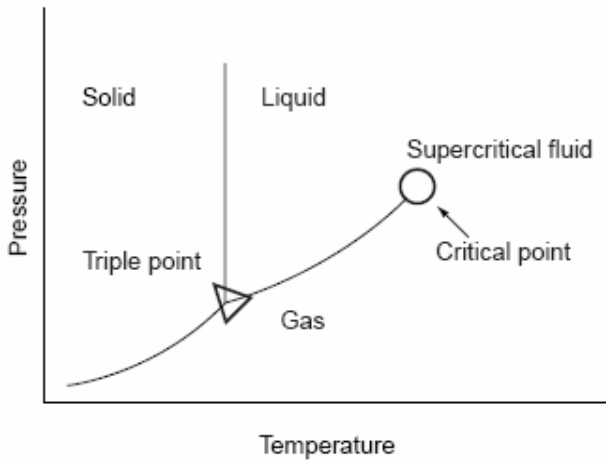

Figure 2-1 Phase behavior of a pure compound as a function of temperature and pressure (Dondeti, 1999)

Table 2-1 Critical conditions for some solvent (Dondeti, 1999)

Solvents	Critical Temperature	Critical Pressure	
	(°C)	(psi)	(MPa)
Ammonia	132.5	1636	11.28
Benzene	289	709	4.88
Carbon dioxide	31.1	1070	7.38
Trichloromonofluoromethane	198.1	640	4.41
Dichlorotetrafluoromethane	146.1	522	3.60
Dichlorodifluoromethane	111.7	579	4.00
Chlorodifluoromethane	96	725	5.00
Chlorotrifluoromethane	28.9	569	3.92
Cyclohexane	280.3	590	4.07
Ethane	32.2	708	4.88
Ethylene	9.3	731	5.04
Isopropanol	235.2	690	4.75
Nitrous oxide	36.5	1050	7.24
p-Xylene	343.1	511	3.52
Propane	96.7	616	4.25
Propylene	91.9	670	4.62
Toluene	318.6	596	4.11
Trichlorofluoromethane	198.1	640	4.41
Water	374.2	3200	22.06

Table 2-1 provides the T_c and P_c for a number of solvents that can be used as SCFs. Many hydrocarbons have a critical pressure close to 650 psi (4481 kPa). The T_c of SCF solvents increases as the molecular weight of the solvent increases or as the polarity or intermolecular hydrogen bonding of the solvent increases. Water is a low molecular weight compound but has a high T_c. It requires a large amount of thermal energy to break the hydrogen bonds between molecules to allow vaporization into the gas phase. The wide range of T_c for gases and liquids suggests the use of a specific SCF for a particular application. Since solvents such as CO_2, ethane and ethylene have T_c close to ambient conditions, they are preferred for processing pharmaceuticals, flavors, thermolabile liquids and reactive monomers. Materials, such

as industrial chemicals and polymers that are less susceptible to temperature, can be processes with C_3- or C_4-hydrocarbons with T_c in the range of 100 to 150 °C. The C_3- or C_4-hydrocarbons are better suited for polymers than the C_2-hydrocarbons. Cyclohexane and benzene with T_c in the range of 250 to 300 °C are used to process nonvolatile substances such as coal and high molecular weight petroleum fractions. Supercritical water (T_c=374.2 °C) is used for hazardous waste detoxification and hydrocarbon reforming.

For pharmaceutical applications, CO_2 is an ideal processing medium. Because of its relatively mild T_c (31.1 °C), it is possible to exploit the advantages of near-critical operation at temperatures lower than 35 °C. Furthermore, carbon dioxide is nontoxic, nonflammable, relatively inexpensive, recyclable and "generally regarded as safe" (Wang *et al*., 2002). Even though the P_c (73.8 bar) of CO_2 is relatively high, such operating pressures and operating equipment thereof are fairly routine in large-scale separation processes involving $scCO_2$ such as the decaffeination of coffee beans and the extraction of hops.

CO_2 is a nonpolar solvent. A common rule of thumb is that if a compound dissolves in hexane, then that compound should also dissolve in $scCO_2$ (Subramaniam, Rajewski and Snavely, 1997). While this rule is valid for many low molar mass compounds that have appreciable vapor pressures, it fails in the case of polymers which have negligible vapor pressures. As such, CO_2 is essentially a nonsolvent for many lipophilic and hydrophilic compounds (which covers most pharmaceutical compounds). $scCO_2$ has been exploited both as a solvent and as a nonsolvent or antisolvent in pharmaceutical applications. The ability to rapidly vary the solvent strength, and thereby the rate of supersaturation and nucleation of dissolved compounds, is a unique aspect of SCT for particle formation.

Solubility Enhancement

SCFs have a tremendous solute capacity near the critical point. The solubility of a solute in SCF can be further increased significantly by the addition of another solute(s) and/or solvent(s). Generally, the solubilities of solutes in supercritical solvents are reported as enhancement factors. The enhancement factor is a dimensionless measure of solvent power, defined as the measured solubility divided

by the ideal gas solubility. The enhancement is relatively insensitive to the solute structure but very dependent on the polarity and density of the solvent. The solubility and selectivity of materials can be increased tremendously by choosing the appropriate SCF. Literature reports indicate that nonpolar solvents such as CO_2, ethane, or ethylene are better solvents for nonpolar molecules. Polar solvents such as fluoroform are preferred for polar compounds and those containing functional groups that can hydrogen-bond with the acidic proton of the solvent (Schmitt and Reid, 1986).

Effect of Cosolvents

The addition of a small amount of cosolvent can have a dramatic effect on SCF phase behavior and may result in the increased solute solubility and/or selectivity. The cosolvents, also known as entrainers, are polar or nonpolar miscible organic solvents which, when added in small quantities (1-5%), modify the polarity and solvent strength of the SCF.

Advantages

Health concerns associated with emissions from conventional pharmaceutical processing involving organic solvents, difficulties associated with residual solvent removal from finished products, and the drive for energy-efficient and inexpensive process have stimulated aggressive research in environment-friendly technologies. Major impetus in this regard has been on the substitution of organic solvents with SCFs which offer numerous advantages. SCFs such as CO_2 and water are inexpensive and abundantly available in nature. They are nontoxic, nonflammable and readily available in high purity. They are chemically inert in reaction conditions and can serve as media for a variety of chemical reactions. Absence of hazardous solvents in SCF processing makes it environmentally acceptable. Ease of solvent removal, low to nonexistent expenses for their disposal and low handling costs, as well as simplified, and fewer processing steps make the SCT attractive and cost effective. The process can be designed to be continuous which reduces the operating costs significantly. Addition of cosolvents can make the process more versatile and efficient. SCFs are advantageous for pharmaceuticals because low operating conditions, temperatures, and pressures can be used for the process.

Applications

SCFs are being more and more widely employed and have applications in numerous industries. Supercritical fluid extraction has been considered as an alternative to distillation solvent extraction by a variety of industries, including the beverage, food, petroleum and synthetic fuel industries. SCFs have been used in the preparation of low-fat and low-cholesterol dairy products, fractionation of vegetable and cotton seed oils, extraction of hops, spices and aromas from plant materials, deasphalting of petroleum and the extraction of liquid fuels from coal. In the environmental industry, supercritical water and CO_2 have been employed to replace hazardous solvents. Supercritical oxidation is used for total treatment of waste waters and sludges and for reactive remediation. Another area of application is the removal of toxic contaminants from soils and industrial waste. In the chemical industry, SCT will have a tremendous impact. SCFs can be used for aerogel production, solvent recovery, polymer and monomer processing, separation of buckminsterfullerene from carbon soot, production of metal catalysts, reclamation of spent catalysts, separation of aromatic organic isomers, extraction of waxy materials, binder removal from ceramics and as a reaction medium for a number of chemical reactions. In cleaning of precision parts, supercritical CO_2 can be used to remove silicone oils, flux residues, machining oils, lubricants, adhesive residues, plasticizers and waxy materials. Some candidates for cleaning purposes include missile gyroscopes, accelerometers, thermal switches, nuclear valve seals, electromechanical assemblies, polymeric containers, special camera lenses and many others. Another interesting area of application for this technology is the forest products industry including pulp and paper processing. SCFs can be used for impregnation of chemical preservatives into wood and in wood-finishing processes.

Although the SCT has been successfully employed on a large scale in the food, polymer and petroleum industries, the pharmaceutical industry is yet to exploit its unique advantages. Recently, the role of SCFs at different stages of pharmaceutical processes has been investigated (Subramaniam, Rajewski and Snavely, 1997).

We have classified the methods of fine particles formation using $scCO_2$ into three groups according to the role of $scCO_2$ and use of the second solvent:

1. *Precipitation from supercritical solutions composed of SCF and solute (s).* Rapid expansion of supercritical solutions (RESS), the RESS process, exemplifies this first group. In this method one dissolves the solute or solutes to be comminuted in a SCF, this mixture is then expanded by means of a restrictor, which causes the solid to precipitate. This technique calls for molecules that are fairly soluble in SCFs, which constitutes a limitation, since most drugs have a poor solubility in $scCO_2$, a commonly used SCF for pharmaceuticals.
2. *Precipitation from solutions using SCFs or compressed gases as antisolvents.* Solids that are insoluble in SCFs or compressed gas can be micronized by means of this approach. The basic principle is to allow a solution of a substrate in a liquid primary solvent of interest to contact a SCF or a dense gas. The simulataneous transfers of CO_2 and primary solvent from one phase to the other lead to supersaturation and the precipitation of the solid. Several applications were developed on this basis, differing from one another in the contact mode of the two phases, in the dispersion device selected, in phase flow direction, and in mode (batch or semicontinuous). Precipitation with a compressed fluid antisolvent (PCA), gas antisolvent (GAS), supercritical antisolvent (SAS), aerosol solvent extraction system (ASES) and solution enhanced dispersion by supercritical fluids (SEDS) are the designations proposed for techniques relevant to this group. As highlighted earlier, since most drugs cannot be operated by the RESS, the antisolvent techniques are effective for a very wide range of compounds.
3. *Precipitation from gas saturated solutions (PGSS),* (and related methods differ from groups). The last group, which consists of PGSS in that the SCF does not act as either solvent or antisolvent. This process involves dissolving an SCF or a compressed gas in the molten material, then expanding the solution through a nozzle.

1. RAPID EXPANSION OF SUPERCRITICAL SOLUTIONS (RESS)

The RESS process relies on the solvent properties of CO_2. Because CO_2 is a nonpolar molecule, this process will be mainly efficient and interesting for micronizing nonpolar molecules. For this reason, a preliminary study on the solubility of the compounds with pressure and temperature is necessary. As usual, the solvent polarity can be modified and enhanced by adding to the $scCO_2$, small quantities of an organic cosolvent. This is primarily because the solvent power of an SCF is strongly dependent on its density, which can be adjusted by small variations of pressure and temperature.

The principle of the technique may be described as follows. The active substance to be micronized is partly solubilized in a continuous stream of pure $scCO_2$, in some cases with the addition of a cosolvent; the mixture so formed is then expanded. The pressure decrease causes the CO_2 to evaporate, leading to supersaturation and precipitation of the solid.

To obtain small enough particles with a uniform particle size distribution, the expansion must be fast ($<10^{-5}$ s) and uniform. This is possible because the pressure variation can be very rapid and travels at the speed of the sound, leading to uniform conditions within the expanding fluid (Sengers, 1994).

Figure 2-2 shows a schematic of the RESS process, which is operated as follows. CO_2 is pumped **[a]** and raised to the desired pressure. When a cosolvent is used, it is pumped in the same way **[b]** and introduced into the CO_2 flow. This flow is then heated to the desired temperature **[c]** and allowed to enter a tank loaded with the active substance **[d]** for extraction. In this part of the process, the solvent power is strong because of the high pressure and because of the possible presence of a cosolvent. This mixture is then depressurized in an expansion vessel **[e]** by means of a capillary or a nozzle, with a typical inner diameter of 50 to 60 µm. The restrictor must be heated to plugging by solid precipitation. The expansion chamber is generally at or near atmospheric pressure. A frit filter is placed at the exit of the expansion chamber to keep the particles formed in the expansion vessel. A cyclone **[f]** separates the solvent from the CO_2, which can be recycled **[g]**.

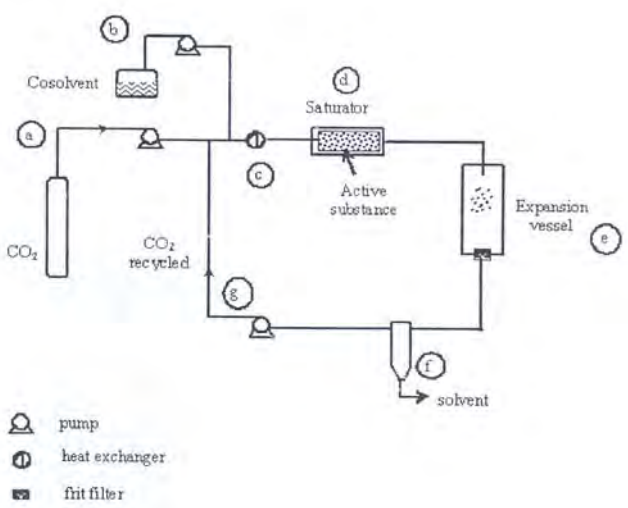

Figure 2-2 Schematic drawing of the RESS process; [a]-[g], see text (Charbit, Badens and Boutin, 2004)

The list that follows, though not exhaustive, gives the key factors to be controlled in this process if the desired particle size and size distribution are to be obtained (Jung and Perrut, 2001):

- Temperature and pressure in the saturator and in the expansion vessel
- Solubility of the active substance in the CO_2 mixture
- Nozzle diameter
- Dimensions of the expansion vessel

As for other supercritical processes, it is possible to micronize one substrate or more, for instance, to encapsulate an active substance in a biocompatible polymer. In such a case, the purpose is to obtain a controlled release system of the active substance and both materials (the active ingredient and the polymer) must be dissolved in the CO_2 mixture. Depending on the relative solubility of the two materials in the supercritical medium, one can obtain an encapsulated product or a composite matrix of the two products (Debenedetti *et al.*, 1993; Kim, Paxton and Tomasko, 1996).

The RESS process, without the use of a cosolvent, is very attractive and probably the most easily managed supercritical process. Unfortunately many molecules are not soluble in pure $scCO_2$, and these require the use of a cosolvent. However, such an addition makes the RESS process less favorable, since it loses its

main advantage of being system free of organic solvent. Any residual solvent in the product must be removed.

2. GAS ANTISOLVENT PROCESS (GAS)

Gallagher *et al*. (1989) first propose the GAS process to overcome limitations encountered with the RESS process. Indeed, many materials, more particularly drugs, are polar compounds that cannot dissolve to an “appreciable” extent in SCFs. Furthermore, the applicability of the RESS remains problematic at large scale owing to the high consumption of SCFs and the high pressures involved. Inspired by classical antisolvent techniques applied to liquid phases (i.e. “salting out”), using SCFs or gases near their vapor pressure as antisolvents.

This attractive technique was first tested to micronize explosives (Gallagher *et al*., 1989; Krukonis *et al*., 1991; Gallagher *et al*., 1992a; Gallagher *et al*., 1992b). Mechanical methods such as milling generate high local temperatures, and therefore are useless in this particular case; the use of $scCO_2$ as an antisolvent allowed comminution to proceed at mild temperatures. As already noted, the GAS process is a batch technique, which entails the gradual introduction of a compressed gas into a liquid solution of the solute of interest in a primary organic solvent. This method is based on the ability of liquids to solubilize large amounts of gases. This solubilization generally induces large volumetric expansions of the liquid phase (severalfold) and a decrease of its density up to a factor 2.

When a solid has been solubilized in the liquid prior to the introduction of the compressed gas, the volumetric expansion is accompanied by a decrease of the liquid solvent strength, which causes the solid to precipitate as ultra fine particles. The physicochemical properties of the solute of interest strongly influence the choice of a solvent/antisolvent pair. The antisolvent should have appreciable mutual solubility with the solvent and should have little or no affinity for the solute. As will be seen, the solute-solvent affinity is also an effective factor that can strongly influence the morphology of the end product.

In schematic of the GAS process shown in Figure 2-3, the compressed gas in tank **[1]** is pumped with a high pressure pump **[2]** and introduced into a buffer vessel

[3]. It can be fed to the crystallization vessel **[4]** either through the top **[5]** or most commonly through the bottom **[6]**, so that it bubbles in the liquid. The autoclave is equipped with a circulating water jacket to maintain the working temperature during the entire process. The autoclave is also provided with a stainless steel frit filter **[7]** and a stirring device **[8]**. At the end of the precipitation step, the fluid content of the precipitator is flushed to atmospheric pressure in a separation vessel **[9]**, where the gas **[10]** and the liquid phase **[11]** are separated.

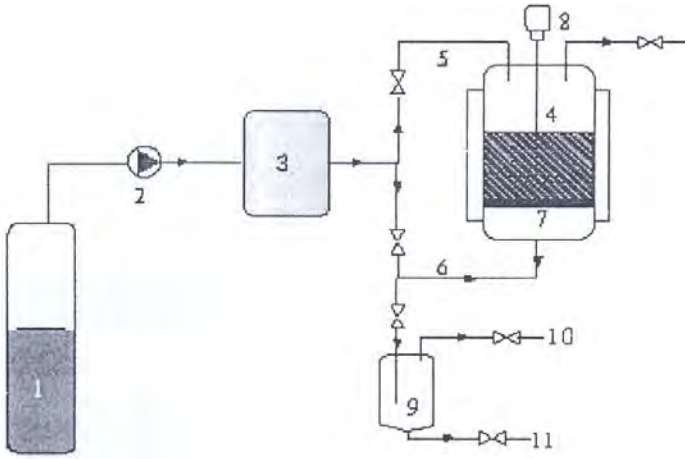

Figure 2-3 Schematic flow diagram of the GAS process; for [1]-[11], see text (Charbit, Badens and Boutin, 2004)

3. PRECIPITATION WITH A COMPRESSED FLUID ANTISOLVENT (PCA), A SUPERCRITICAL ANTISOLVENT (SAS) AND THE AEROSOL SOLVENT EXTRACTION SYSTEM (ASES) PROCESSES

Dozens of drugs have been recrystallized by means of the precipitation with a compressed fluid antisilvent (PCA) and the supercritical antisolvent (SAS) and aerosol solvent extraction system (ASES) processes.

These three precipitation processes involve the dispersion of a solution of the substrate of interest, dissolved in an organic solvent, through a capillary or a nozzle and into a continuous supercritical or subcritical antisolvent phase, which generally sweeps the vessel. In most cases, the experimental procedure is as follows (see Figure 2-4). The antisolvent is first introduced into the precipitation vessel. When the experimental pressure has been reached, an outlet valve is opened to maintain a constant pressure and a constant antisolvent flow rate. Then, there are two

alternatives. Pure solvent is introduced upon reaching and the steady state (constant ratio of antisolvent and solvent), the liquid phase turns from pure solvent to the liquid solution of the substrate. The other alternative is to introduce the solution of the substrate directly into the pure antisolvent phase. In that case, the supercritical phase composition evolves and a certain time is required before the steady state is reached. In both cases, the solution is introduced through a capillary or a nozzle. The dispersed liquid phase can form a liquid jet or can be atomized in fine droplets depending on the injection device (geometry, orifice diameter), the liquid flow rate, the operating pressure and temperature, and so on. During the process, the precipitation results from two phenomena: the fast diffusion of the antisolvent into the liquid phase and the evaporation of the organic solvent into the continuous phase, generally in a supercritical state. Both transfers rapidly yield supersaturation, which causes the substrate to precipitate in the form of nano- or microparticles. The fluid mixture (antisolvent+solvent) flows to a cold trap at atmospheric pressure, where the separation of gas and liquid occurs.

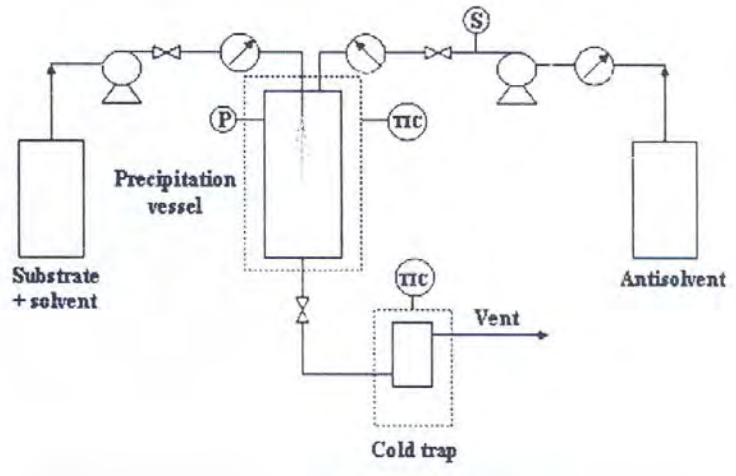

Figure 2-4 Apparatus for PCA, SAS and ASES processes: TIC, temperature indicator/ controller (Charbit, Badens and Boutin, 2004)

When the injection of liquid is finished, a washing step is carried out to remove the organic solvent and to prevent it from condensing during the depressurization step. For this purpose, the feed of pure antisolvent is maintained, to renew the vessel content. The vessel pressure is then reduced to atmospheric pressure, and solid particles are collected on a filter at the bottom of the vessel and/or on the

walls of the vessel; in some cases, metallic or polymeric baskets are used for the particle harvesting.

4. SOLUTION ENHANCED DISPERSION BY SUPERCRITICAL FLUIDS (SEDS) PROCESS

The SEDS process appeared not long after the other antisolvent processes just described, and it was first developed and patented by Bradford Particle Design (Hanna and York, 1995). The general principle is the same as that for SAS process: $scCO_2$ and the organic solution are introduced cocurrently in the reactor, and precipitation of the solid is due to the antisolvent effect. The essential difference is related to the way of introducing the different phase; in SEDS, a coaxial nozzle is used. The liquid solution is introduced in the inner channel while CO_2 flows in the outer tube; however; the inverse process was also proposed. Whatever the configuration used, the geometry given to these two channels results in a premixing chamber located just above the injection point in the supercritical medium. This premixing favors turbulence, hence the dispersion of the organic solution in the CO_2 was efficacy of the mass transfer. It normally leads to small particles with nanometric or micrometric size. This process was used for many substrates that are difficult to manufacture by the RESS process. Compared with the other antisolvent techniques, SEDS is distinguished by two specific features. First the coaxial introduction of $scCO_2$ and liquid solution with a high velocity of CO_2, leads to turbulent flow and to improved conditions for mixing and particle formation. Furthermore, the use of coaxial introduction fixes the composition solvent, $scCO_2$ and solid material from the mixing point, which should induce uniform conditions for particle formation.

5. PARTICLES FROM GAS SATURATED SOLUTIONS (PGSS)

The so-called PGSS process was described by Weidner et al. in a series of patents filed beginning in 1994 (Weidner *et al.*, 1994; Weidner *et al.*, 1997; Weidner *et al.*, 2000). Unlike the RESS process, in this technique the compressed gas is dissolved in the material(s) to be treated; thus, the PGSS process takes advantage of a much higher solubility of gases in liquids or solids than that of solids or liquids in compressed gases at same conditions. When the material to be treated is a solid, it is first melted, and the compressible gas is added to the molten material until saturation is reached; the solution thus formed may typically contain 5 to 50% wt/wt of the

compressed gas. The temperature of the solution is preferably adjusted to around 50 K above or below the melting point of the solid under atmospheric pressure. The mixture formed is discharged through a nozzle or other expansion device. The operating conditions of the decompression are turned in such a way that nearly all the compressed fluid turns to gas, facilitating its further separation from the particles. The evaporation and/or the Joule-Thomson effect results in noticeable cooling of the mixture, which causes the temperature to fall below the melting point of the material, which then precipitates. Additionally, it must be noted that the melting point of the solid is decreases owing to its pressurization with dense gases.

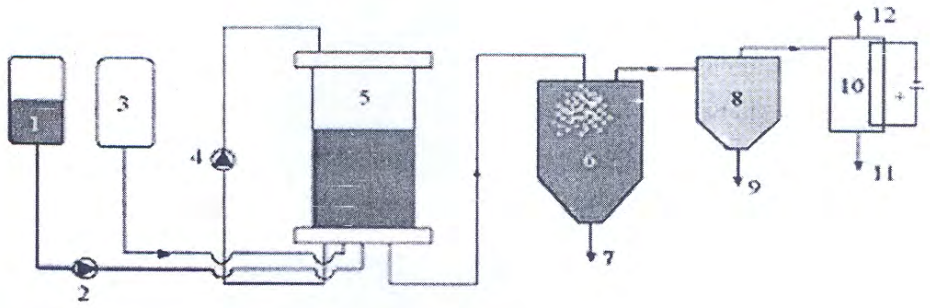

Figure 2-5 Schematic flow diagram of the PGSS process; for [1]-[12], see text (Charbit, Badens and Boutin, 2004)

The apparatus for carrying out the PGSS process is described in Figure 2-5. The solid or solids to be treated must first be melted in a feed vessel **[3]** and sucked in the autoclave **[5]**. A compressible fluid stored in a tank **[1]** is fed to the autoclave by means of a high pressure pump **[2]**. To enhance the mass transfer between the liquid and gaseous phases, the liquid is drawn off at the bottom of the autoclave and recycled to the top by means of a high pressure circulating pump **[4]**. The expanded liquid phase so formed is then sprayed into a tower **[6]** through suitable devices (nozzle, capillary, valve, orifice, etc.). The spray tower is designed in such a way that particles with an equivalent diameter equal or greater than 10 µm deposit and are collected at the bottom of the tower **[7]**. The gaseous phase issued from the spray tower is conveyed to a cyclone **[8]**, which allows for the removal of particles with diameter above 1 µm **[9]**. The smallest particles leave the cyclone suspended in the gas stream, which is operated by an electrostatic precipitator. Subject to an intense electric field (20 kV) solid particles gather on the central wire. Periodically the solid

is shaken off and collected at the bottom of the precipitator **[11]** while the purified gas is extracted at the top **[12]** and recycled to the autoclave.

According to Kramer and Thodos (1989) studied the solubility of 1-octadecanol [$CH_3(CH_2)_{16}CH_2OH$] and stearic acid [$CH_3(CH_2)_{16}COOH$] in dense $scCO_2$ has been established at 318, 328 and 338 K and pressures ranging from 140 to 467 bar. Maximum solubilities were observed for both systems at 318 K and pressures of 280-300 bar. The results of the 1-octadecanol-carbon dioxide system at 328 and 338 K and those for the stearic acid-carbon dioxide system at 338 K were correlated with the mole fraction of the solute and the reduced density of the pure solvent. This approach yielded deviations of 5.85% (13 points) for 1-octadecanol and 3.39% (5 points) for stearic acid. The Hansen three-dimensional solubility parameter was also applied to the Flory-Huggins theory for the development of a different model which yielded deviations of 24.0% (17 points) for 1-octadecanol and 5.14% (17 points) for stearic acid.

According to Zhong, Han and Yan (1997) studied the effect of methyl acetate and acetic acid on the solubility of stearic acid in supercritical CO_2. The main objective was to study how the difference between acetic acid and methyl acetate affects solubility. The solubility of stearic acid in CO_2+acetic acid and CO_2+methyl acetate binary mixtures was measured at 318.15 K in the pressure range 90-165 bar and the cosolvent concentration range 0.0-5.1 mol%. The solubility data are discussed qualitatively on the basis of the chemical association principle, which indicates that the larger solubility enhancement by acetic acid is primarily caused by the stronger hydrogen bond between the solute and acetic acid. Solubility increases significantly with pressure at lower cosolvent concentrations and lower pressures, but increases slowly with pressure at higher pressures or higher cosolvent concentrations.

According to Guan, Han and Yan (1998) studied the effect of acetic acid and n-octane on the solubility of stearic acid in supercritical CO_2. The solubility of stearic acid in supercritical CO_2 with n-octane and acetic acid cosolvents was measured at 308.15 K in the pressure range from 80 to 160 bar and the cosolvent concentrations range from 0.0 to 3.5 mol%. The solubility increases with the concentrations of the cosolvents and pressure. However, the solubility increases very slowly with the

concentrations of the cosolvents at higher the concentrations of the cosolvents when acetic acid is used as a cosolvent, mainly because acetic acid can associate with itself. In CO_2-acetic acid mixture, the solubility increases with the concentrations of the cosolvents provided that the apparent density of CO_2 is fixed. In CO_2-n-octane mixture, the solubility also increases with the concentrations of the cosolvents at higher the apparent density of CO_2. However, at lower the apparent density of CO_2 and the concentrations of the cosolvents the solubility decreases with the concentrations of the cosolvents at fixed the apparent density of CO_2. It was found that clustering between CO_2 and the cosolvent reduces the efficiency of CO_2 to dissolve the solute.

Lubricant in the Tabletting Process

It is rare to find a solid oral dosage product consisting of drug alone. To produce a final product that is not only practical and convenient to handle but also facilitates patient compliance, the drug substance needs to be processed with other excipients. The “fillers” or “excipients” serve many purposes in the formulation. One class of functional excipients that is essential in the most tablet formulations is “lubricants”.

As with other classes of pharmaceutical excipients, solid lubricating agents are added to the formulation of solid dosage form to aid in the manufacturing technologies used and ensure appropriate quality parameters for the finished products, reflective of uniform accuracy, safety and therapeutic efficacy.

In tabletting, the mixture of granules and fine powders developed by wet granulation and slugging technologies similarly must flow from hopper orifices. In these cases, the flow is to a consecutive series of fast-moving dies, set in the rotating, circular tabletop of a tablet press. Glidant lubricants added to such formulations assist in good weight and content control. Lubricating agents also reduce friction between tablet surfaces and die wall to ensure easy tablet ejection upon the upstroke of the lower tablet punches. A third function of lubricating agents is to ensure complete release (antiadherent) of solids from the upper and lower faces.

In the filling of hard gelatin, two-piece capsules by automatic equipment the blend of medicated powders and excipients must flow rapidly and uniformly from hoppers to he units containing the empty capsule bodies in order to ensure proper capsule weight and content uniformity. Lubricating agents of the glidant type are added to overcome powder cohesiveness and achieve appropriate flow.

In dusting powder, the blend of fine particle-size solids must flow readily and uniformly from the sprinkle-top container to the skin and thereafter spread evenly over the skin surface without significant rubbing, that is, produce a glidant effect. Likewise, it is desirable for such powder blends to reduce friction between skin surfaces and clothing to avoid chafing and irritation. Lubricating agents are present in such formulations to achieve these desirable effects.

The pharmaceutical literature identifies three interrelated types of lubricating agents used in compressed tablet formulations: lubricants, glidants and antiadherents (Miller, 1988). Strickland (1959) first outlined this interrelationship as follows:

- Lubricant excipients reduce the friction between tablet surface and the die wall during and after compaction to ensure easy ejection of the tablet from the die
- Glidant excipients improve the flow characteristics of tablet granulations (and capsule powder blends)
- Antiadherent excipients reduce adhesion between tablet punch faces and tablet surfaces to prevent sticking of solid particles to punch surfaces

Lubricants can be subdivided into water-soluble (e.g. Magnesium lauryl sulfate) and water-insoluble (e.g. Magnesium stearate and Stearic acid) categories. Water-insoluble lubricants are hydrophobic and, as such, can harm drug bioavailability, disintegration and dissolution times and tablet strength. Lubricants in solid dosage forms and suggested percentage are summarized in the Table 2-2.

Table 2-2 Lubricants in solid dosage forms and suggested percentage (Zanowiak, 1994)

Lubricant	Suggested Percentage
Water-insoluble	
Stearic acid	1-2
Magnesium stearate	0.5-2
Calcium stearate	0.5-2
Zinc stearate	0.5-2
Talc	5-10
Starch	5-10
Glyceryl behenate	0.5-4
Sodium stearyl fumarate	0.5-2
Light mineral oil	1-3
Hydrogenated vegetable oils	1-2
Calcium stearate, sodium stearate and lauryl sulfate mixture (Stearowet C)	0.5-2
Water-soluble	
Polyethylene glycols (400, 600)	2-10
Sodium acetate	5-10
Sodium benzoate	2-5
Sodium chloride	5-20
DL-leucine	1-5
Sodium lauryl sulfate	1-3
Magnesium lauryl sulfate	1-3

A significant number of hydrophobic lubricants can be grouped chemically in the following way (Miller, 1988):

- *Fatty acids*: stearic acid, palmitic acid
- *Fatty alcohols*: stearyl alcohol, palmityl alcohol
- *Hydrocarbons*: mineral oil, paraffins, waxes (mineral and vegetable), hydrogenated vegetable oils

- *Fatty acid esters*: glyceryl mono- and distearate, glyceryl tristearte, palmitate and myristate, glyceryl tribehenate, glyceryl palmitostearate, sucrose monostearate and palmitate, sorbitan monostearate, sodium stearyl fumarate

Some of the commonly used tablet lubricants are stearic acid, magnesium stearate, glycerol esters of fatty acids, DL-leucine and sodium benzoate (Turkoglu *et al*., 2005).

Stearic acid is an example of a fatty acid. Fatty acids are long molecules consisting of a hydrocarbon chain with a carboxylic acid group (-COOH) at the end. Figure 2-6 shows the long tail of the molecule, made up of carbon and hydrogen, is not attracted to water and is said to be hydrophobic (literally, water-fearing). It is hydrophobic and, as such, can harm drug bioavailability, disintegration and dissolution times and tablet strength. The carboxylic acid "head" can form hydrogen bonds with water, and is therefore strongly attracted to water. It is said to be hydrophilic (literally, water-loving) (Grant, 1997).

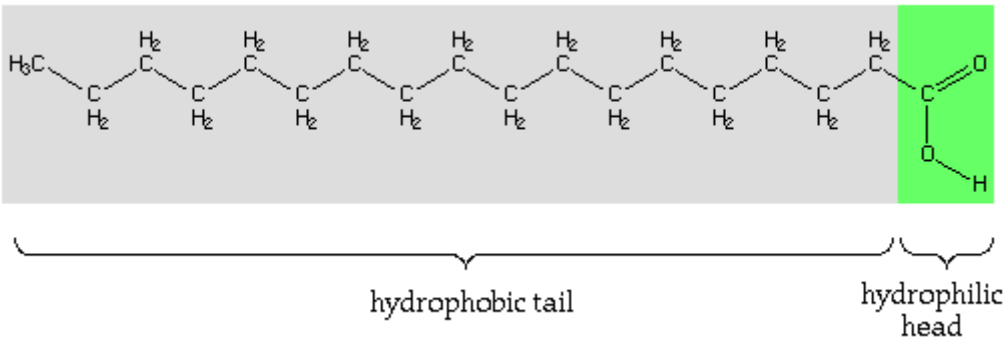

Figure 2-6 Structure of stearic acid: hydrophilic head and hydrophobic tail (Grant, 1997)

Stearic acid, a wax-like material, is a hard, white or faintly yellow-colored, some what glossy, crystalline solid or a white or yellowish white powder that has a chemical name of octadecanoic acid, a molecular formula of $C_{18}H_{36}O_2$ and a molecular weight of 284.47 daltons (for pure material). It has a slight odor and taste suggesting tallow. It is practically insoluble in water but freely soluble in benzene,

carbon tetrachloride, chloroform and ether, and soluble in ethanol, hexane and propylene glycol. The melting point of stearic acid is reported at about 60 °C (Allen, 1994).

According to Miller and York (1985) investigated physical and chemical characteristics of some high purity magnesium stearate and palmitate powders. High purity magnesium stearate and palmitate powders have been prepared at two batch sizes under different pH environments. Larger batch products were analyzed for chemical and physical character using gas chromatography, atomic absorption, surface area estimation, scanning electron microscopy, thermal analysis (moisture evolution analysis, DSC, TGA, hot stage microscopy), infrared and X-ray diffraction techniques. Powder particles produced under acid conditions had a thin, regular, plate-like appearance which those manufactured from alkaline conditions had more irregular structure. Acid-manufactured powders were found to be associated with two molecules of water and had a small degree of structure which was disrupted on drying. Materials precipitated from alkaline conditions appeared to consist of two species, the major one being one molecule of magnesium stearate or palmitate associated with two molecules of water, and the second minor component probably associated with equimolar proportions of water. Estimates of activation energy associated with the major thermal transitions confirmed the low level molecular structure in prepared materials.

According to Hussain *et al*. (1988) studied of the formation of magnesium stearate film on sodium chloride using energy-dispersive X-ray analysis. Scanning electron microscopy (SEM) and energy-dispersive X-ray (EDX) analysis techniques have been successfully applied to make direct measurements of the lubricant distribution on selected excipient particles. Sodium chloride was chosen as a model to represent a tabletting excipient and the formation of a magnesium stearate film on its surface was studied. Percentage surface coverage by the lubricant has been estimated from the EDX data for 0.1%, 0.5% and 2% wt/wt lubricant for several magnesium stearate samples. Film formation by lubricants from different manufacturers was examined and results suggested similarity in mechanism but different degree of host surface coverage for equivalent mixing conditions. Data also indicated that a molecular film is formed initially which, on further blending, was followed by the

build-up of a particulate layer that may have been initiated at gross defect points on the host particle surface. Lubricant film formation on sodium chloride has been confirmed as being of the Langmuir type. The influence of the specific surface area of the lubricant on excipient surface coverage has also been discussed.

According to Jannin *et al*. (2003) compared the lubricant performance of Compritol® 888 ATO either used by classical blending or by hot melt coating onto Lactopress by compression tests. In physical mix, the Compritol concentration does not affect the compressibility. The same compressibility is obtained with lactose coated by 0.5 or 1% of Compritol, but a higher compressibility can be observed with 2 and 3%. Cohesiveness of lactose depends on the process: hot melt coating induces a decrease of tablet tensile strength. In terms of forces transmission during compression phase and axial ejection pressures, Compritol used by hot melt coating allows for a concentration of 0.5% to directly obtain the lubricant performance of 3% of Compritol used by blending. These results suggest that the hot melt coating process induces a homogenous repartition of the lubricant on the lactose surface, contrary to classical blending procedure. Thus, lubrication by hot melt coating seems to be a very efficient procedure. It can be used specifically for large surface area particulate systems producing a lot of friction.

According to Aoshima *et al*. (2005) compared glycerin fatty acid esters (triglycerin full behenate (TR-FB®) and triglycerin half behenate (TR-HB®)) as a new lubricant of tablets with magnesium stearate (Mg-St) and a sucrose fatty acid ester (SSE) with regard to lubrication properties, tablet characteristics and stability of the preparation. Granules containing 50% acetaminophen were prepared and improvements in their fluidity by the lubricants were compared. The lubricant effects of TR-FB and TR-HB during tablet punching (pressure transmission ratio, ejection force) were similar to those of Mg-St and were better than those of SSE. When the lubricant content, mixing time and tabletting pressure were changed, TR-FB® and TR-HB® provided better tablet hardness than Mg-St. TR-FB® and TR-HB® made tablets more disintegratable than Mg-St. When the effects of these lubricants on the stability of acetylsalicylic acid (ASA) were compared, Mg-St promoted its hydrolysis, but TR-FB® or TR-HB® did not affect its stability.

According to Turkoglu, Sahin and San (2005) evaluated hexagonal boron nitride (HBN) as a new lubricant for pharmaceutical tablet manufacturing. The other conventional lubricants such as magnesium stearate (MGST), stearic acid (STAC) and glyceryl behenate (COMP) were also tested along with HBN. Tablets were manufactured on an instrumented single-station tablet press to monitor and quantify the lower punch ejection force (LPEF). The force ratio, tablet crushing strength, disintegration time and thickness were measured. The lubricant film formation and lubricant distribution in tablets were studied using the scanning electron microscopy (SEM) and electron probe micro analyzer (EPMA). Based on the force ratio, a good lubrication was obtained at 1% for MGST and HBN; in contrast, STAC and COMP did not show a good lubrication. After 1%, all lubricants performed well. MGST was found to be the most effective lubricant based on LPEF-lubricant concentration profile. HBN provided a 50% decrease in LPEF at 2% lubricant concentration and was rated as an effective tablet lubricant. HBN was better than either STAC or COMP. Unlike MGST, HBN had no significant prolongation effect on tablet disintegration times.

According to Uğurlu and Turkoğlu (2008) investigated the lubrication properties of hexagonal boron nitride (HBN) as a new tablet lubricant and compare it with conventional lubricants such as magnesium stearate (MGST), stearic acid (STAC) and glyceryl behenate (COMP). Tablets were manufactured on an instrumented single-station tablet press to monitor lower punch ejection force (LPEF) containing varied lubricants in different ratio (0.5, 1 and 2%). Tablet crushing strength, disintegration time and thickness were measured. Tensile strength of compacted tablets were measured by applying a diametrical load across the edge of tablets to determine mechanical strength. The deformation mechanism of tablets was studied during compression from the Heckel plots with or without lubricants. MGST was found to be the most effective lubricant based on LPEF-lubrication concentration profile and LPEF of HBN was found very close to that of MGST. HBN was better than both STAC and COMP. A good lubrication was obtained at 0.5% for MGST and HBN (189 and 195 N, respectively). Where COMP and STAC showed 20 and 35% more LPEF compare to that of MGST (239 and 288 N, respectively). Even at the concentration of 2% COMP and STAC did not decrease LPEF as much as 0.5% of MGST and HBN. Like all conventional lubricants the higher the concentration of

HBN the lower the mechanical properties of tablets because of its hydrophobic character. However, this deterioration was not as pronounced as MGST. HBN had no significant effect on tablet properties. Based on the Heckel plots, it was observed that after the addition of 1% lubricant granules showed less plastic deformation.

Surface Modification and/or Particle Coating

Surface modification to alter the properties of powders (such as flowability, wettability, time release, flavor, color, taste, etc.) is very important to many industries. Typically, surface modification of particles to form a barrier or film between the particle and its environment has been done by wet coating methods such as pan coaters and a variety of fluidized bed coaters or by wet chemistry-based techniques such as coacervation, interfacial polymerization and urea/formaldehyde deposition. However, wet coating methods have become less desirable because of environmental concerns over the resulting waste solutions and possible volatile organic compound emissions. Dry particle coating, which directly attaches fine materials (guest particles) onto the surface of larger core particles (host particles) by mechanical means without using any solvents, binders or even water, is a promising alternative approach (Kono *et al*., 1990). Apart from forming a barrier as in wet coating, dry particle coating can be used for making significant changes in the functionality or the properties of the original host particles, and thus creating engineered particulates.

Several dry coating methods have been developed, including SCT, magnetically assisted impact coating (MAIC), hybridization, mechanofusion and fluidized bed coating. These methods generally allow for the application of high shearing stresses or high impaction forces to achieve coating. The strong mechanical forces and the accompanying heat generated can cause layering and even embedding of the guest particles onto the surface of the host particles. Soft coating methods that can attach the guest particles onto the host particles with a minimum degradation of particle size, shape and composition caused by the build up of heat are the better candidates for materials which are sensitive to heat, and may be deformed by severe mechanical forces.

According to Tsutsumi *et al*. (1995) described a novel fluidized-bed coating of fine particles by rapid expansion of supercritical fluid solutions. Experiments were

conducted in a 50 mm circulating fluidized bed with an internal nozzle in the center of the riser. Microspheroidal catalyst particles (average particle size 56 μm) were used as the core particles. Supercritical carbon dioxide solutions of paraffin were expanded through the nozzle into the bed that was fluidized by air. The coating mass and coating rates were measured by a sampling method. Mercury porosimetry was used to determine the quality of the coated particles. A stable coating of fine particles was achieved without the formation of agglomerates at room temperature. The present study examines the effects of hydrodynamics and solute concentration on coating rate and coating efficiency. It was found that there was no significant agglomeration during coating. This is because the coating material is deposited directly on the surface of core particles without the presence of liquid droplets which act as a binder for particles. The coating mass was proportional to coating time, indicating a constant coating rate. The increase in paraffin concentration increases coating efficiency slightly. The fluidized-bed coating process by the rapid expansion of supercritical solutions allows not only fine particle coating, but also solventless and low temperature coating. This suggests the possibility of wide application in industry.

According to Liang, Ueno and Shinohara (2000) investigated the effectiveness of UV attenuation involving dispersibility changes with the coating ratio of surface composite particles and different sizes of coarse particles. Titanium dioxide powder was used as the fine particles to coat coarse nylon and polyethylene particles by high-speed rotational impact blending. The effects of the coating ratio and size of the coarse particles on the effectiveness of UV attenuation were investigated. The effectiveness of UV protection was found to be increased by decreasing the coating ratio, as this led to a lower level of surface agglomerates being formed. A further advantage of coating large polymer particles with fine titanium dioxide was an improvement in the bulk dispersion, which resulted in optimum UV protection.

According to Wang *et al.* (2001) studied mechanism of particle coating granulation with RESS process in a fluidized bed. In this study, the rapid expansion of supercritical fluid solution (RESS) process was employed for the coating granulation of fine particles in a fluidized bed and its mechanism was examined. The rapid expansion of the supercritical solution causes very high supersaturating ratio of solute in the spraying flow, forming a large number of superfine nuclei. The superfine nuclei

deposited on the surface of the particles form a thin film. It was found that the fine particles were all covered with the thin film. This coating mechanism has been confirmed by SEM inspection. The granules with fine particles adhered were circulated through the spraying region and were covered with the binder or coating material (solute) in the region in the form of a film, resulting in the fine particles being cumulatively coated on core particles layer by layer. The temperature at the nozzle inlet was found to be an important factor affecting the coating granulation process.

According to Schreiber *et al.* (2002) investigated fluidized bed coating at supercritical fluid conditions. As a model system, silica-particles and glass beads were encapsulated with a wax, which is common in technical coating applications. For this a homogeneous mixture of molten paraffin and supercritical carbon dioxide is prepared in an autoclave and injected into the fluidized bed from the bottom through a nozzle with an orifice diameter of 50 or 100 µm. Due to different conditions in the mixing-autoclave and the fluidized bed the paraffin precipitates in the vicinity of the nozzle and adheres to the solid particles. The coating experiments were carried out at fluid velocities up to 2.23 times the minimum fluidization velocity. The operating conditions for the coating process were determined by the investigation of the system paraffin-CO_2 by means of solubility and differential scanning calorimetry measurements. An even distribution of the coating material within the fluidized bed was observed at fluid velocities higher than 1.2 times the minimum fluidization velocity. SEM-images of the achieved coatings show different morphologies according to the process parameters and solids used. In the case of glass beads with a diameter of 100-200 µm a uniform, thin but incomplete coating was produced.

According to Wang *et al.* (2002) studied a modified RESS process for particle coating with a solution of polymer in supercritical CO_2. This technique involves extracting the polymer with supercritical CO_2, with or without a cosolvent in an extraction vessel, and then precipitating the polymer onto the surface of host particles in a second precipitation vessel by adjusting the pressure and temperature inside the precipitator to lower its solubility. The research was performed using a pilot-scale supercritical apparatus, glass beads as host particles and two different polymers as coating materials. Experiments showed that the coating of glass beads with polyvinyl

chloride-co-vinyl acetate (PVCVA) and hydroxypropyl cellulose (HPC) was successfully achieved. Scanning electron microscopy (SEM), energy dispersive X-ray spectrometry (EDS), energy dispersive X-ray mapping and thermogravimetric analysis (TGA) were used to characterize the coatings obtained. The results indicate that the process of particle coating with supercritical solution is a promising environmentally friendly, alternative coating method with little or no organic solvents required.

According to Mujumdar *et al.* (2004) developed a simple, potentially cost-effective technique to preserve the pyrotechnic properties of ground magnesium by dry coating wax or silica onto the surface of ground magnesium particles. The main idea is that the coating with materials that are hydrophobic will delay the formation of magnesium hydroxide, hence increasing the shelf-life of the ground magnesium. Dry particle coating is used to enhance the moisture resistance of ground magnesium powder (primary size 75 μm) by coating its surface with carnauba wax (primary size 15 μm). Coating was done using MAIC and two high-speed impaction-coating devices, the hybridizer and mechanofusion. The uncoated and coated samples are characterized by scanning electron microscopy (SEM), humidity tests and X-ray diffraction (XRD). SEM images indicate that in MAIC the coated wax is mainly observed in and around the cracks, whereas in the hybridizer and mechanofusion the wax was softened and spread more evenly over the magnesium surface. The results of 150-h humidity tests as well as extended 400-h tests show a significant improvement in the moisture resistance of ground magnesium powder after coating in all three devices. Extended 400-h tests show that in some cases, the wax-coated samples perform similar to atomized magnesium. In particular, the mechanofusion-coated product showed moisture resistance comparable to atomized magnesium, with an amount of wax as little as 2%. These results are also verified by XRD analysis to measure the amount of hydroxide formation. Thus the wax coating increases humidity resistance by delaying hydroxide formation, hence increasing the shelf life of the coated ground magnesium.

According to Wang, Dave and Pfeffer (2004) described a new method using supercritical CO_2 as an anti-solvent (SAS) for nanoparticle coating/encapsulation. A model system, using silica nanoparticles as host particles and Eudragit polymer as the

coating material, was chosen for this purpose. The SAS process causes a heterogeneous polymer nucleation with the nanoparticles acting as nuclei and a subsequent growth of polymer on the surface of the nanoparticles induced by mass transfer and phase transition. A polymer matrix structure of encapsulated nanoparticles is formed by agglomeration of the coated nanoparticles. Field emission scanning electron microscopy, transmission electron microscopy, electron energy loss spectroscopy and Fourier transform infrared spectroscopy were used to characterize the coated/encapsulated silica nanoparticles.

According to Yuwadee Phoonphetmongkon (2004) studied particle coating in fluidized bed coater enhanced with electrostaticity. Experimental results of coating of glass beads with aqueous solution containing HPMC as a coating liquid within a 16 liters top-spray fluidized bed enhanced by electrostaticity was significantly dependant on operating variables which were fluidizing air velocity (2.2 to 4.3 m/sec), flow rate of coating agent (10 to 20 ml/min), size of core particles (590 and 1,033 μm) and electricity potential applied to a spraying nozzle (0 to (-4) kV). Coating efficiency, coating film thickness and packed bulk of coated particles were affected by those operating variables. Increasing of fluidizing air velocity, coating efficiency and coating film thickness became hindered due to the higher evaporating rate of sprayed droplets became promoted with the increasing air velocity then they transformed to fine particulate dispersing away before coming into contact with core particles. While larger core particles led to more difficulty to be fluidized, resulting in a less contact among the core particles and sprayed droplets. On the other hand, an increase in flow rate of coating liquid could increase the coating film thickness and the coating efficiency. This could be implied that the higher the flow rate the larger the droplets sprayed out from the nozzle which increased the possibility of contact among the core particles and droplets. Meanwhile, an increase in electrical potential applied to the nozzle would lead to an increase in the attractive force among the charged droplets and the core particles therefore the coating efficiency could become more enhanced.

According to Kröber and Teipel (2005) examined microencapsulation of particles using supercritical carbon dioxide. In this contribution a novel fluidized-bed coating process is introduced to encapsulate heat-sensitive materials with particle sizes below 100 μm. Supercritical carbon dioxide is used as solvent for the coating

material as well as carrier fluid for the core material. The behaviour of the high pressure fluidized-bed was investigated for different process parameters and materials. It is shown that the fluidization starts at lower fluid velocities if the pressure is increased and it was possible to fluidized particles with a mean size below 10 µm. The coating of glass beads with stearyl alcohol was carried out and layers with a thickness of 1-8 µm were achieved.

According to Yang *et al*. (2005) investigated dry particle coating for improving the flowability of cohesive powders. Several dry processing techniques are used to coat cohesive corn starch powder with different size silica particles. For nanosized silica guest particles, FESEM images show that both the magnetic assisted impaction coater (MAIC) and the hybridizer (HB) produce particles that are significantly more uniformly coated than using either a V-shape blender or simple hand mixing. Image analysis confirms that MAIC and HB provide higher surface coverage for the amount of guest material (flow aid) used. The improvement in flowablity of coated corn starch is determined from angle of repose measurements using a Hosokawa powder tester. These measurements show that nanosized silica provides the best flowability enhancement, whereas mono-dispersed 500-nm silica does not improve the flow properties of corn starch at all. This observation agrees with a simple theoretical derivation based on the original Rumpf model, which shows that the flowability improvement is inversely proportional to the guest particle size for a given host particle size or size of surface asperities. Experimental results also indicate that surface-treated hydrophobic silica is more effective in improving the flowability of corn starch particles than untreated hydrophilic silica. An increase in processing time using MAIC and the V-blender also improves the flowability of the corn starch since the guest particles are more deagglomerated and better dispersed, the longer the processing time.

According to Calderone *et al*. (2008) developed a new supercritical co-injection process to coat microparticles. The process was first set up with micron-sized glass beads as model particles and then applied to two powdered active pharmaceutical ingredients. A lipid was used as coating material. The mass balance core/shell in the obtained particles was performed using both differential scanning calorimetry (DSC) and pycnometry measurements and showed a good reproducibility

of the process when particles above 20 µm size were considered. Fourier transform infrared (FT-IR) spectra and environmental scanning electronic microscope (ESEM) characterization were used to ensure that a shell of coating surrounded the raw particles. Both methods showed a different deposition mode of the lipid between the coated particles and a physical mixture of glass beads and lipid. Release tests in distilled water performed with coated active compounds showed a slowed down dissolution kinetics. The study of the polymorphism of the crystallized lipid revealed a solid/solid transition with time. The supercritical co-injection process is a promising way to discretely coat particles with relatively low diameters (20-50 µm) and is particularly suited to coat sensitive pharmaceutical molecules such as proteins.

According to Narh, Agwedicham and Jallo (2008) studied dry coating polymer powder particles with deagglomerated carbon nanotubes to improve their dispersion in nanocomposites. Deagglomerated multi-walled carbon nanotubes (MWCNTs) were dry coated onto the surfaces of polyethylene oxide powder particles by MAIC. The deagglomeration of the tightly agglomerated MWCNTs was carried out using two procedures: rapid expansion of supercritical suspension (RESS) of MWCNTs and CO_2, and high-intensity ultrasonic agitation of a suspension of MWCNTs in acetone, using an ultrasonic probe. FESEM images show that the high-intensity ultrasonic probe was more effective in deagglomerating the agglomerated MWCNTs than the RESS method. Furthermore, it was found that the extent of PEO particle surface coverage by MWCNTs greatly depends on the extent of deagglomeration.

According to Liu *et al*. (2008) investigated the properties of the modified sulfur and the sulfur coated urea particles. The shell of sulfur coated urea was easily cracked due to sulfur being friable. Sulfur was modified with dicyclopentadiene (DCPD) to increase its strength and abrasion resistance. SEM images showed that the micro-structure of modified sulfur was denser and more uniform than pure sulfur. The strength of modified sulfur increased with the DCPD/Sulfur ratio. Experiments of urea particle coating with sulfur and modified sulfur were carried out in a fluidized bed coater. The shell of coated urea particles with modified sulfur was more compact than that with pure sulfur. The modification retarded the sulfur phase transformation from monoclinic to orthorhombic, avoiding the crack formation in the coating shell of

sulfur. The modified sulfur coated urea particles can be produced with thinner shell and higher strength, and had better controlled release properties.

According to Rojo, Marienfeld and Cocero (2008) examined RESS process in coating applications in a high pressure fluidized bed environment: Bottom and top spray experiments. As a model system, glass beads particles ($d_{p,s}$=176 μm) were encapsulated with paraffin (T_m=52-54 °C). Two different ways of injecting the coating solutions of paraffin in the $ScCO_2$ in the fluidized bed were tested, bottom and top spray. The operation variables were kept in the following ranges for the saturation step: pressure from 18 to 22 MPa and temperature from 35 to 55 °C. In the coating process the pressure range from 8 to 10 MPa and temperature from 35 to 50 °C. Yields of the global process up to 70% were achieved. SEM images of the achieved coatings show complete coating films with no agglomeration in the top spray experiments.

CHAPTER III

EXPERIMENTAL

1. Materials

The following substances were obtained from commercial sources.

- Corn starch of pharmaceutical grade (Purity® 21A, Batch no. MGB2001, obtained as gift sample from Siam Medicare Co., Ltd., Bangkok, Thailand)
- Stearic acid (Octadecanoic acid, Lot no. A80626-13, Natural Oleochemicals Sdn. Bhd., Johor, Malaysia)
- Spray-dried lactose (LACTOSE SUPERTAB ANHYDROUS, Batch no. HR020011, DMV-FONTERRA, Taranaki, New Zealand)
- Microcrystalline cellulose (CEOLUS® PH-102, Batch no. 24B2, ASAHI KASEI Chemicals Corporation, Tokyo, Japan)
- Magnesium stearate (Radiastar® 1100, Batch no. 1758, OLEON NV, Ertvelde, Belgium)
- Talcum (Lot no. CH/294/07, CHINA CHEMICAL INDUSTRY, China)
- Colloidal silicon dioxide (Aerosil®, Lot no. ZB55869, Wacker Chemie AG, München, Germany)
- Liquefied carbon dioxide of industrial grade (99.5 %) in cylinders equipped with dip tube (Purchased from Thai Industrial Gases Public Co., Ltd., Samut Prakan, Thailand)
- Polyoxyethylene sorbitan monooleate (Tween 80, Lot no. 507864, NOF Corporation, Tokyo, Japan)
- Methanol HPLC grade (Lot no. I7AG1H, Honeywell Burdick & Jackson, Michigan, USA)

2. Equipments

- Supercritical Fluid Extractor (Model SFE-400, SUPELCO INC., Bellefonte, Pennsylvania, USA)

- Analytical Balance (Model AJ180, PB303, PB3002, PB602-L and XP205, METTLER TOLEDO, Schwerzenbach, Switzerland)
- Scanning Electron Microscope (Model JSM-5410LV, JEOL Ltd., Tokyo, Japan)
- Laser Diffraction Particle Sizer (Model Mastersizer 2000, Malvern Instruments Ltd., Worcestershire, UK)
- Density Analyzer (Model Ultrapycnometer 1000, QUANTACHROME INSTRUMENTS, Florida, USA)
- Differential Scanning Calorimeter (Model DSC822^{e}, METTLER TOLEDO, Schwerzenbach, Switzerland)
- Thermogravimetric Analyzer (Model TGA/SDTA851^{e}, METTLER TOLEDO, Schwerzenbach, Switzerland)
- X-ray diffractometer (Model D8-Discover, Bruker AXS, Karlsruhe, Germany)
- Fourier Transform Infrared Spectrometer (Model Spectrum One, Perkin Elmer Ltd., Massachusetts, USA)
- Hot Air Oven (Model UL80, MEMMERT, Munich, Germany)
- Halogen Moisture Analyzer (Model HR83, METTLER TOLEDO, Schwerzenbach, Switzerland)
- Dynamic Vapour Sorption Apparatus (Model DVS INTRINSIC, Surface Measurement Systems Ltd., London, United Kingdom)
- Karl Fischer Volumetric Titrator (Model AF8, ORION, Houston, Texas, USA)
- Jolting Volumeter (Modified by Department of Manufacturing Pharmacy, Faculty of Pharmaceutical Sciences, Chulalongkorn University, Thailand)
- Ultrasound Transonic Digital Sonicator (Model T680/H, ELMA, Singen, Germany)
- Single Punch Tablet Press (Model PMA 3, KORSCH America Inc., Massachusetts, USA)
- Tablet Hardness Tester (Model DHT-250, THERMONIK, Mumbai, India)
- Tablet Friability Tester (Model TAR 10, ERWEKA GmbH, Heusenstamm, Germany)

- Disintegration Apparatus (Model ZT 31, ERWEKA GmbH, Heusenstamm, Germany)

3. Methods

1. Preliminary study on surface modification of starch grains by coating with stearic acid using supercritical fluid technology

Possibility of application of supercritical fluid technology with RESS process in coating of starch grains with stearic acid was investigated. A schematic diagram of the RESS apparatus (Model SFE-400, SUPELCO INC., Bellefonte, Pennsylvania, USA) is illustrated in Figure 3-1. The amount of corn starch (2.0 grams) was mixed with 1.0 gram of stearic acid and introduced carefully into the 10 mL extraction vessel in order to avoid dusting and compaction, and insert into oven. Liquefied carbon dioxide was charged to a high pressure pump, compressed up to 4500 psi, heated to 60 °C and delivered to the 10 mL extraction vessel for 40 minutes of circulation time, then depressurizing the fluid after 20 minutes of equilibration time. After depressurizing, the 10 mL extraction vessel was kept in the dessicator for 24 hours. The coated starches were collected from vessel into the appropriate sample bottle and then kept in the dessicator for further characterization.

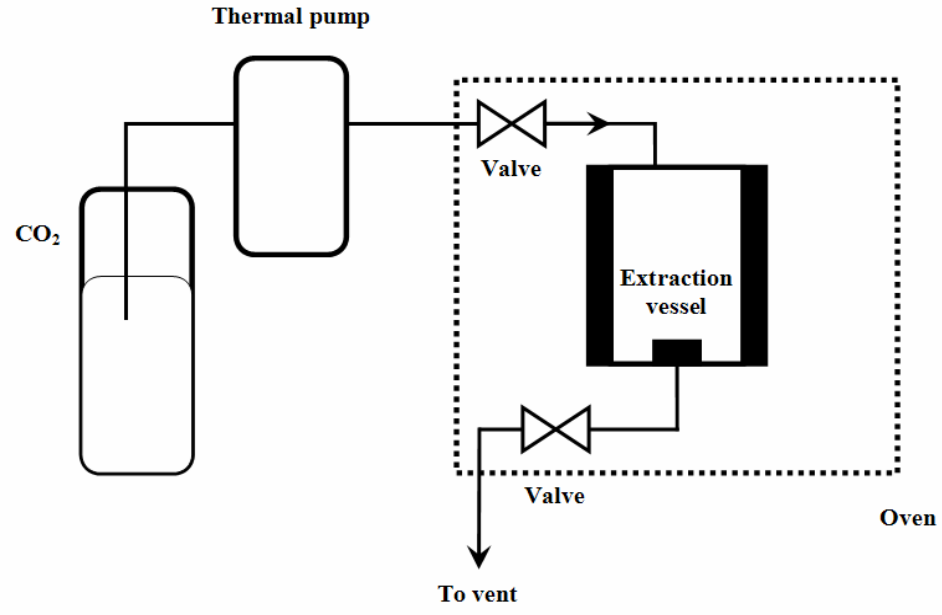

Figure 3-1 Schematic diagram of RESS apparatus

2. Effect of temperature and pressure on the surface modification of starch grains

The coated starches were prepared using procedure from section (1) to investigate the effect of temperature and pressure on the surface modification of starch grains. The pressures and temperatures of the process were varied as presented in Table 3-1, while ratio of corn starch and stearic acid with total weight of 3.0 grams at ratio of 2.0:1.0 grams, circulation time for 40 minutes and equilibration time for 20 minutes were kept constant.

Table 3-1 Formation codes with pressures and temperatures used for RESS-N process

Formulation	Pressure (psi)	Temperature (°C)
AA_46	4500	60
AA_45	4500	50
AA_44	4500	40
AA_36	3000	60
AA_35	3000	50
AA_34	3000	40
AA_16	1500	60
AA_15	1500	50
AA_14	1500	40

3. Effect of corn starch and stearic acid ratios on the surface modification of starch grains

The coated starches were prepared using procedure as described in section (1) and optimum conditions from the study in section (2) were used to investigate the effect of corn starch and stearic acid ratios on the surface modification of starch grains. The different weight ratios of corn starch and stearic acid and operation parameters are shown in Table 3-2 and 3-3, respectively.

Table 3-2 Different weight ratios of corn starch and stearic acid with total weight of 3.00 grams

Formulation	Corn starch (g)	Stearic acid (g)	Ratio (g)
BB_36	2.20	0.80	1 : 0.36
CC_36	2.40	0.60	1 : 0.25
DD_36	2.60	0.40	1 : 0.15
EE_36	2.80	0.20	1 : 0.07
FF_36	2.85	0.15	1 : 0.05
GG_36	2.90	0.10	1 : 0.03
HH_36	2.95	0.05	1 : 0.02

Table 3-3 Operation parameters used for coated starches preparation

Operation parameters	Level
Pressure	3000 psi
Temperature	60 °C
Circulation time	40 minutes
Equilibration time	20 minutes

4. Physical characterization of raw materials and/or coated starches

Powder samples were characterized based on the physical properties of shape, surface topography, mean size, size distribution, moisture content and sorption, powder flowability and densities. The different techniques used for characterization included image analysis, laser light diffraction, loss on drying (LOD) using a halogen moisture balance, gravimetric vapour sorption analysis, Karl Fischer titration, tapped density and pycnometry measurement. These techniques are briefly described in the following sections.

4.1 Morphology Observation

The shape, size and surface topography of uncoated corn starch, stearic acid and coated starches (formulation EE_36, GG_36 and HH_36) were determined by scanning electron microscope (SEM; Model JSM-5410LV, JEOL Ltd., Tokyo, Japan). Samples were mounted on SEM stub with double-sided adhesive tape and

coated with gold by gold sputtering technique prior SEM examination. Scanning electron micrographs of corn starch, stearic acid and coated starches were taken in different magnifications of x100, x500, x5000 and x7500 at 15 kV.

4.2 Particle Size and Size Distribution

The particle size and size distribution of uncoated corn starch, stearic acid and coated starches (formulation EE_36, GG_36 and HH_36) were measured by laser light scattering technique (Model Mastersizer 2000, Malvern Instruments Ltd., Worcestershire, UK). Prior to each measurement, the powder samples were suspended in 2% (wt/vol) TWEEN 80. The suspension samples were dispersed in 2% (wt/vol) TWEEN 80 for measurement. All measurements were repeated three times for each powder materials and a mean particle size distribution was calculated. It is important to note that diameters from the laser diffraction method are calculated assuming spherical particles, so incorrect values may be obtained for irregular or needle-shaped particles. Thus the size distribution for all the test powders was checked by image analysis using a scanning electron microscope, as discussed in section 4.1.

4.3 Moisture Content

The moisture content by weight of uncoated corn starch both before and after drying at 70 °C for 3 hours was determined using Halogen Moisture Analyzer (Model HR83, METTLER TOLEDO, Schwerzenbach, Switzerland). The analyzer consists of a halogen heating unit, a sample plate and an electronic weighing balance. The instrument works on the thermogravimetric principle: the moisture analyzer determines the weight of the sample at the start. About 2.5 grams of the uncoated corn starch were accurately weighed and uniformly spread as thin layer on an aluminium plate. Then, the sample is then quickly heated approximately 105 °C by the integral halogen heating module and the moisture vaporizes. During the drying process, the instrument continually measures the weight of the sample and displays the reduction in moisture. Once the drying has been completed as indicated by no further reduction in sample weight, the moisture or solids content of the sample is displayed as the final result. The moisture content in terms of loss on drying (LOD) was calculated automatically. The measurements were carried out in triplicate and an average value was determined.

4.4 Gravimetric Vapour Sorption Analysis

The vapour sorption of uncoated corn starch and coated starches (formulation EE_36, GG_36 and HH_36) were carried out gravimetrically using Dynamic Vapour Sorption apparatus (Model DVS INTRINSIC, Surface Measurement Systems Ltd., London, United Kingdom). About 5 milligrams of sample powders were accurately weighed into the stainless steel pan and analyzed to determine the percentage of mass change of sample. Prior to each experiment, 0% relative humidity was carried out by exposing the powder sample to dry nitrogen flowing environment during one hour in order to stabilize the sample mass. The required humidity is achieved by mixing dry and water-vapour-saturated nitrogen gas flows, with the help of flow controllers, before they enter the chambers. Using this method of obtaining humidified gas can achieve relative humidity value to 75% RH at 25 °C. The system was considered to reach equilibrium if the rate of change in mass was less than 0.002% (dm/dt inferior to 0.002%/minute) at 75% RH. The percentage of mass change of three aliquots of each sample was determined in this way, and the mean and standard deviation were calculated.

4.5 Determination of Moisture Absorption Property

The total water content of uncoated corn starch and coated starches (formulation EE_36, GG_36 and HH_36) before and after exposed to 75% RH for 0, 7, 14, 21, 28, 35 and 42 days at room temperature were determined using Karl Fischer Volumetric Titrator (Model AF8, ORION, Houston, Texas, USA). About 10 milligrams of each sample was accurately weighed into the titration vessel and analyzed to determine the % (wt/wt) water content of sample. The total water content of three aliquots of each sample was determined in this way, and the mean and standard deviation were calculated.

4.6 Flow Rate

Accurately weighed amount of 25 grams of the uncoated corn starch, stearic acid and coated starches (formulation EE_36, GG_36 and HH_36) were introduced carefully into the dry glass funnel in order to avoid dusting and compaction with orifice diameter of 1.2 centimeters fixed on the clamp in a strictly vertical position and height 8.5 centimeters from the floor. The funnel was unblocked and the time the entire powder needed to flow out of the funnel measured. The flow

rate was averaged from three determinations and expressed in gram per seconds of sample.

4.7 Angle of Repose

The device used to measure the static angle of repose in the current study consisted of a glass conical funnel. The angle of repose (α) was measured from a heap built up by falling of 25 grams of the uncoated corn starch, stearic acid and coated starches (formulation EE_36, GG_36 and HH_36) through the dry glass funnel with an outlet diameter of 1.2 centimeters and fixed on a metal stand. The funnel outlet was kept at a height of 8.5 centimeters above the base. Average result from three determinations was reported. The angle of repose was calculated from the following equation:

$$\alpha = \tan^{-1} \frac{h}{r}$$

in which "*h*" is the height of powder samples and "*r*" is the radius of shallow petri dish.

4.8 Bulk Density, Tapped Density and Compressibility Index

The bulk densities (ρ_b) of uncoated corn starch, stearic acid and coated starches (formulation EE_36, GG_36 and HH_36) were determined by pouring 10 grams of the powder samples into a 50 milliliters graduated cylinder and measuring the volume of samples. The graduated cylinder was tapped on a Jolting Volumeter (Modified by Department of Manufacturing Pharmacy, Faculty of Pharmaceutical Sciences, Chulalongkorn University, Thailand) until a constant volume was obtained. This was taken as the tapped volume which was used for calculating the tapped densities (ρ_t). All measurements were done in triplicate and an average value was reported. The bulk and tapped densities were used to calculate the Carr's compressibility index (Carr's CI) to provide a measure of the flow properties and compressibility of powders as presented in Table 3-4. The Carr's CI was calculated as following equation:

$$\% \text{ Compressibility} = \left[\frac{\rho_t - \rho_b}{\rho_t} \right] x 100$$

Table 3-4 Flow property and corresponding flowability parameters (USP 30)

Flow Property	Angle of Repose (°)	Compressibility Index (%)
Excellent	≤ 30	≤ 10
Good	31-35	11-15
Fair	36-40	16-20
Passable	41-45	21-25
Poor	46-55	26-31
Very poor	56-65	32-37
Very very poor	> 66	> 38

4.9 Apparent Density

The apparent densities of uncoated corn starch, stearic acid and coated starches were determined using helium gas displacement pycnometer (Model Ultrapycnometer 1000, QUANTACHROME INSTRUMENTS, Florida, USA). The small amount of uncoated corn starch, stearic acid and coated starches approximately 0.5-1.0 grams was weighed into a micro cell. The apparent densities were averaged from five determinations and were reported in term of g/cm^3.

5. Physicochemical characterization of raw materials and coated starches

5.1 Differential Scanning Calorimetry (DSC)

DSC analysis of uncoated corn starch, stearic acid, coated starches (formulation EE_36, GG_36 and HH_36), and the physical mixtures of corn starch and stearic acid at different weight ratios were carried out using differential scanning calorimeter (Model DSC822^e, METTLER TOLEDO, Schwerzenbach, Switzerland). The small amount of uncoated corn starch, stearic acid, coated starches (formulation EE_36, GG_36 and HH_36), and the physical mixtures of corn starch and stearic acid at different weight ratios of approximately 5 milligrams were weighed into a 40 µl aluminum pan. DSC sample pans were sealed with aluminum piece by hermetically sealed and placed in sample holder of DSC822^e instrument with an empty pan as a

reference. Samples were heated from 25 to 250 °C at a heating rate 5 °Cmin^{-1} under a protective nitrogen atmosphere at a flow rate 60 mLmin^{-1}.

5.2 Thermogravimetric Analysis (TGA)

The TG curves of uncoated corn starch, stearic acid, coated starches (formulation EE_36, GG_36 and HH_36), and the physical mixtures of corn starch and stearic acid at different weight ratios were performed using thermogravimetric analyzer (Model TGA/SDTA851^{e}, METTLER TOLEDO, Schwerzenbach, Switzerland). The small amount of uncoated corn starch, stearic acid, coated starches, and the physical mixtures of corn starch and stearic acid at different weight ratios approximately 5 milligrams were weighed into aluminum pan 70 µl and placed in sample holder of TGA/SDTA851^{e} instrument. Samples were heated from 25 to 250 °C at a heating rate 5 °Cmin^{-1} under a protective nitrogen atmosphere at a flow rate 50 mLmin^{-1}.

5.3 X-ray Powder Diffractometry (XRPD)

The XRPD patterns of uncoated corn starch (formulation EE_36, GG_36 and HH_36), stearic acid, coated starches, and the physical mixtures of corn starch and stearic acid at different weight ratios were carried out using the X-ray diffractometer (Model D8-Discover, Bruker AXS, Karlsruhe, Germany) equipped with a Ni-filtered Cu-Kα radiation at 40 kilovolts and 40 milliamps. The X-ray source had a wavelength of 1.542 Å and the diffraction patterns were recorded at Bragg angles (2θ) of 5° to 50° with scanning speed, step angle and step time were 0.2 sec/step, 0.0188° and 96 seconds, respectively at room temperature.

5.4 Fourier Transform Infrared (FT-IR) Spectroscopy

The FT-IR spectra of uncoated corn starch, stearic acid, coated starches (formulation EE_36, GG_36 and HH_36), and the physical mixtures of corn starch and stearic acid at different weight ratios were determined by FT-IR spectrometer (Model Spectrum One, Perkin Elmer Ltd., Massachusetts, USA). The powder samples were blended with potassium bromide and laminated. The FT-IR spectra were investigated in the wave number range from 4000 to 450 cm^{-1}. The scanning and scanning resolution was 16 times and 4.0 cm^{-1}, respectively.

6. Evaluation of coated starches used as lubricant in tabletting process

The coated starches were applied as lubricant in tabletting process in comparison with conventional lubricants. The compositions of tablet for each formulation are shown in Table 3-5 and 360 milligrams per tablet was prepared using direct compression technique. The various direct compression diluents were weighed and mixed in plastic bag for 10 minutes. Corn starch, coated starches (formulation EE_36, GG_36 and HH_36), stearic acid through SCT at critical pressure of 3000 psi and critical temperature of 60 ^{o}C (SS_36), stearic acid through an 80-mesh sieve (SA_80) and magnesium stearate for using as lubricant of each formulation were added and mixed for 2 minutes. Powder mixes were compressed using a single punch tablet press (Model PMA 3, KORSCH America Inc., Massachusetts, USA) and 3/8-inch beveled edge punch. The compression force of each formulation was adjusted to obtain an upper punch force of 25, 30 and 35 kilonewtons.

Table 3-5 Compositions of tablet for each formulation code

Ingredients	Formulation							
	BL (%)	**CS (%)**	**EE (%)**	**GG (%)**	**HH (%)**	**SS (%)**	**SA (%)**	**MG (%)**
Spray-dried lactose	87.5	86.5	86.5	86.5	86.5	86.5	86.5	86.5
Microcrystalline cellulose (PH 102)	10.0	10.0	10.0	10.0	10.0	10.0	10.0	10.0
Corn starch	0	1.0	0	0	0	0	0	0
EE_36	0	0	1.0	0	0	0	0	0
GG_36	0	0	0	1.0	0	0	0	0
HH_36	0	0	0	0	1.0	0	0	0
SS_36	0	0	0	0	0	1.0	0	0
SA_80	0	0	0	0	0	0	1.0	0
Magnesium stearate	0	0	0	0	0	0	0	1.0
Talcum	2.0	2.0	2.0	2.0	2.0	2.0	2.0	2.0
Silicon dioxide	0.5	0.5	0.5	0.5	0.5	0.5	0.5	0.5

6.1 Characterization of Powder Mixes Before Tabletting

6.1.1 Flow Rate

The amounts of about 40 grams for each formulation were characterized using procedure as described in section 4.6 to investigate the flowability of powder mixtures.

6.1.2 Angle of Repose

The amounts of about 40 grams for each formulation were characterized using procedure from section 4.7 to investigate the angle of repose of powder mixtures.

6.1.3 Bulk Density, Tapped Density and Compressibility Index

The amounts of about 25 grams for each formulation were characterized using procedure as described in section 4.8 to investigate the bulk densities, tapped densities and Carr's compressibility index of powder mixtures.

6.2 Characterization of Tablet Properties

6.2.1 Tablet Hardness, Thickness and Diameter

The hardness, thickness and diameter of tablets (n=20) were determined using the tablet hardness tester (Model DHT-250, THERMONIK, Mumbai, India). The mean and standard deviation of twenty determinations for each formulation were calculated.

6.2.2 Tablet Friability

The tablet friability (n=20) was determined according to the USP30 using the tablet friability tester (Model TAR 10, ERWEKA GmbH, Heusenstamm, Germany) at a speed of 25 rpm for 4 minutes. The percentage weight loss was expressed as the tablet friability.

6.2.3 Disintegration Time of Tablet

The disintegration time of tablets (n=6) were evaluated according to the USP30 using the disintegration apparatus (Model ZT 31, ERWEKA GmbH, Heusenstamm, Germany). The apparatus was operated using deionized water as the immersion fluid maintained at a temperature of 37 ± 2 °C during the test. The mean and standard deviation of six determinations for each formulation were calculated.

CHAPTER IV

RESULTS AND DISCUSSION

1. Investigation of surface modification of starch grains by adsorption of stearic acid using supercritical fluid technology

In this study, the surface of corn starch grains were modified by coating with stearic acid using SCT by application of RESS-N process. Stearic acid is practically insoluble in water but freely soluble in benzene, carbon tetrachloride, chloroform and ether, and soluble in ethanol, hexane and propylene glycol. The melting point of stearic acid is reported at about 60 °C (Allen, 1994). CO_2 is a nonpolar solvent. The critical temperature and pressure for carbon dioxide is 31.1°C and 1070 psi, respectively. A common rule of thumb is that if a compound dissolves in hexane, then that compound should be also dissolved in $scCO_2$ (Subramaniam *et al*., 1997). Kramer and Thodos (1989) studied the solubility of 1-octadecanol [$CH_3(CH_2)_{16}CH_2OH$] and stearic acid [$CH_3(CH_2)_{16}COOH$] in dense $scCO_2$ using temperatures of 318, 328 and 338 K, and pressures ranging from 140 to 467 bar. It was found that stearic acid could be solubilized in $scCO_2$, which a maximum solubility occured at temperature of 318 K (45 °C) and pressure around 280-300 bar (4061.06-4351.13 psi). Also a first preliminary investigation of surface modification was performed by using ratio of corn starch and stearic acid of 2.0:1.0 grams with total weight of 3.0 grams, pressure of 4500 psi and temperature of 60 °C. Before the liquid CO_2 passed into the 10 mL extraction vessel, it was pressurized to the desired pressure and heated to the specified temperature by the means of a pump to reach the supercritical state. After the pressurization, $scCO_2$ was delivered into the extraction vessel containing corn starch and stearic acid inside for 20 minutes (circulation time). The pressure of $scCO_2$ dropped about 200 psi after $scCO_2$ was delivered into the extraction vessel but $scCO_2$ was pressurized again to the desired pressure within about 1 minute. After completion of the circulation time, the thermal pump was closed and $scCO_2$ was equilibrated in the extraction vessel for 20 minutes (equilibration time). $scCO_2$ was then released out the extraction vessel. After processing, the extraction

vessel with coated starch inside was kept in the dessicator for 24 hours. It was found that the flake of stearic acid still remained.

So, a second preliminary investigation of surface modification was performed by using the same ratio of corn starch and stearic acid, conditions of pressure and temperature, and equilibration time but the circulation time was increased from 20 to 40 minutes. After surface modification, this coated starch was kept in the dessicator for 24 hours. It was found that no flake of stearic acid remained.

Furthermore, the effects of pressure and temperature on the surface modification of starch grains were investigated. The pressures were varied in the range form 1500, 3000 to 4500 psi and temperatures were varied in the range from 40, 50 to 60 °C, as previously shown in Table 3-1. The appearance of product obtained is presented in Table 4-1. It was found that formulation AA_46, AA_36, AA_16, AA_45, AA_35 and AA_15 gave a white cake and no flake of stearic acid remained. Formulation AA_44 and AA_34 were in white cake and the flake of stearic acid remained and formulation AA_14 after processing showed no different character of the powder before processing.

Table 4-1 Effects of pressure and temperature on the surface modification of starch grains

Formulation	Conditions		Appearance
	Pressure (psi)	Temperature (°C)	
AA_46	4500	60	no flake of stearic acid remained
AA_36	3000	60	”
AA_16	1500	60	”
AA_45	4500	50	”
AA_35	3000	50	”
AA_15	1500	50	”
AA_44	4500	40	Flake of stearic acid remained
AA_34	3000	40	”
AA_14	1500	40	Similar with raw materials

Then the optimum condition using pressure of 3000 psi and temperature of 60 °C was selected to investigate the effect of corn starch and stearic acid ratios on the surface modification of starch grains. Various ratios of corn starch and stearic acid were investigated, as previously shown in Table 3-2. The characteristic of powder obtained is presented in Table 4-2. It was found that Formulation BB_36, CC_36 and DD_36 were in white cake and without the flake of stearic acid but the cohesiveness of white cake reduced, when compared with the corn starch and stearic acid ratio of 2.0:1.0 grams. This result was due to the corn starch and stearic acid ratio of formulation BB_36, CC_36 and DD_36 were reduced. Formulation EE_36, FF_36, GG_36 and HH_36 were in white powder with some agglomerate and no flake of stearic acid remained.

Table 4-2 Effect of corn starch and stearic acid ratios on the surface modification of starch grains

Formulation	Ratio of corn stach and stearic acid	Appearance	Cohesiveness
BB_36	1 : 0.36	no flake of stearic acid remained	+++++++
CC_36	1 : 0.25	”	++++++
DD_36	1 : 0.15	”	+++++
EE_36	1 : 0.07	”	++++
FF_36	1 : 0.05	”	+++
GG_36	1 : 0.03	”	++
HH_36	1 : 0.02	”	+

2. Physical characterization of raw materials and/or coated starches

2.1 Morphology Observation

From the photographs of SEM, the uncoated corn starch particles are rather irregular shape and their surface is uneven with numerous small depressions or pores. Also particles with completely smooth surface are observed (Figure 4-1). The SA_ 80 (through sieving) and SS_36 (through SCT) particles are flake, but the particle size of SA_80 was larger as compared with SS_36, as shown in Figure 4-2 and 4-3, respectively.

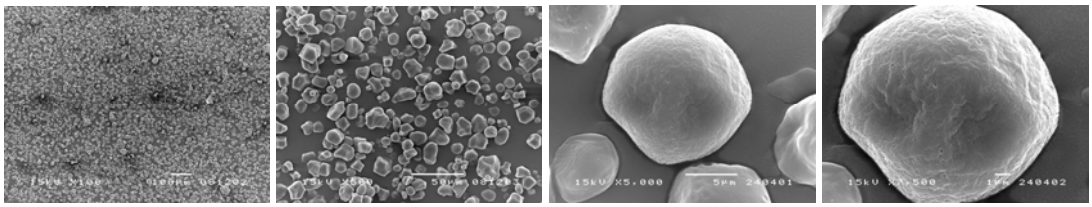

(a) (b) (c) (d)

Figure 4-1 Scanning electron photomicrograph of uncoated corn starch in magnification of (a) x100, (b) x500, (c) x5000 and (d) x7500

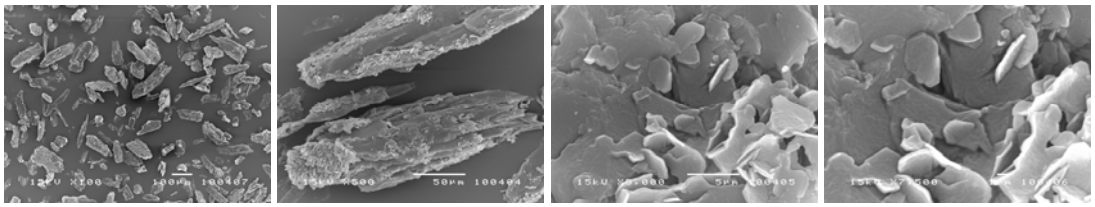

(a) (b) (c) (d)

Figure 4-2 Scanning electron photomicrograph of SA_80 (through sieving) in magnification of (a) x100, (b) x500, (c) x5000 and (d) x7500

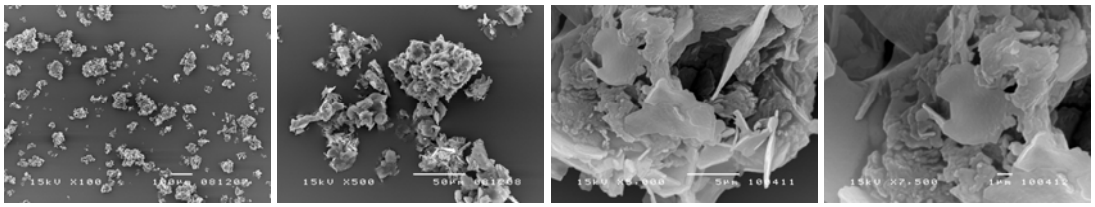

(a) (b) (c) (d)

Figure 4-3 Scanning electron photomicrograph of SS_36 (through SCT) in magnification of (a) x100, (b) x500, (c) x5000 and (d) x7500

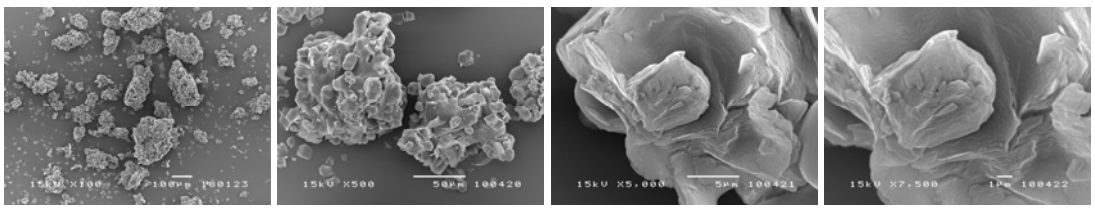

(a) (b) (c) (d)

Figure 4-4 Scanning electron photomicrograph of AA_46 in magnification of (a) x100, (b) x500, (c) x5000 and (d) x7500

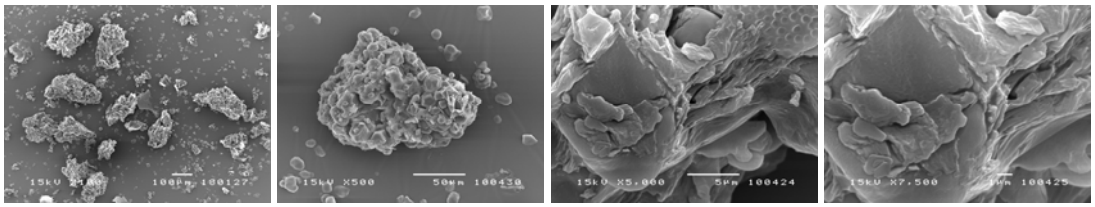

(a) (b) (c) (d)

Figure 4-5 Scanning electron photomicrograph of AA_45 in magnification of (a) x100, (b) x500, (c) x5000 and (d) x7500

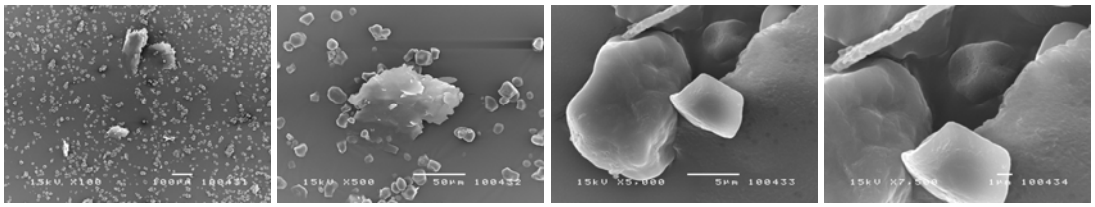

(a) (b) (c) (d)

Figure 4-6 Scanning electron photomicrograph of AA_44 in magnification of (a) x100, (b) x500, (c) x5000 and (d) x7500

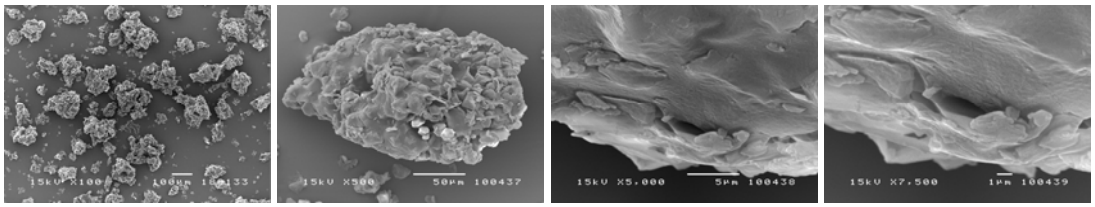

(a) (b) (c) (d)

Figure 4-7 Scanning electron photomicrograph of AA_36 in magnification of (a) x100, (b) x500, (c) x5000 and (d) x7500

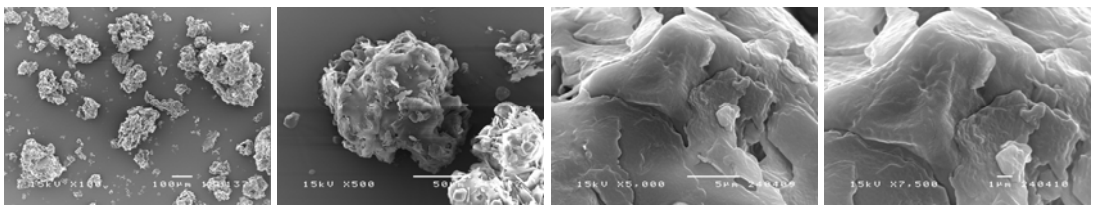

(a) (b) (c) (d)

Figure 4-8 Scanning electron photomicrograph of AA_35 in magnification of (a) x100, (b) x500, (c) x5000 and (d) x7500

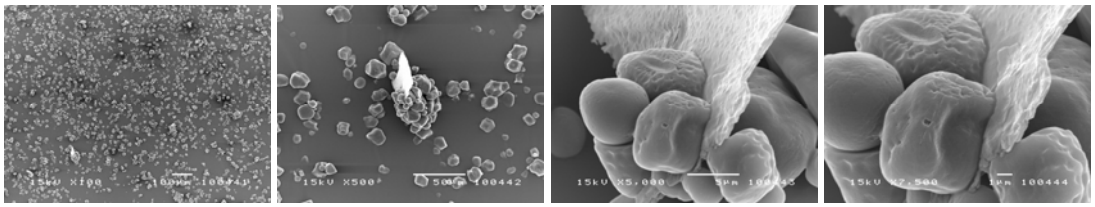

(a) (b) (c) (d)

Figure 4-9 Scanning electron photomicrograph of AA_34 in magnification of (a) x100, (b) x500, (c) x5000 and (d) x7500

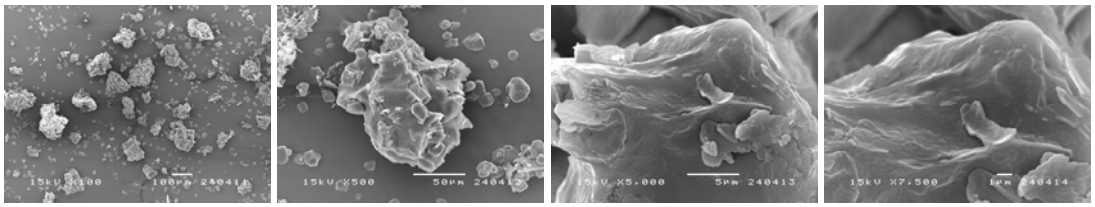

(a) (b) (c) (d)

Figure 4-10 Scanning electron photomicrograph of AA_16 in magnification of (a) x100, (b) x500, (c) x5000 and (d) x7500

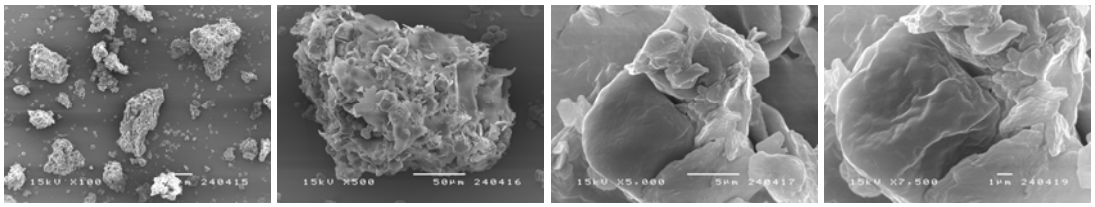

(a) (b) (c) (d)

Figure 4-11 Scanning electron photomicrograph of AA_15 in magnification of (a) x100, (b) x500, (c) x5000 and (d) x7500

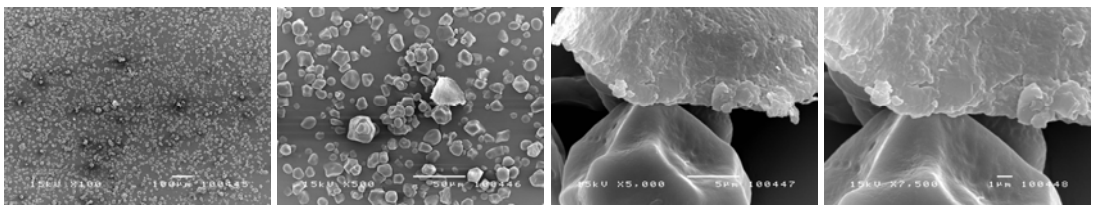

(a) (b) (c) (d)

Figure 4-12 Scanning electron photomicrograph of AA_14 in magnification of (a) x100, (b) x500, (c) x5000 and (d) x7500

SEM images of formulation AA_46, AA_45, AA_36, AA_35, AA_16 and AA_15 (Figure 4-4, 4-5, 4-7, 4-8, 4-10 and 4-11, respectively) showed that these coated starches were rather irregular shape. Stearic acid deposited onto the surface of corn starch particles, but the coated starches formed agglomerate particles. This result was due to the excessive ratio of stearic acid. Formulation AA_44, AA_34 and AA_14 were individual particles of corn starch particles and stearic acid particles, as shown in Figure 4-6, 4-9 and 4-12, respectively. This result was due to the lower temperature of supercritical carbon dioxide. Some stearic acid did not dissolve and deposite onto the surface of corn starch particles.

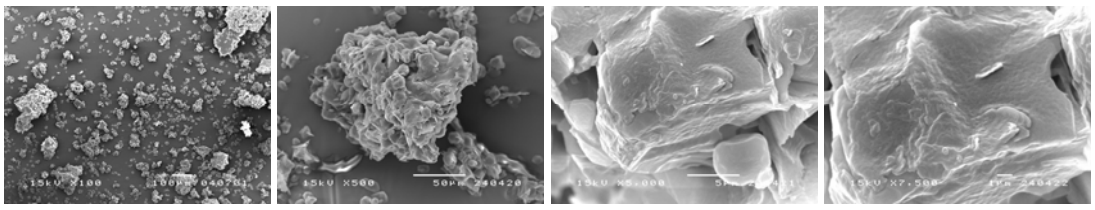

(a) (b) (c) (d)

Figure 4-13 Scanning electron photomicrograph of BB_36 in magnification of (a) x100, (b) x500, (c) x5000 and (d) x7500

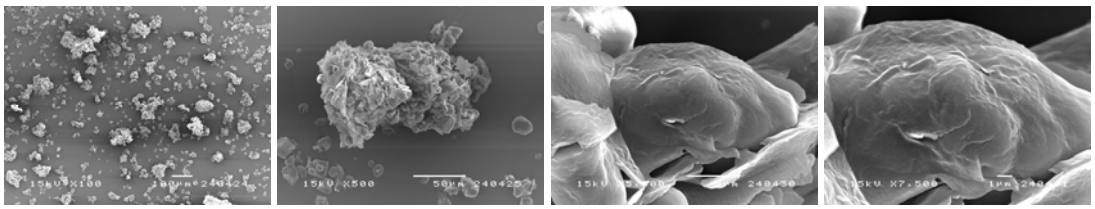

(a) (b) (c) (d)

Figure 4-14 Scanning electron photomicrograph of CC_36 in magnification of (a) x100, (b) x500, (c) x5000 and (d) x7500

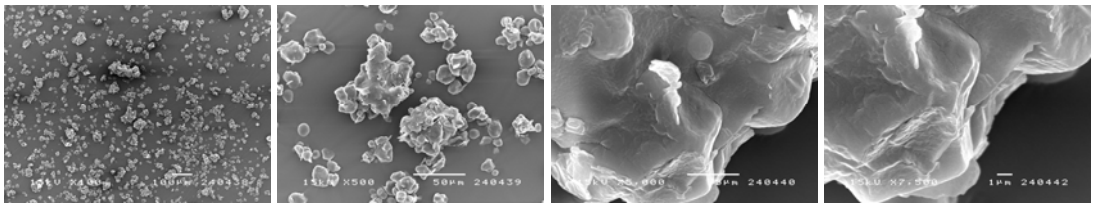

(a) (b) (c) (d)

Figure 4-15 Scanning electron photomicrograph of DD_36 in magnification of (a) x100, (b) x500, (c) x5000 and (d) x7500

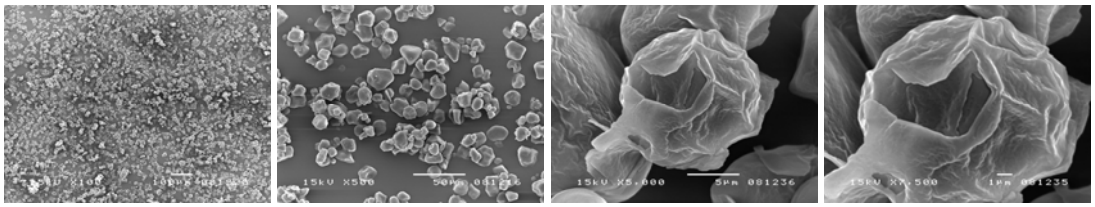

(a) (b) (c) (d)

Figure 4-16 Scanning electron photomicrograph of EE_36 in magnification of (a) x100, (b) x500, (c) x5000 and (d) x7500

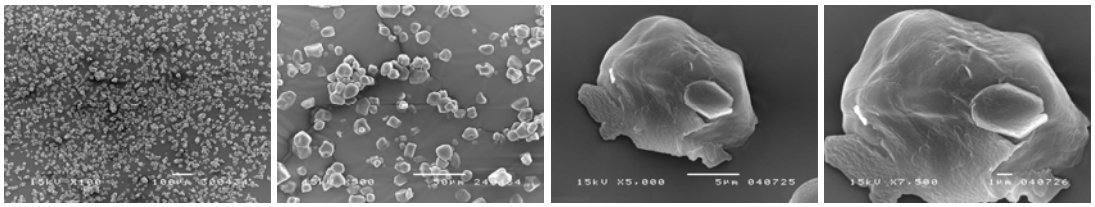

(a) (b) (c) (d)

Figure 4-17 Scanning electron photomicrograph of FF_36 in magnification of (a) x100, (b) x500, (c) x5000 and (d) x7500

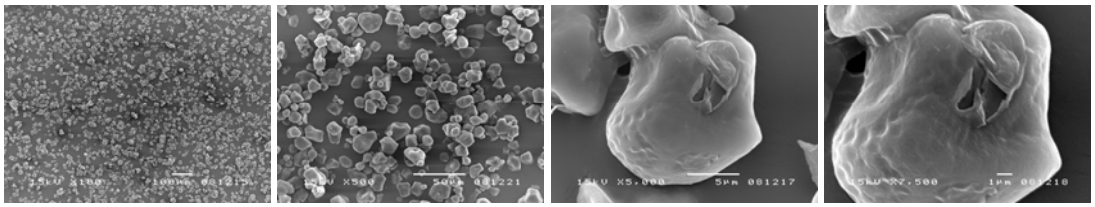

(a) (b) (c) (d)

Figure 4-18 Scanning electron photomicrograph of GG_36 in magnification of (a) x100, (b) x500, (c) x5000 and (d) x7500

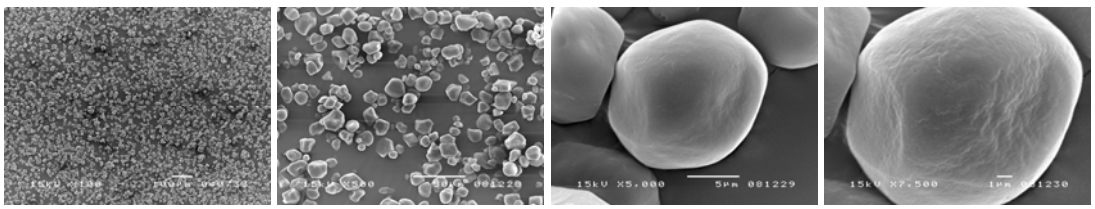

(a) (b) (c) (d)

Figure 4-19 Scanning electron photomicrograph of HH_36 in magnification of (a) x100, (b) x500, (c) x5000 and (d) x7500

SEM images of formulation BB_36, CC_36 and DD_36 (Figure 4-13, 4-14 and 4-15, respectively) shows that these coated starches were rather irregular shape. Stearic acid deposited onto the surface of corn starch particles. The coated starches were in agglomerate particles but the agglomerate particles of formulation BB_36, CC_36 and DD_36 were in lower degree as compared with those formulations AA, which using the corn starch and stearic acid ratio of 2.0:1.0 grams. This result was due to the corn starch and stearic acid ratio of formulation BB_36, CC_36 and DD_36 were reduced (Table 3-2). Formulation EE_36, FF_36 and GG_36 were discrete particles and no agglomerate was formed because of the suitable reduction in ratio of corn starch and stearic acid. The corn starch and stearic acid ratio of formulation EE_36, FF_36 and GG_36 were 2.80:0.20, 2.85:1.50 and 2.90:1.00 grams, respectively. SEM images of formulation EE_36, FF_36 and GG_36 (Figure 4-16, 4-17 and 4-18, respectively) indicate that stearic acid would form a thin film deposited onto the surface of corn starch grains, but the distribution of stearic acid on the surface of starch grains might not be uniform. Formulation HH_36 (Figure 4-19) shows that stearic acid deposited onto the surface of starch grains formed a thin, uniform and smooth film, because it had probably suitable percentage amount of stearic acid as compared with other formulations, as shown in Table 3-2. After surface modification, formulation EE_36, GG_36 and HH_36 were selected for further characterization because coated starches were discrete particles and no agglomerate, and stearic acid was deposited onto the surface of corn starch particles.

2.2 Particle Size and Size Distribution

The particle size and size distribution of uncoated corn starch, stearic acid (both SA_80 and SS_36) and coated starches (formulation EE_36, GG_36 and HH_36) were determined by laser light diffraction technique and the results are presented in Table 4-3.

The particle size of coated starches (formulation EE_36, GG_36 and HH_36) were relatively larger as compared with uncoated corn starch, but both uncoated corn starch and coated starches had the narrow particle size distribution. It was corresponding with the results obtained from SEM, as shown in Figure 4-1, 4-16, 4-18 and 4-19. The uncoated corn starch particles had the mean volume diameter (D [4, 3]) of 16.73±0.02 μm, whereas the coated starch particles of formulation EE_36, GG_36 and HH_36 had the longer mean volume diameter of 19.35±0.13, 18.00±0.19

and 16.75±0.01 µm, respectively. The standard deviation given for the mean volume diameter was calculated on the basis of three particles size measurements performed on the same sample. Considering both standard deviations of uncoated and of coated particles, it appears that the coated samples get a longer diameter than the uncoated ones. This may be due to the deposition of the stearic acid film on the corn starch particles. This assumption was verified by SEM investigations. In addition, the particle size of SA_80 was larger as compared with SS_36, but both SA_80 and SS_36 had the wide particle size distribution. The particle size of SA_80 and SS_36 were 84.52±0.05 and 22.47±0.04 µm, respectively.

Table 4-3 Particle size and size distribution of uncoated corn starch, stearic acid and coated starches [average (SD)]

Sample name	*d* (*v*, 0.1) µm	*d* (*v*, 0.5) µm	*d* (*v*, 0.9) µm	*D* [4, 3] µm	Span	Uniformity
Corn starch	8.34 (0.01)	16.27 (0.01)	26.73 (0.03)	16.73 (0.02)	1.13 (0.00)	0.36 (0.00)
SA_80	14.52 (0.05)	68.43 (0.12)	173.10 (0.05)	84.52 (0.05)	2.32 (0.02)	0.72 (0.01)
SS_36	2.72 (0.08)	20.44 (0.06)	44.38 (0.03)	22.47 (0.04)	2.03 (0.00)	0.62 (0.00)
EE_36	9.18 (0.14)	16.56 (0.15)	32.62 (0.56)	19.35 (0.13)	1.56 (0.01)	0.54 (0.01)
GG_36	8.91 (0.17)	16.33 (0.10)	29.93 (0.24)	18.00 (0.19)	1.41 (0.02)	0.48 (0.01)
HH_36	8.66 (0.12)	16.30 (0.02)	26.76 (0.02)	16.75 (0.01)	1.56 (0.00)	0.42 (0.00)

Note: - *d* (*v*, 0.5) is the size at which 50% of the sample is smaller and 50% is larger (mass median diameter).

- *d* (*v*, 0.1) and *d* (*v*, 0.9) are the size of particle below which 10% and 90% of the sample lies, respectively.

- *D* [4, 3] is the mean volume diameter.

- The span is the measurement of the width of the distribution, defined as the differences between the diameter at the 90 and the 10 percentage points relative to the median diameter. ((*D*90 −*D*10)/*D*50)

- The uniformity is a measure of the absolute deviation from the median.

2.3 Moisture Content

The moisture content of uncoated corn starch was presented in terms of loss on drying (%LOD). The moisture contents of uncoated corn starch both before and after drying at 70 °C for 3 hours were 11.85±0.09 and 8.51±0.33%, respectively.

2.4 Gravimetric Moisture Sorption Analysis

The percentages of mass change of uncoated corn starch and coated starches (formulation EE_36, GG_36 and HH_36) when exposed to 75% RH at 25 °C were determined using a DVS apparatus (Figure 4-20). The percentages of mass change of uncoated corn starch, formulation EE_36, GG_36 and HH_36 before exposed to 75% RH were 100 %. The percentage of mass change when exposed to 75% RH was found to be lower for coated starches as compared with uncoated corn starch. The coated starch of EE_36 was the lowest percentage of mass change of 105.38±0.01%, whereas formulation GG_36 and HH_36 were the higher percentage of mass change of 106.10±0.07 and 107.35±0.00%, respectively. The uncoated corn starch was the highest percentage of mass change of 115.06±0.05 %.

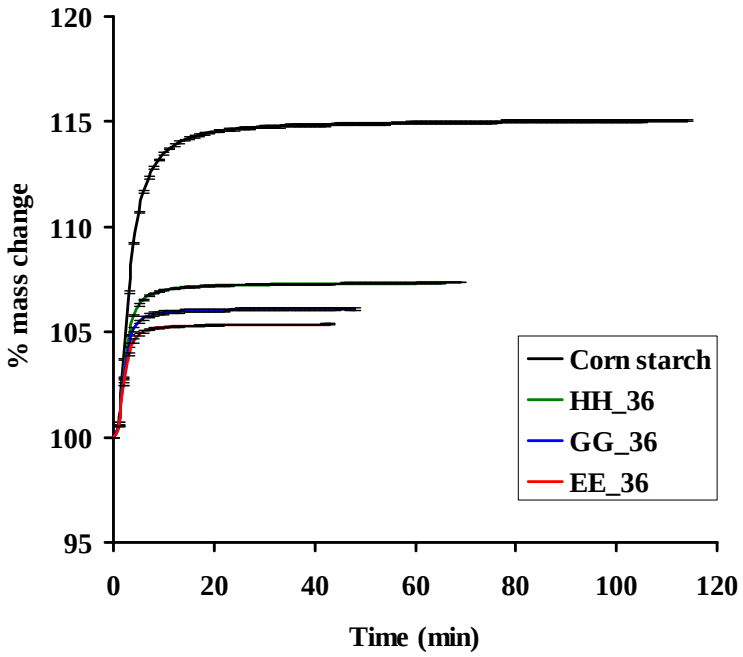

Figure 4-20 Percentage of mass change of uncoated corn starch and coated starches when exposed to 75% RH at 25 °C

Similarly, the times of saturation moisture sorption after exposure of coated starches (formulation EE_36, GG_36 and HH_36) were lower as compared with uncoated corn starch. Formulation EE_36 gave the shortest time of saturation moisture sorption of 42.67±0.58 minutes, whereas GG_36 and HH_36 gave the longer time of saturation moisture sorption of 47.33±1.15 and 69.33±1.53 minutes, respectively. The uncoated corn starch showed the longest time of saturation moisture

sorption of 114.33±4.51 minutes. Based on these results obtained, the ratio of stearic acid increased, the percentages of mass change and the times of saturation moisture sorption of coated starches were lower. It is indicated that the coating stearic acid on starch grains could prevent moisture absorption into the starch grains, which confirmed that the stearic acid film was formed on the surface of corn starch particles. This result shows a significant improvement in the moisture resistance of starch grains via the surface modification with the RESS-N process.

2.5 Determination of Moisture Absorption Property

The percentages of total water content of uncoated corn starch and coated starches (formulation EE_36, GG_36 and HH_36) before and after exposure to 75% RH for 0, 7, 14, 21, 28, 35 and 42 days at room temperature are presented in Figure 4-21.

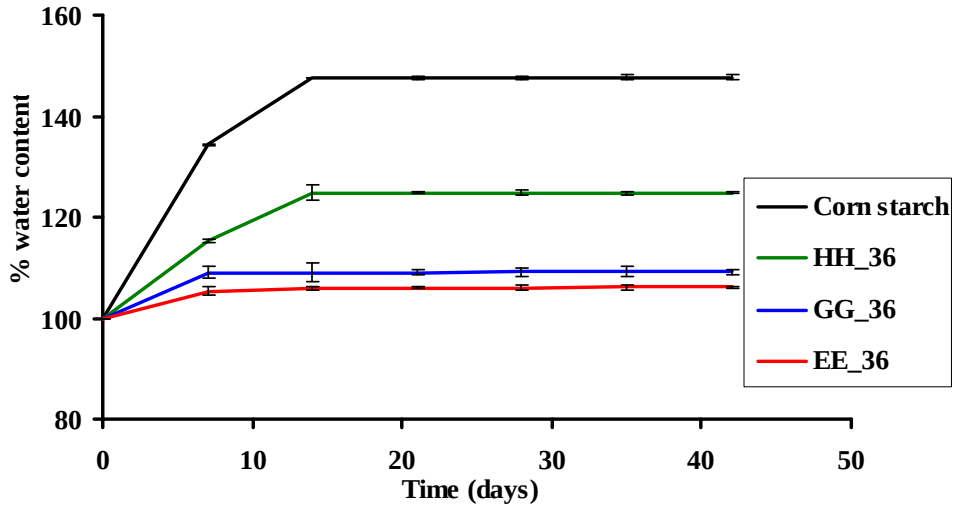

Figure 4-21 Percentage of total water content of uncoated corn starch and coated starches before and after long exposure to 75% RH for 0, 7, 14, 21, 28, 35 and 42 days at room temperature

The percentages of total water content of uncoated corn starch, formulation EE_36, GG_36 and HH_36 before long exposure to 75% RH were 100%. The percentage of total water content after long exposure to 75% RH for 42 days was found to be lower for coated starches (formulation EE_36, GG_36 and HH_36) as compared with uncoated corn starch. Formulation EE_36 was the lowest percentage of total water content of 106.09±0.11 %, whereas formulation GG_36 and HH_36 had

higher percentage of total water content of 109.17±0.57 and 124.86±0.13 %, respectively. The uncoated corn starch had the highest percentage of total water content of 147.71±0.42 %. Based on the results obtained, the percentages of total water content of coated starches were reduced when the ratio of stearic acid increased, the result using the Karl Fischer method was corresponding with the results obtained from the gravimetric moisture sorption analysis.

2.6 Flow Rate

The flow rates of uncoated corn starch, stearic acid (both SA_80 and SS_36) and coated starches (formulation EE_36, GG_36 and HH_36) are presented in Table 4-4. It was found that the flow rate of all powder samples are not available due to all powder samples did not flow out of the funnel, which could produce particulate arching or bridging over the orifice opening nearest to the funnel's central section.

Sometimes, powder arching or bridging are formed at the funnel, leading to intermittent flow or a no flow scenario. Arching can form in bulk solids because of two reasons: particle interlocking or an increase in cohesive strength. Particle interlocking occurs when particles lock together mechanically at the outlet. Particles with irregular shapes have a greater chance of forming arches. Cohesive arches can form where particles bond together physically, chemically or electrostatically.

Table 4-4 Flow rate, angle of repose, bulk and tapped density, compressibility index and apparent density of uncoated corn starch, stearic acid and coated starches [average (SD)]

Sample name	Flow rate (g/sec)	Angle of repose (°)	Bulk density (g/cm^3)	Tapped density (g/cm^3)	Compressibility Index (%)	Apparent density (g/cm^3)
Corn starch	N/A	N/A	0.47 (0.01)	0.75 (0.01)	36.89 (0.49)	1.5044 (0.0021)
SA_80	N/A	N/A	N/A	N/A	N/A	1.0144 (0.0025)
SS_36	N/A	N/A	N/A	N/A	N/A	0.8312 (0.0034)
EE_36	N/A	N/A	0.31 (0.00)	0.50 (0.01)	37.84 (0.81)	1.4538 (0.0020)
GG_36	N/A	N/A	0.34 (0.00)	0.55 (0.00)	37.47 (0.22)	1.4835 (0.0024)
HH_36	N/A	N/A	0.36 (0.00)	0.58 (0.01)	37.46 (0.75)	1.5013 (0.0072)

Note: N/A means not available

2.7 Angle of Repose

The angle of reposes of uncoated corn starch, stearic acid (both SA_80 and SS_36) and coated starches (formulation EE_36, GG_36 and HH_36) are presented in Table 4-4. It was found that the angle of repose of all powder samples are not available due to all powder samples did not flow out of the funnel, as described in section 2.6.

2.8 Bulk Density, Tapped Density and Compressibility Index

The bulk densities, tapped densities and Carr's CI of uncoated corn starch, stearic acid (both SA_80 and SS_36) and coated starches (formulation EE_36, GG_36 and HH_36) are presented in Table 4-4. The uncoated corn starch was higher bulk and tapped density as compared with coated starches. The uncoated corn starch had bulk density of 0.47±0.01 g/cm^3, whereas the coated starch of HH_36, GG_36 and EE_36 had lower bulk density of 0.36±0.00, 0.34±0.00 and 0.31±0.00 g/cm^3, respectively. Similarly, the uncoated corn starch had the tapped density of 0.75±0.01 g/cm^3, whereas the coated starch of HH_36, GG_36 and EE_36 had the lower tapped density of 0.58±0.01, 0.55±0.00 and 0.50±0.01 g/cm^3, respectively.

Flow character is classified based on compressibility index. Lower Carr's CI of a material indicates better flow properties than higher ones. The Carr's CI of ≤ 10 is considered "excellent" flow whereas CI of > 38 is considered "very very poor" flow. There are intermediate scales for the Carr's CI between 11-15 is considered "good" flow, CI between 16-20 is considered "fair" flow, CI between 21-25 is considered "passable" flow, CI between 26-31 is considered "poor" flow and CI between 32-37 is considered "very poor" flow. The uncoated corn starch was the lower Carr's CI as compared with coated starches. The uncoated corn starch had the Carr's CI of 36.89±0.49 %, whereas the coated starch of EE_36, GG_36 and HH_36 had the higher Carr's CI of 37.84±0.81, 37.47±0.22 and 37.46±0.75 %, respectively. The bulk density, tapped density and Carr's CI of stearic acid (both SA_80 and SS_36) are not available. Based on the results obtained, flowing behavior of both uncoated corn starch and coated corn starch were classified as "very poor", in terms of its flow based on the Carr's CI values. These results indicated that the ratio of stearic acid reduced, the bulk density and tapped density of coated starches were higher, and the Carr's CI of coated starches was lower, as reported in Table 4-4.

2.9 Apparent Density

The apparent density of uncoated corn starch, stearic acid (both SA_80 and SS_36) and coated starches (formulation EE_36, GG_36 and HH_36) were determined using helium gas displacement pycnometer are presented in Table 4-4. Because helium gas could penetrate into the smallest pores or crevices and was not adsorbed by the material, it was generally conceded that the helium method gave the closest approximation to true density. As shown in Table 4-4, the apparent density was found to be higher for uncoated corn starch as compared with coated starches. The uncoated corn starch had the apparent density of 1.5044±0.0021 g/cm^3, whereas the coated starch of HH_36, GG_36, EE_36, SA_80 and SS_36 had the lower apparent density of 1.5013±0.0072, 1.4835±0.0024, 1.4538±0.0020, 1.0144±0.0025 and 0.8312±0.0034 g/cm^3, respectively. The result of this experiment was found that coated starches had lower apparent density than uncoated corn starch. Because the coated starch particles were coated with stearic acid, the helium gas could not penetrate into the smallest pores or crevices.

3. Physicochemical characterization of raw materials and coated starches

3.1 Differential Scanning Calorimetry (DSC)

DSC thermograms of uncoated corn starch, stearic acid, coated starches (formulation EE_36, GG_36 and HH_36) and the physical mixtures of corn starch and stearic acid at different weight ratios of 2.80:0.20 (PE), 2.90:0.10 (PG) and 2.95:0.05 (PH) were carried out using differential scanning calorimetry and all DSC thermograms are shown in Figure 4-22. DSC thermogram of uncoated corn starch showed the water loss endothermic peak of 92.66 °C (Figure 4-22 (G) and Table 4-5) and stearic acid showed that there was only one sharp endothermic peak of 58.35 °C. The result was corresponding with its melting point (Figure 4-22 (H) and Table 4-5). The melting point of stearic acid was reported at about 60 °C (Allen, 1994). The coated starches of formulation EE_36, GG_36 and HH_36 showed combined of water loss endothermic peak of corn starch and melting endotherm of stearic acid approximately of 91-93 and 57 °C, respectively (Figure 4-22 (A) to (C)), the DSC thermogram of coated starches is similar to the DSC thermograms of physical mixture of uncoated corn starch and stearic acid, as shown in Figure 4-22 (D) to (F). DSC thermograms of the coated starches and the physical mixture of uncoated corn starch and stearic acid exhibited similar patterns but significant difference of the sharp

endothermic peak of stearic acid. The results of this experiment indicated that the ratio of stearic acid reduced, the sharp endothermic peak of stearic acid became lower.

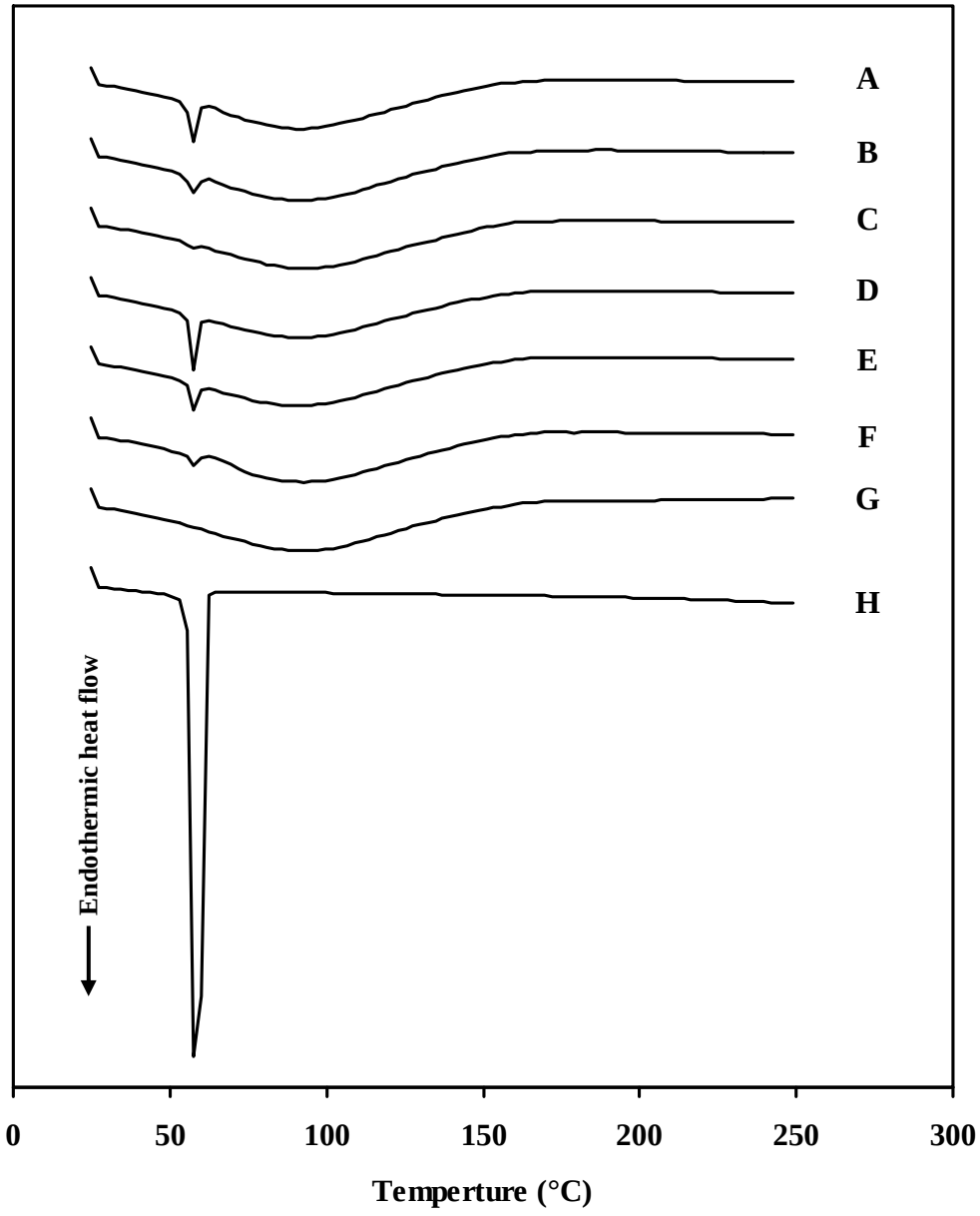

Figure 4-22 DSC thermograms of (A) EE_36, (B) GG_36, (C) HH_36, (D) PE, (E) PG, (F) PH, (G) uncoated corn starch and (H) stearic acid

Table 4-5 Thermal properties of the uncoated corn starch and stearic acid

Sample Name	T_{onset} (°C)	T_{peak} (°C)	T_{endset} (°C)
Uncoated corn starch	25.16	92.66	171.21
Stearic acid	56.26	58.35	60.76

3.2 Thermogravimetric Analysis (TGA)

The TG curves of uncoated corn starch, stearic acid, coated starches (formulation EE_36, GG_36 and HH_36) and the physical mixtures of corn starch and stearic acid at different weight ratios were performed using thermogravimetry and the TG curves are illustrated in Figure 4-23.

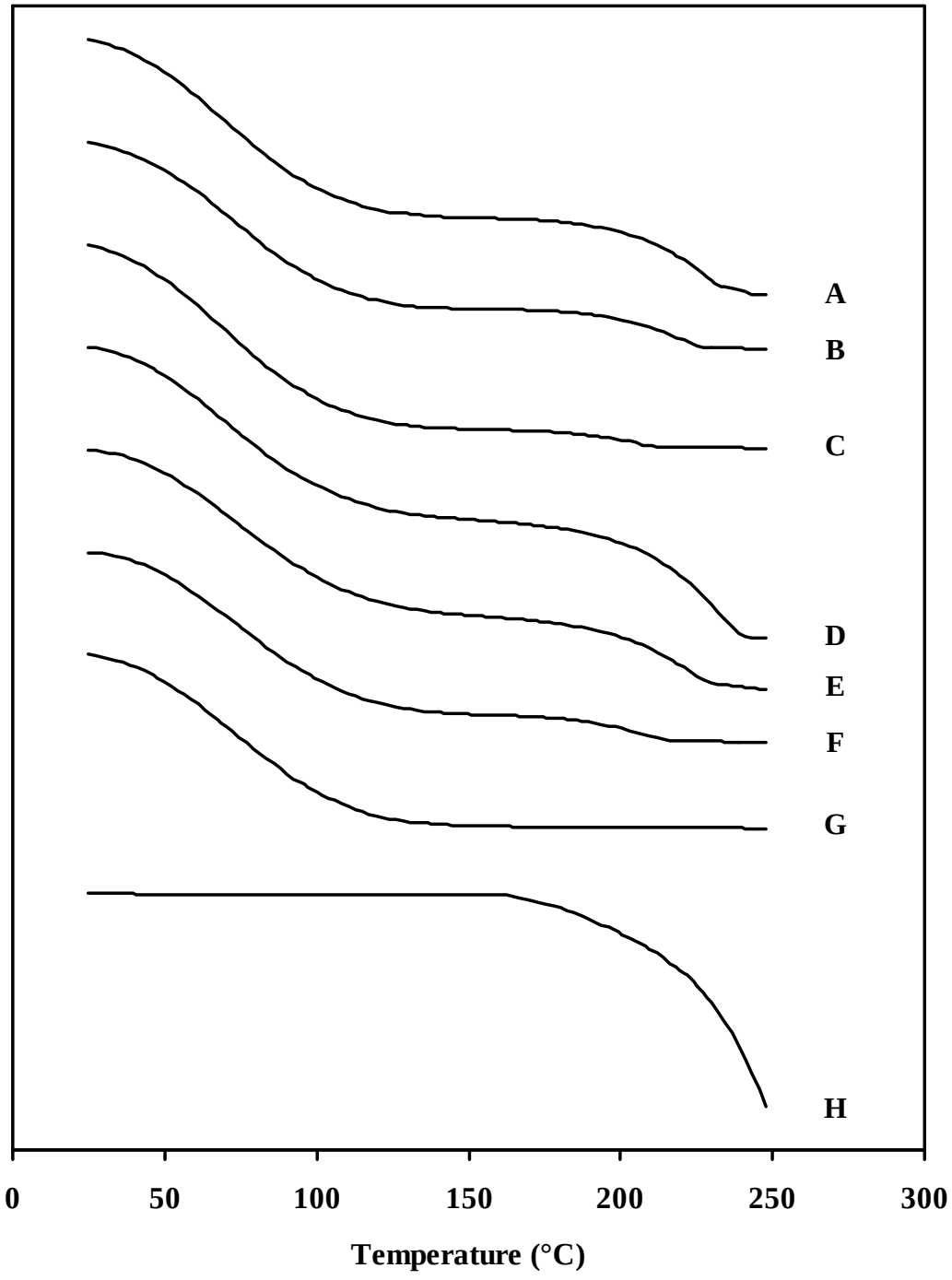

Figure 4-23 TG curves of (A) EE_36, (B) GG_36, (C) HH_36, (D) PE, (E) PG, (F) PH (G) uncoated corn starch and (H) stearic acid

In TG curve of the uncoated corn starch (Figure 4-23 (G)), a weight loss below 100 °C was mainly ascribed to water loss, therefore, it was designated as dehydration and from 100 °C to the decomposition onset temperature was related to the volatilization of water. While stearic acid was shown a weight loss curves at above 160 °C, as shown in Figure 4-23 (H). In TG curve of stearic acid, it started to decompose at above 160 °C and the temperature range of decomposition stage is very broad. The forms of mass loss curves were similar for these coated starches and the physical mixtures of corn starch and stearic acid but significant difference at the end of TG curve as compared with TG curve of uncoated corn starch. The TG curves of coated starches and the physical mixture of uncoated corn starch and stearic acid indicated that the ratio of stearic acid reduced, the end of TG curves was higher, as shown in Figure 4-23 (A) to (F). The TG curves of formulation HH_36 and PH, the least ratio of stearic acid, had similar pattern with uncoated corn starch.

3.3 X-ray Powder Diffractometry (XRPD)

X-ray powder diffraction measurements were performed to investigate the change of the crystallinity of starch. The XRPD studies have shown that starch exists in three crystal forms designated A, B and C. These forms are dependent on the botanical source of the starch. Pattern A is observe for cereal grain starches, whereas pattern B is characteristic of tuber, fruit and stem starches. Pattern C is intermediate between the A and B patterns and has been attributed to mixtures of A and B type crystallites. The A type pattern is commonly observed for corn starch (Ann *et al*., 2007).

The XRPD patterns for the uncoated corn starch, stearic acid, coated starches (formulation EE_36, GG_36 and HH_36) and the physical mixtures of corn starch and stearic acid at different weight ratios are presented in Figure 4-24. The uncoated corn starch exhibits an A type crystallinity pattern. The uncoated corn starch was found to have some crystalline character as evidenced by the broad peaks present. The uncoated corn starch had sharp diffraction peaks at Bragg angle (2θ) = 15°, 17°, 18° and 23°, which indicated typical A pattern of cereal starch (Zobel, 1988), as shown in Figure 4-24 (G). The pattern is indicative of a crystalline material and is similar to the A type pattern, but a definite determination of the form is difficult based on the quality of the pattern. While stearic acid had sharp diffraction peaks at 2θ = 7°, 21° and 24°, as shown in Figure 4-24 (H). In the diffraction pattern of coated starches

and the physical mixtures of corn starch and stearic acid retained their respective peaks at their positions. Almost no change was detected in their diffraction patterns, as shown in Figure 4-24 (A) to (F). As result, the XRPD patterns of coated starches of formulation EE_36, GG_36 and HH_36 and the physical mixtures of uncoated corn starch and stearic acid of PE, PG and PH showed the combined XRPD patterns of uncoated corn starch and stearic acid.

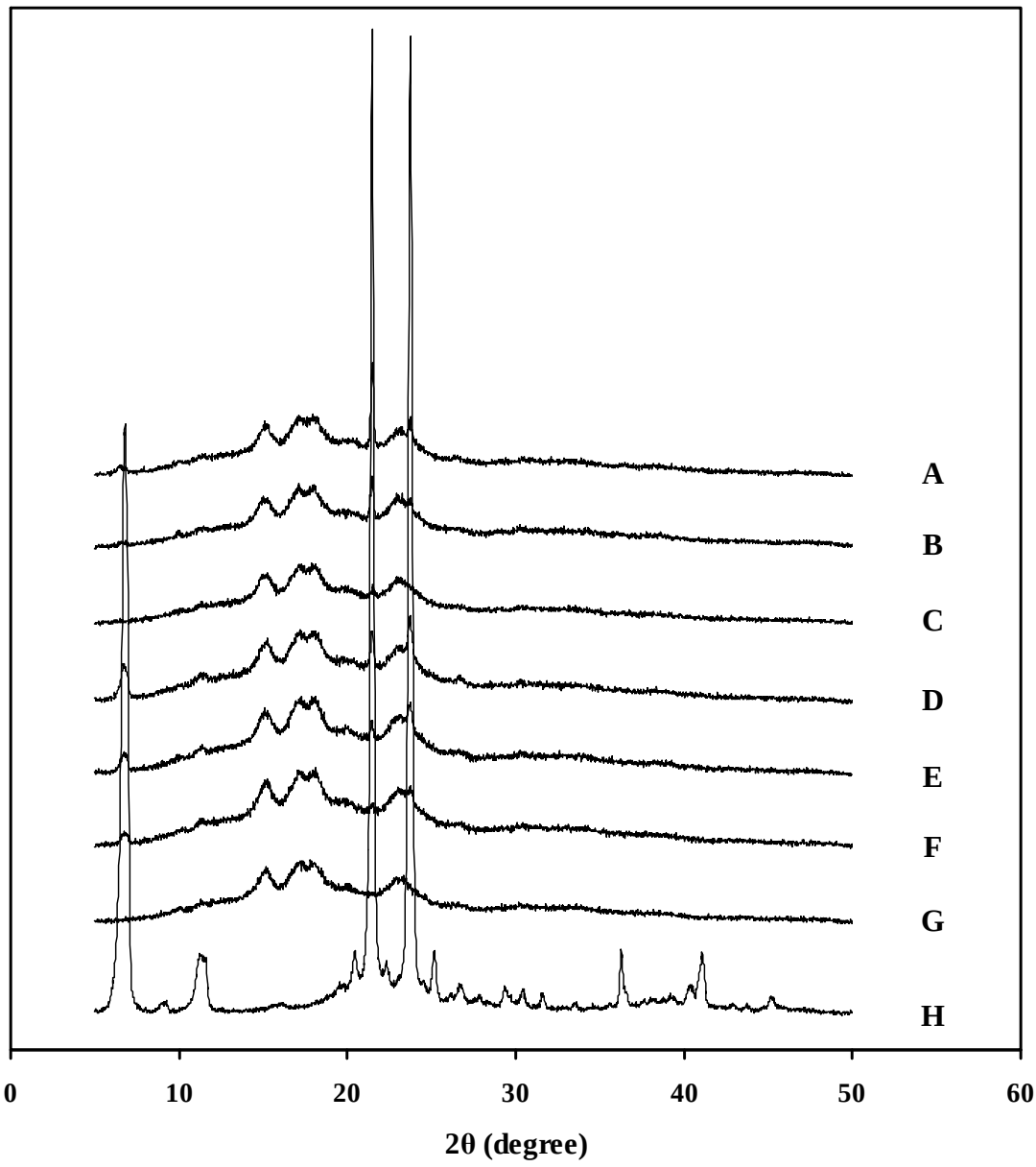

Figure 4-24 XRPD patterns of (A) EE_36, (B) GG_36, (C) HH_36, (D) PE, (E) PG, (F) PH, (G) uncoated corn starch and (H) stearic acid

3.4 *Fourier transform Infrared (FT-IR) Spectroscopy*

The FT-IR spectra of uncoated corn starch, stearic acid and coated starches (formulation EE_36, GG_36 and HH_36) are shown in Figure 4-25. In the spectra of uncoated corn starch (Figure 4-25 (G)), there are several discernible absorbencies at 1158, 1082, 1015 and 929 cm^{-1}, which were attributed to the C-O bond stretching vibration. A strong absorption band at 1015 cm^{-1}, probably due to the stretching of the C-OH bond, was present in the spectra of the starches consistent with the earlier report by Marcazzan *et al.* (1999). A characteristic peak occurred at 1643 cm^{-1}, which is presumably a feature of tightly bound water present in the starch. Additional characteristic absorption bands appeared at 995, 929, 861, 765 and 575 cm^{-1} due to the entire anhydroglucose ring stretching vibrations. The band at 2931 cm^{-1} is characteristic of the C-H stretching vibration. An extremely broad band resulting from vibration of the hydroxyl groups (O-H) appears at 3434 cm^{-1} which was attributed to the complex vibrational stretches associated with free, inter and intramolecular bound hydroxyl groups which make up the gross structure of starch. Meanwhile, the spectra of stearic acid (Figure 4-25 (H)), the characteristic absorptions that appear at 1705 cm^{-1} are attributed to the C=O bond stretching vibration. The band at 2918 and 2850 cm^{-1} is characteristic of the C-H stretching vibration. In Figure 4-25 show the FT-IR spectra of formulation EE_36, GG_36 and HH_36 and the physical mixtures of uncoated corn starch and stearic acid of PE, PG and PH. All of these spectra have similar profiles. Identical peaks of coated starches and the physical mixtures in all spectra are described as follows. In comparison with the spectra of the uncoated corn starch, the major change is the presence of a carbonyl C=O absorption frequency at 1705 cm^{-1}. The C-H stretching absorbance centered on 2918 cm^{-1} is increased in intensity upon surface modification. The occurrence of a shoulder at 2850 cm^{-1} on the absorbance centered at 2918 cm^{-1} in the spectra was attributed to the C-H stretching bands. The strong O-H stretching band at 3434 cm^{-1} in the uncoated corn starch decreased only slightly in intensity following the surface modification. The intensity of the C-H stretching bands at 2918 and 2850 cm^{-1} increased with increasing carbon chain length relative to the O-H absorbance (3434 cm^{-1}). In summary, similar spectroscopic profiles to the coated starches of formulation EE_36, GG_36 and HH_36 and the physical mixtures of uncoated corn starch and stearic acid of PE, PG and PH were obtained in all cases. These revealed the similar structures of their, with all presenting an intense ester carbonyl band at 1705 cm^{-1}. These new absorptions

suggested that the coated starch products were coated with stearic acid via the RESS-N process.

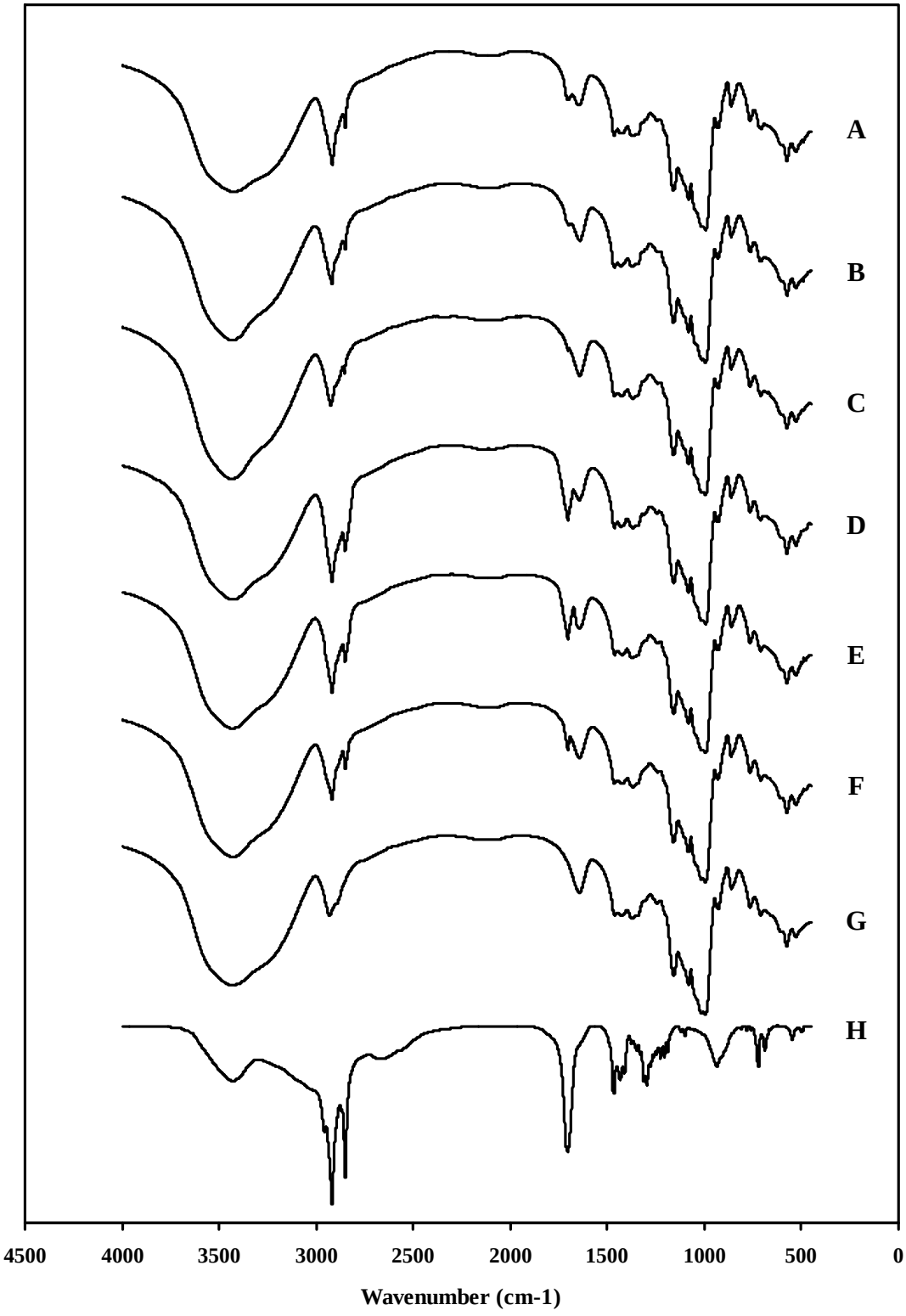

Figure 4-25 FT-IR spectra of (A) EE_36, (B) GG_36, (C) HH_36, (D) PE, (E) PG, (F) PH (G) uncoated corn starch and (H) stearic acid

4. Evaluation of coated starches used as lubricant in tabletting process

4.1 Characterization of Powder Mixes Before Tabletting

4.1.1 Flow Rate

The flow rate of each formulation is exhibited in Table 4-6. Formulation EE had the highest flow rate of 9.48±0.13 g/sec. Formulation GG, SS, SA, HH, BL and CS had the lower flow rate of 9.12±0.18, 8.86±0.04, 8.75±0.08, 8.61±0.08, 8.58±0.07 and 8.55±0.11 g/sec, respectively. Formulation MG had the lowest flow rate of 8.29±0.03 g/sec. The flow rate of formulation EE and GG were found to be higher as compared with other formulation, whereas formulation HH was higher as compared with formulation BL, CS and MG but lower as compared with formulation SS and SA. Based on the results obtained, when the ratio of stearic acid in coated starch was reduced (formulation EE, GG and HH), the flow rates became lower.

Table 4-6 Flow rate, angle of repose, bulk density, tapped density and compressibility index of powder mixes [average (SD)]

Formulation	Flow rate (g/sec)	Angle of repose (°)	Bulk density (g/cm^3)	Tapped density (g/cm^3)	Compressibility index (%)
BL	8.58 (0.07)	26.65 (0.14)	0.64 (0.00)	0.78 (0.01)	17.87 (0.13)
CS	8.55 (0.11)	26.77 (0.40)	0.63 (0.00)	0.79 (0.01)	19.83 (0.73)
EE	9.48 (0.13)	26.00 (0.09)	0.64(0.00)	0.85 (0.00)	24.36 (0.00)
GG	9.12 (0.18)	26.26 (0.41)	0.64 (0.00)	0.84 (0.00)	23.25 (0.30)
HH	8.61 (0.08)	26.73 (0.39)	0.64 (0.00)	0.80 (0.00)	20.17 (0.30)
SS	8.86 (0.04)	27.28 (0.08)	0.67 (0.00)	0.85 (0.01)	25.17 (0.13)
SA	8.75 (0.08)	27.02 (0.09)	0.67 (0.00)	0.84 (0.00)	24.66 (0.36)
MG	8.29 (0.03)	27.49 (0.14)	0.67 (0.00)	0.85 (0.01)	25.42 (0.19)

4.1.2 Angle of Repose

The angle of repose of each formulation is reported in Table 4-6. Flowability is indicated based on the angle of repose. The angle of repose of < 30° indicates “excellent” flow whereas a value of > 66° is considered “very very poor” flow. There are intermediate scales indicates “good” (θ between 31-35°), “fair” (θ between 36-40°), “passable which may hang up” (θ between 41-45°), “poor which must be agitated or vibrated” (θ between 46-55°) and “very poor” (θ between 56-65°).

MG had the highest angle of repose of 27.49±0.14°. Formulation SS, SA, CS, HH, BL and GG had the lower angle of repose of 27.28±0.08, 27.02±0.09, 26.77±0.40, 26.73±0.39, 26.65±0.14 and 26.26±0.41°, respectively. Formulation EE had the lowest angle of repose of 26.00±0.09°. Based on the results obtained, flowability of all formulations were classified as “excellent”, in terms of its flow based on the angle of repose values.

4.1.3 Bulk Density, Tapped Density and Compressibility Index

The bulk and tapped densities of each formulation are shown in Table 4-6. The bulk densities of all powder mixes were similar within the range of 0.63±0.00-0.67±0.00 g/cm^3. The tapped densities of formulation EE, SS and MG were the highest of 0.85±0.01 g/cm^3, whereas formulation GG, SA, HH and CS had the lower tapped density of 0.84±0.00, 0.84±0.00, 0.80±0.00 and 0.79±0.01 g/cm^3, respectively. Formulation BL without lubricant had the lowest tapped density of 0.78±0.01 g/cm^3.

The Carr’s CI were also calculated based on the equation presented in CHAPTER III (section 4.8) and are presented in Table 4-6. Formulation BL had the lowest Carr’s CI of 17.87±0.13 %, whereas formulation CS, HH, GG, EE, SA and SS had the higher Carr’s CI of 19.83±0.73, 20.17±0.30, 23.25±0.30, 24.36±0.00, 24.66±0.36 and 25.17±0.13 %, respectively. Formulation MG had the highest Carr’s CI of 25.42±0.19 %. As describes in section 2.8 and based on the results obtained, flowing behavior of formulation BL, CS and HH were classified as “fair”, whereas formulation GG, EE, SA, SS and MG were classified as “passable”, in terms of its flow based on the Carr’s CI values.

Thus flow of powder mixes for formulation BL, CS, and HH were better as compared with formulation EE, GG, SS, SA and MG based on the Carr’s CI. However, based on the flow rate and angle of repose results, formulation EE was better than other formulations. This discrepancy might be due to very qualitative nature of the scale of measurements and ratings for flow properties based on these methods.

4.2 Characterization of Tablet Properties

Tablets (360 milligrams per tablet) were prepared using a single punch tablet press and 3/8-inch beveled edge punch. Coated starches (formulation EE_36, GG_36 and HH_36) were used as lubricant and compared with corn starch, stearic acid

through SCT at critical pressure of 3000 psi and critical temperature of 60 ^{o}C (SS_36), stearic acid through an 80-mesh sieve (SA_80) and magnesium stearate. The compression force was adjusted to obtain an upper punch force of 25, 30 and 35 kilonewtons. After tabletting, tablets of each formulation were characterized for hardness, friability and disintegration time. Formulation BL and CS were found to be difficult for tablet as compared with other formulations. Because the powder mixes of formulation BL and CS had not lubricant in tablet formulation.

4.2.1 Tablet Thickness, Diameter and Hardness

The tablet thickness, diameter and hardness of each formulation using an upper punch force of 25, 30 and 35 kilonewtons are presented in Table 4-7 to 4-9, respectively. At an upper punch force of 25, 30 and 35 kilonewtons, the tablet hardness of each formulation was shown similar trends and can be ranked in the following order: BL > CS > SS > HH > SA > MG > GG > EE. Base on the results obtained, higher tablet hardness were found with increasing compression force. The tablet hardness of formulations containing coated starch of EE_36 and GG_36 were lower, whereas of HH_36 was higher as compared with those formulations containing SA_80 (through sieving) and magnesium stearate. In addition, the formulations containing coated starch of EE_36, GG_36 and HH_36 were lower tablet hardness than the formulations containing corn starch and SS_36 (through SCT).

Table 4-7 Physical properties of tablet for each formulation using an upper punch force of 25 kilonewtons

Formulation	Physical Properties				
	Thickness (mm)	Diameter (mm)	Hardness (kp)	Friability (%)	Disintegration time (min)
BL_25	4.12±0.01	9.55±0.00	9.33±0.29	0.439±0.029	00:56±0.00
CS_25	4.00±0.02	9.58±0.03	8.75±0.49	0.458±0.024	00:45±0.00
EE_25	4.02±0.02	9.61±0.02	6.49±0.30	0.417±0.055	03:50±0.00
GG_25	4.04±0.02	9.60±0.03	6.54±0.74	0.366±0.046	03:15±0.00
HH_25	4.03±0.03	9.57±0.03	7.72±0.33	0.444±0.086	01:01±0.00
SS_25	3.98±0.03	9.61±0.02	8.05±0.17	0.403±0.060	06:24±0.00
SA_25	4.01±0.02	9.62±0.01	6.93±0.20	0.430±0.055	05:11±0.00
MG_25	3.99±0.03	9.62±0.02	6.68±0.39	0.384±0.035	10:38±0.00

Table 4-8 Physical properties of tablet for each formulation using an upper punch force of 30 kilonewtons

Formulation	Physical Properties				
	Thickness (mm)	Diameter (mm)	Hardness (kp)	Friability (%)	Disintegration time (min)
BL_30	3.88±0.01	9.60±0.03	15.79±0.54	0.333±0.014	04:24±0.00
CS_30	3.83±0.02	9.56±0.01	15.60±0.76	0.375±0.000	03:56±0.00
EE_30	3.81±0.03	9.62±0.02	11.08±0.63	0.310±0.008	06:58±0.00
GG_30	3.82±0.02	9.61±0.03	11.38±0.79	0.278±0.090	06:38±0.00
HH_30	3.84±0.02	9.62±0.02	12.39±0.79	0.352±0.089	04:56±0.00
SS_30	3.79±0.02	9.60±0.01	13.75±0.59	0.306±0.084	09:44±0.00
SA_30	3.82±0.02	9.61±0.03	12.05±0.42	0.315±0.022	08:14±0.00
MG_30	3.77±0.03	9.59±0.01	11.97±0.63	0.296±0.064	10:51±0.00

Table 4-9 Physical properties of tablet for each formulation using an upper punch force of 35 kilonewtons

Formulation	Physical Properties				
	Thickness (mm)	Diameter (mm)	Hardness (kp)	Friability (%)	Disintegration time (min)
BL_35	3.70±0.03	9.58±0.03	21.70±0.55	0.236±0.013	06:58±0.00
CS_35	3.65±0.02	9.58±0.02	20.45±0.76	0.278±0.069	06:57±0.00
EE_35	3.69±0.03	9.60±0.01	13.91±0.94	0.236±0.024	09:00±0.00
GG_35	3.69±0.03	9.58±0.01	14.87±0.30	0.222±0.048	07:48±0.00
HH_35	3.71±0.03	9.59±0.02	18.44±0.52	0.264±0.099	07:04±0.00
SS_35	3.66±0.03	9.60±0.03	19.03±0.60	0.236±0.049	12:05±0.00
SA_35	3.69±0.02	9.58±0.02	16.18±0.54	0.236±0.087	10:35±0.00
MG_35	3.65±0.01	9.61±0.01	14.98±0.97	0.236±0.036	12:21±0.00

4.2.2 Tablet Friability

The percentage of tablet friability for each formulation using an upper punch force of 25, 30 and 35 kilonewtons are presented in Table 4-7 to 4-9, respectively. All formulations gave tablet friability less than 1 %. At an upper punch force of 25, 30 and 35 kilonewtons, tablet friability of each formulation was shown similar trends and can be ranked in the following order: CS > HH > BL > SA > EE >

SS > MG > GG. Base on the results obtained, lower tablet friability were found with increasing compression force.

4.2.3 Disintegration Time of Tablet

The disintegration time of tablet for each formulation using an upper punch force of 25, 30 and 35 kilonewtons are presented in Table 4-7 to 4-9, respectively. At an upper punch force of 25, 30 and 35 kilonewtons, the disintegration time of tablet for each formulation was shown similar trends and can be ranked in the following order: MG > SS > SA > EE > GG > HH > BL > CS. Base on the results obtained, longer disintegration time of tablet were found with increasing compression force. The tablet disintegration time of formulations containing coated starch of EE_36, GG_36 and HH_36 were shorter as compared with the formulations containing SS_36 (through SCT), SA_80 (through sieving) and magnesium stearate. Moreover, in comparison of the tablet disintegration time of formulation containing uncoated corn starch (formulation CS) and coated starches (formulation EE, GG and HH) were found that coated starches (formulation EE_36, GG_36 and HH_36) used as lubricant in this study affecting disintegration time of tablet. Because coated starches were coated with stearic acid, the tablet disintegration time of formulations containing coated starches were longer as compared with the formulation containing uncoated corn starch.

CHAPTER V

CONCLUSIONS

The rapid expansion of supercritical solutions with a nonsolvent (RESS-N) process was applied to modify the surface of starch grains by coating with stearic acid. Corn starch and stearic acid were chosen as core particles and coating agent, respectively. The effects of temperature, pressure, and ratio of starch and stearic acid on the surface modification of corn starch grains were investigated. The coating process was performed by introducing supercritical carbon dioxide ($scCO_2$) at pressures and temperatures into extraction vessel containing mixture of corn starch and stearic acid. The physical and physicochemical properties of coated starches were characterized to compare with uncoated starch and/or stearic acid, and applied as lubricant in tabletting process. It can be concluded that:

- The pressure of $scCO_2$ did not affect but temperature of $scCO_2$ and ratio of corn starch and stearic acid had significant effect on surface modification of starch grains.

- SEM images showed that stearic acid deposited onto the surface of starch grains forming a thin, uniform and smooth film when reducing the content of stearic acid using pressure of 3000 psi and temperature of 60 °C. This result was supported by an increase in particle size of coated starch which corresponding with the amount of stearic acid used in the mixture.

- The gravimetric vapour sorption analysis of coated starches showed the percentage of mass change lower than uncoated corn starch. This result was corresponding with the result obtained from the determination of moisture absorption property (Karl Fischer method). It indicated that the starches coated with stearic acid, a hydrophobic material, rarely absorb moisture.

- The bulk and tapped density, compressibility index and apparent density were showed different between uncoated corn starch and coated starches.

- Physicochemical characterizations of coated starches indicated that no change and/or evidence of interaction between corn starch and stearic acid.

- The coated starches were applied as lubricant in order to compare the tablet properties with conventional lubricants such as stearic acid and magnesium stearate. The results suggest that coated starch could be useful as a lubricating agent in tablet formulations.

In conclusion, coating of starch grains with stearic acid was possible via RESS with a nonsolvent:

1) The RESS-N process can be used to coating of particle. In the present study, this process was applied for coating the surface of starch grains with stearic acid.

2) The process could be useful for coating fine particles of pharmaceuticals for surface modification, taste masking and stability improvement.

REFERENCES

Allen, L.V. Stearic acid. In R.C. Rowe; P.J. Sheskey; and P.J. Weller (eds.), Handbook of pharmaceutical excipients, 4th ed, pp. 615-617. Washington, D.C.: American Pharmaceutical Association, 1994.

Aoshima, H., Miyagisnima, A., Nozawa, Y., Sadzuka, Y., and Sonobe, T. Glycerin fatty acid esters as a new lubricant of tablets. International Journal of Pharmaceutics. 293 (2005): 25-34.

Calderone, M., Rodier, E., Lochard, H., Marciacq, F., and Fages, J. A new supercritical co-injection process to coat microparticles. Chemical Engineering and Processing. 47 (2008): 2228-2237.

Charbit, G., Badens, E., and Boutin, O. Methods of particle production. In P. York; U.B. Kompella; and B.Y. Shekunov (eds.), Supercritical fluid technology for drug product development, vol. 138, pp. 159-212. New York: Marcel Dekker, 2004.

Debenedetti, P.G., Tom, J.W., Yeo, S., and Lim, G. Application of supercritical fluids for the production of sustained delivery devices. Journal of Controlled Release. 24 (1993): 21-44.

Dondeti, P., and Desai, Y. Supercritical fluid technology in pharmaceutical research. In J. Swarbrick; and J.C. Boylan (eds.), Encyclopedia of pharmaceutical technology, vol. 18, pp. 219-248. New York: Marcel Dekker, 1999.

Fages, J., Lochard, H., Letourneau, J.J., Sauceau, M., and Rodier, E. Particle generation for pharmaceutical applications using supercritical fluid technology. Powder Technology. 141 (2004): 219-226.

Gallagher, P.M., Coffey, M.P., Krukonis, V.J., Klasutis, N. Gas antisolvent recrystallization: New process to recrystallize compounds insoluble in supercritical fluids. In J.M.L. Penniger (ed.), Supercritical fluid science and technology, pp. 334-354. Washington, D.C.: American Chemical Society, 1989.

Gallagher, P.M., Krukonis, V.J., and Coffey, M.P. US patent 5 389 263, 1992a.

Gallagher, P.M., Coffey, M.P., Krukonis, V.J., and Hillstrom, W.W. Gas anti-solvent recrystallization of RDX: Formation of ultra-fine particles of a difficult-to-comminute explosive. Journal of Supercritical Fluids. 5 (1992b): 130-142.

Grant, C. Stearic Acid, a Fatty Acid [Online]. 1997. Available from: http://chemlabs.uoregon.edu/GeneralResources/models/stearic_acid.html. [2008, November 7]

Guan, B., Han, B., and Yan, H. Solubility of stearic acid in supercritical CO_2-acetic acid and CO_2-n-octane mixtures at 308.15 K. Journal of Supercritical Fluids. 12 (1998): 123-128.

Hanna, M.H., and York, P. Method and apparatus for the formation of particles. World patent WO 95/01 221, 1995.

Hussain, M.S.H., York, P., and Timmins, P. A study of the formation of magnesium stearate film on sodium chloride using energy-dispersive X-ray analysis. International Journal of Pharmaceutics. 42 (1988): 89-95

Jannin, V., Bérard, V., N'Diaye, A., Andrès, C., and Pourcelot, Y. Comparative study of the lubricant performance of Compritol® 888 ATO either used by blending or by hot melt coating. International Journal of Pharmaceutics. 262 (2003): 39-45.

Joshi, A.A., and Duriez, X. Added functionality excipients: an answer to challenging formulations. Pharmaceutical Technology, Excipients and Solid Dosage Forms. (2004): 12-19.

Jung, J., and Perrut, M. Particle design using supercritical fluids: Literature and patent survey. Journal of Supercritical Fluids. 20 (2001): 179-219.

Kara, A., Tobyn, M. J., and Stevens, R. An application for zirconia as a pharmaceutical die set. Journal of the European Ceramic Society. 24 (2004): 3091-3101.

Kim, J., Paxton, T., and Tomasko, D. Microencapsulation of naproxen using rapid expansion of supercritical solutions. Biotechnology progress. 12 (1996): 650-661.

Kono, H. O., Huang, C. C., and Xi, M. Function and mechanism of flow conditioners under various loading pressure conditions in bulk powders. Powder Technology. 63 (1990): 81-86.

Kramer, A., and Thodos, G. Solubility of 1-octadecanol and stearic acid in supercritical carbon dioxide. Journal of Chemical & Engineering Data. 34 (1989): 184-187.

Krukonis, V. J., Gallagher, P. M., and Coffey, M. P. US patent 5 360 478, 1991.

Kröber, H., and Teipel, U. Microencapsulation of particles using supercritical carbon dioxide. Chemical Engineering and Processing. 44 (2005): 215-219.

Liang, H., Ueno, A., and Shinohara, K. UV protection effectiveness of plastic particles coated with titanium dioxide by rotational impact blending. Trans IChemE. 78 (2000): 49-54.

Liu, Y.H., Wang, T.J., Qin, L., and Jin, Y. Urea particle coating for controlled release by using DCPD modified sulfur. Powder Technology. 183 (2008): 88-93.

Marcazzan, M., Vianello, F., Scarpa, M., and Rigo, A. An ESR assay for a-amylase activity toward succinylated starch, amylose and amylopectin. Journal of Biochemical and Biophysical Methods. 38 (1999): 191-202.

Marshall, K., and Rudnic, E.M. Tablet dosage forms. New York: Marcel Dekker, 1990.

Miller, T.A., and York, P. Physical and chemical characteristics of some high purity magnesium stearate and palmitate powders. International Journal of Pharmaceutics. 23 (1985): 55-67.

Miller, T.A., and York, P. Pharmaceutical tablet lubrication. International Journal of Pharmaceutics. 41 (1988): 1-19.

Mujumdar, A., Wei, D., Dave, R.N., Pfeffer, R., and Wu, C.Y. Improvement of humidity resistance of magnesium powder using dry particle coating. Powder Technology. 140 (2004): 86– 97.

Narh, K.A., Agwedicham, A.T., and Jallo, L. Dry coating polymer powder particles with deagglomerated carbon nanotubes to improve their dispersion in nanocomposites. Powder Technology. 186 (2008): 206-212.

Phoonphetmongkon, Y. Particle coating in fluidized bed coater enhanced with electrostaticity. Master's Thesis, Department of Chemical Engineering, Graduate School, Chulalongkorn University, 2004.

Rojo, S.R., Marienfeld, J., and Cocero, M.J. RESS process in coating applications in a high pressure fluidized bed environment: Bottom and top spray experiments. Chemical Engineering Journal. 144 (2008): 531-539.

Schmitt, W.J., and Reid, R.C. Solubility of monofunctional organic solids in chemically diverse supercritical fluids. Journal of Chemical and Engineering Data. 31 (1986): 204-212.

Schreiber, R., Vogt, C., Werther, J., and Brunner, G. Fluidized bed coating at supercritical fluid conditions. Journal of Supercritical Fluids. 24 (2002): 137-151.

Sengers, J.V. Effects of critical fluctuations on the thermodynamic and transport properties of supercritical fluids. In E. Kiran; and J.M.H.L. Sengers (eds.), Supercritical fluids: Fundamentals for application, pp. 231-271. Dordrecht: Kluwer Academic, 1994.

Subramaniam, B., Rajewski, R.A., and Snavely, K. Pharmaceutical processing with supercritical carbon dioxide. Journal of Pharmaceutical Sciences. 86 (1997): 885-890.

Tsutsumi, A., Nakamoto, S., Mineo, T., and Yoshida, K. A novel fluidized-bed coating of fine particles by rapid expansion of supercritical fluid solutions. Powder Technology. 85 (1995): 275-278.

Turkoglu, M., Sahin, I., and San, T. Evaluation of hexagonal boron nitride as a new tablet lubricant. Pharmaceutical Development and Technology. 10 (2005): 381-388.

Uğurlu, T., and Turkoğlu, M. Hexagonal boron nitride as a tablet lubricant and a comparison with conventional lubricants. International Journal of Pharmaceutics. 353 (2008): 45-51.

Wang, T.J., Tsutsumi, A., Hasegawa, H., and Mineo, T. Mechanism of particle coating granulation with RESS process in a fluidized bed. Powder Technology. 118 (2001): 229-235.

Wang, Y., Wei, D., Dave, R., Pfeffer, R., Sauceau, M., Letourneau, J.J., and Fages, J. Extraction and precipitation particle coating using supercritical CO_2. Powder Technology. 127 (2002): 32-44.

Wang, Y., Dave, R.N., and Pfeffer, R. Polymer coating/encapsulation of nanoparticles using a supercritical anti-solvent process. Journal of Supercritical Fluids. 28 (2004): 85–99.

Weidner, E., Knez, Z., and Novak, Z. Slovenian patent 940 079, 1994.

Weidner, E., Knez, Z., and Novak, Z. US patent 6 056 791, 1997.

Weidner, E., Knez, Z., and Novak, Z. European patent 0 744 990, 2000.

Yang, J., Sliva, A., Banerjee, A., Dave, R.N., and Pfeffer, R. Dry particle coating for improving the flowability of cohesive powders. Powder Technology. 158 (2005): 21-33.

Zanowiak, P. Lubrication in solid dosage form design and manufacture. In J. Swarbrick; and J.C. Boylan (eds.), Encyclopedia of pharmaceutical technology, vol. 9, pp. 87-111. New York: Marcel Dekker, 1994.

Zhong, M., Han, B., and Yan, H. Solubility of stearic acid in supercritical CO_2 with cosolvents. Journal of Supercritical Fluids. 10 (1997): 113-118.

Zobel, H.F. Molecules to granules: A comprehensive starch review. vol. 40, pp. 44-50. Weinheim: WILEY-VCH Verlag GmbH & Co. KGaA, 1988.

APPENDICES

APPENDIX A

Physical characterization of raw materials and/or coated starches

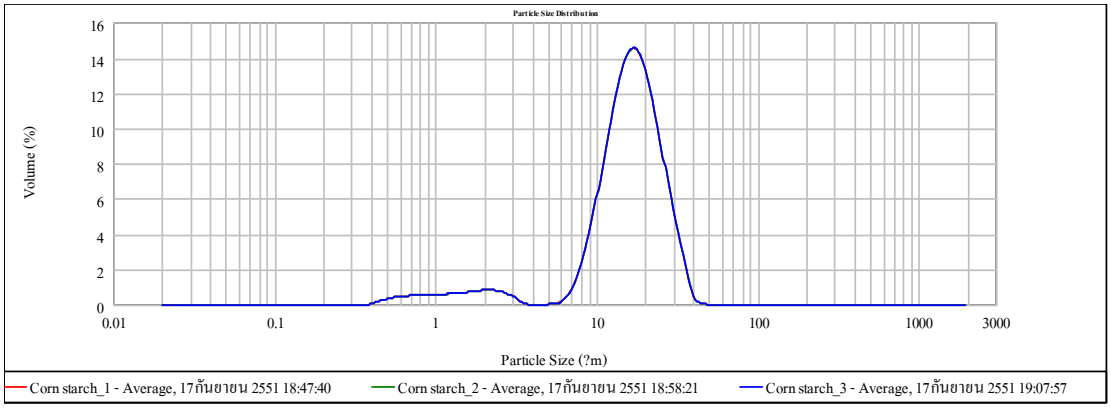

Figure 7-1 Particle size and size distribution of uncoated corn starch

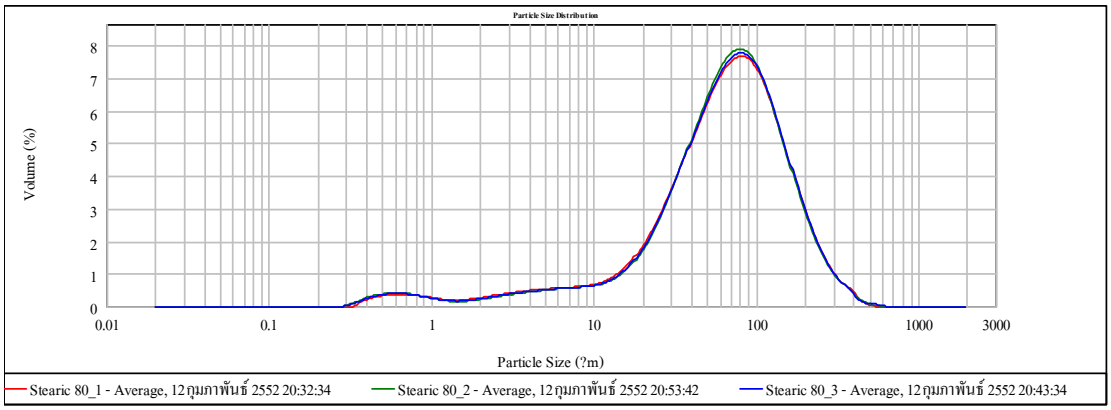

Figure 7-2 Particle size and size distribution of stearic acid through an 80-mesh sieve (SA_80)

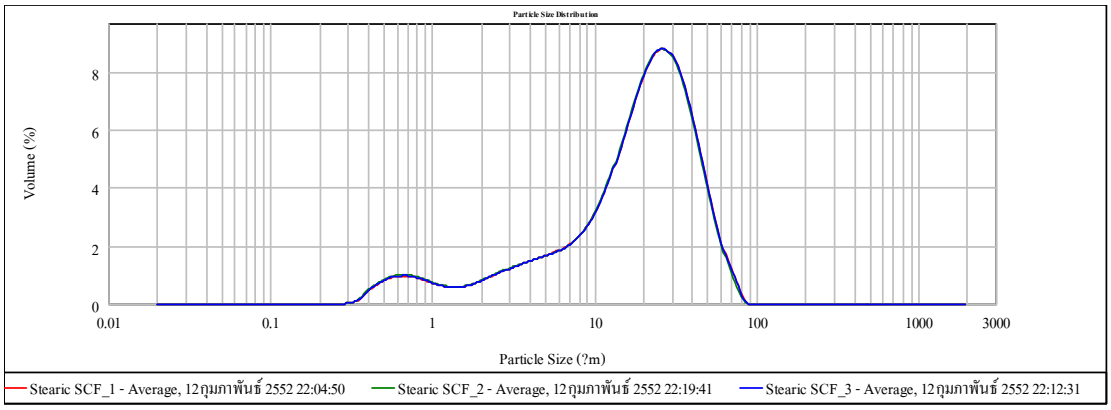

Figure 7-3 Particle size and size distribution of stearic acid through SCT at pressure of 3000 psi and temperature of 60 ^{o}C (SS_36)

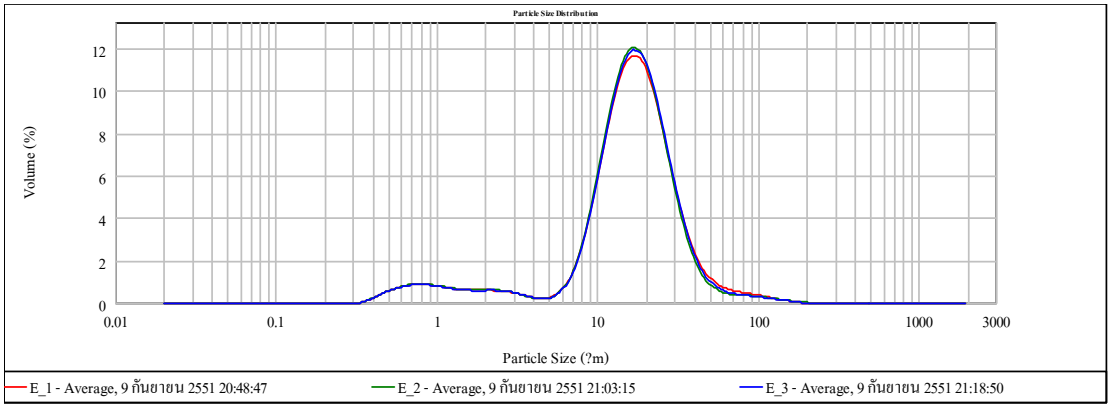

Figure 7-4 Particle size and size distribution of coated starch at ratio of corn starch and stearic acid of 2.8 : 0.2 grams, pressure 3000 psi and temperature 60 ^{o}C (EE_36)

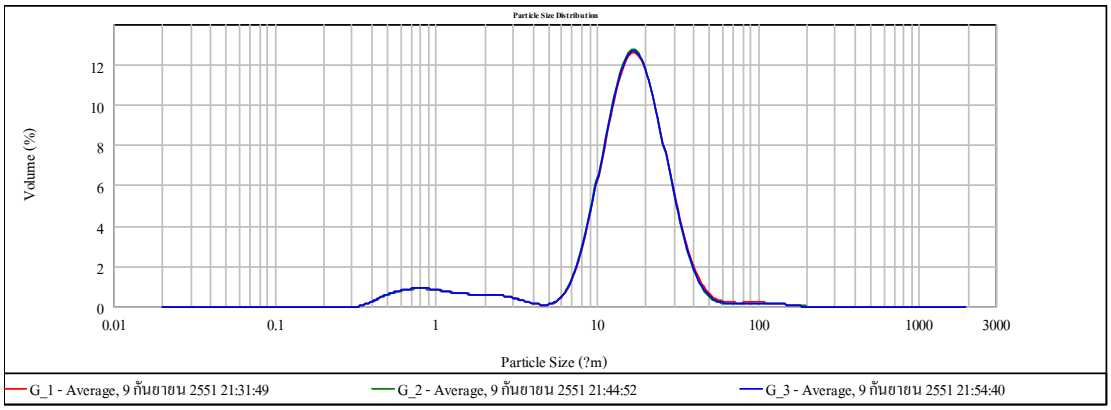

Figure 7-5 Particle size and size distribution of coated starch at ratio of corn starch and stearic acid of 2.9 : 0.1 grams, pressure 3000 psi and temperature 60 ^{o}C (GG_36)

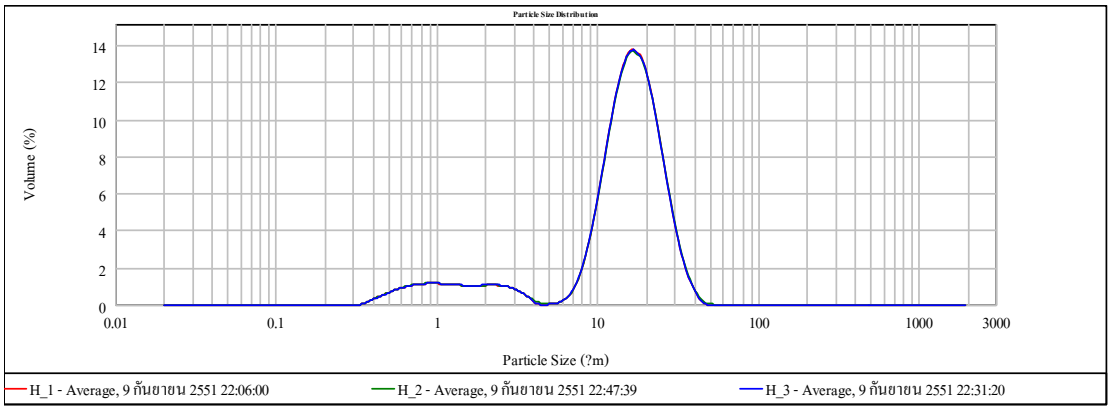

Figure 7-6 Particle size and size distribution of coated starch at ratio of corn starch and stearic acid of 2.95 : 0.05 grams, pressure 3000 psi and temperature 60 ^{o}C (HH_36)

Table 7-1 Moisture content by weight of uncoated corn starch both before and after drying at 70 °C for 3 hours using Halogen Moisture Analyzer

Sample No.	before drying		after drying	
	Weight (g)	Moisture content (%)	Weight (g)	Moisture content (%)
1	2.473	11.77	2.471	8.86
2	2.474	11.84	2.472	8.21
3	2.472	11.94	2.473	8.45
Average (SD)	**2.473 (0.00)**	**11.85 (0.09)**	**2.472 (0.00)**	**8.51 (0.33)**

Table 7-2 Percentage of mass change of uncoated corn starch when exposed to 75% RH at 25 °C using Dynamic Vapour Sorption Apparatus

Time (min)	Percentage of mass change				SD
	1	2	3	Average	
0	100.00	100.00	100.00	100.00	0.00
1	100.70	100.71	100.70	100.70	0.01
2	103.72	103.65	103.66	103.68	0.04
3	106.94	106.90	106.84	106.89	0.05
4	109.22	109.27	109.21	109.23	0.03
5	110.64	110.74	110.71	110.70	0.05
6	111.59	111.70	111.70	111.67	0.06
7	112.27	112.37	112.36	112.33	0.06
8	112.77	112.85	112.80	112.81	0.04
9	113.14	113.22	113.18	113.18	0.04
10	113.42	113.52	113.51	113.48	0.05
11	113.64	113.72	113.73	113.70	0.05
12	113.82	113.90	113.90	113.87	0.05
13	113.96	114.04	114.04	114.01	0.05
14	114.07	114.16	114.16	114.13	0.05
15	114.16	114.25	114.25	114.22	0.05
16	114.25	114.33	114.33	114.30	0.05
17	114.31	114.39	114.39	114.36	0.05
18	114.37	114.45	114.45	114.43	0.05
19	114.42	114.50	114.50	114.47	0.05
20	114.46	114.55	114.55	114.52	0.05
21	114.50	114.58	114.58	114.55	0.05
22	114.53	114.62	114.62	114.59	0.05
23	114.56	114.65	114.64	114.62	0.05
24	114.58	114.67	114.67	114.64	0.05
25	114.60	114.70	114.70	114.67	0.06
26	114.62	114.71	114.71	114.68	0.06
27	114.63	114.73	114.73	114.70	0.05
28	114.65	114.75	114.75	114.72	0.06
29	114.66	114.76	114.76	114.73	0.06
30	114.68	114.78	114.78	114.75	0.06
31	114.69	114.79	114.79	114.75	0.06
32	114.70	114.80	114.80	114.77	0.06
33	114.71	114.82	114.82	114.78	0.06
34	114.72	114.83	114.83	114.79	0.06
35	114.73	114.84	114.83	114.80	0.06
36	114.74	114.85	114.85	114.81	0.06
37	114.75	114.86	114.85	114.82	0.06
38	114.76	114.87	114.86	114.83	0.06

Table 7-2 Percentage of mass change of uncoated corn starch when exposed to 75% RH at 25 °C using Dynamic Vapour Sorption Apparatus (cont.)

Time (min)	Percentage of mass change				SD
	1	2	3	Average	
39	114.76	114.87	114.87	114.83	0.06
40	114.77	114.88	114.88	114.84	0.06
41	114.78	114.89	114.88	114.85	0.06
42	114.78	114.89	114.89	114.85	0.06
43	114.79	114.90	114.89	114.86	0.06
44	114.80	114.90	114.90	114.86	0.06
45	114.80	114.92	114.91	114.88	0.06
46	114.81	114.92	114.92	114.88	0.06
47	114.82	114.92	114.92	114.89	0.06
48	114.82	114.93	114.92	114.89	0.06
49	114.83	114.94	114.93	114.90	0.06
50	114.83	114.95	114.94	114.91	0.07
51	114.84	114.95	114.95	114.91	0.06
52	114.84	114.95	114.95	114.91	0.07
53	114.85	114.95	114.95	114.92	0.06
54	114.85	114.96	114.95	114.92	0.06
55	114.85	114.96	114.96	114.92	0.06
56	114.85	114.97	114.96	114.93	0.06
57	114.86	114.97	114.96	114.93	0.06
58	114.86	114.97	114.96	114.93	0.06
59	114.86	114.97	114.97	114.94	0.06
60	114.87	114.98	114.98	114.94	0.07
61	114.87	114.98	114.98	114.95	0.06
62	114.88	114.98	114.98	114.95	0.06
63	114.88	114.99	114.98	114.95	0.06
64	114.88	114.99	114.98	114.95	0.06
65	114.88	114.99	114.99	114.96	0.06
66	114.89	115.00	114.99	114.96	0.06
67	114.89	115.00	115.00	114.96	0.06
68	114.89	115.00	115.00	114.97	0.06
69	114.90	115.01	115.00	114.97	0.06
70	114.90	115.01	115.00	114.97	0.06
71	114.90	115.01	115.01	114.97	0.06
72	114.91	115.01	115.01	114.98	0.06
73	114.91	115.02	115.01	114.98	0.06
74	114.91	115.02	115.02	114.98	0.06
75	114.92	115.02	115.02	114.98	0.06
76	114.92	115.03	115.02	114.99	0.06
77	114.92	115.03	115.03	114.99	0.06

Table 7-2 Percentage of mass change of uncoated corn starch when exposed to 75% RH at 25 °C using Dynamic Vapour Sorption Apparatus (cont.)

Time (min)	Percentage of mass change				SD
	1	2	3	Average	
78	114.92	115.04	115.03	115.00	0.07
79	114.92	115.04	115.03	115.00	0.06
80	114.93	115.04	115.03	115.00	0.06
81	114.93	115.04	115.04	115.00	0.06
82	114.93	115.04	115.04	115.00	0.06
83	114.93	115.04	115.04	115.01	0.06
84	114.94	115.04	115.04	115.01	0.06
85	114.94	115.04	115.04	115.01	0.06
86	114.94	115.05	115.04	115.01	0.06
87	114.94	115.05	115.04	115.01	0.06
88	114.95	115.05	115.05	115.01	0.06
89	114.95	115.05	115.05	115.01	0.06
90	114.95	115.05	115.05	115.02	0.06
91	114.95	115.05	115.05	115.02	0.06
92	114.95	115.05	115.05	115.02	0.05
93	114.96	115.05	115.05	115.02	0.05
94	114.96	115.06	115.05	115.02	0.05
95	114.96	115.06	115.05	115.02	0.05
96	114.96	115.06	115.05	115.03	0.05
97	114.97	115.07	115.06	115.03	0.05
98	114.97	115.07	115.06	115.03	0.05
99	114.97	115.07	115.06	115.03	0.05
100	114.98	115.07	115.06	115.04	0.05
101	114.98	115.07	115.06	115.04	0.05
102	114.98	115.07	115.06	115.04	0.05
103	114.98	115.07	115.06	115.04	0.05
104	114.98	115.08	115.07	115.04	0.05
105	114.98	115.08	115.07	115.04	0.05
106	114.99	115.08	115.07	115.04	0.05
107	114.99	115.08	115.07	115.05	0.05
108	115.00	115.08	115.08	115.05	0.05
109	115.00	115.08	115.08	115.05	0.04
110	115.01	115.08	115.08	115.06	0.04
111	115.01	N/A	115.08	115.05	0.05
112	115.01	N/A	115.08	115.05	0.05
113	115.02	N/A	115.09	115.05	0.05
114	115.02	N/A	115.09	115.06	0.05
115	N/A	N/A	115.09	115.09	N/A
116	N/A	N/A	115.10	115.10	N/A

Table 7-2 Percentage of mass change of uncoated corn starch when exposed to 75% RH at 25 °C using Dynamic Vapour Sorption Apparatus (cont.)

Time (min)	Percentage of mass change				SD
	1	2	3	Average	
117	N/A	N/A	115.10	115.10	N/A
118	N/A	N/A	115.10	115.10	N/A
119	N/A	N/A	115.10	115.10	N/A

Table 7-3 Percentage of mass change of EE_36 when exposed to 75% RH at 25 °C using Dynamic Vapour Sorption Apparatus

Time (min)	Percentage of mass change				SD
	1	2	3	Average	
0	100.00	100.00	100.00	100.00	0.00
1	100.52	100.55	100.51	100.52	0.02
2	102.49	102.45	102.47	102.47	0.02
3	104.02	103.87	103.96	103.95	0.07
4	104.64	104.48	104.58	104.57	0.08
5	104.91	104.79	104.86	104.85	0.06
6	105.05	104.96	105.00	105.00	0.05
7	105.13	105.06	105.09	105.09	0.04
8	105.18	105.12	105.15	105.15	0.03
9	105.22	105.16	105.18	105.19	0.03
10	105.24	105.19	105.21	105.22	0.03
11	105.26	105.22	105.23	105.24	0.02
12	105.28	105.24	105.25	105.25	0.02
13	105.29	105.25	105.26	105.27	0.02
14	105.30	105.26	105.27	105.28	0.02
15	105.31	105.27	105.28	105.29	0.02
16	105.31	105.28	105.29	105.30	0.02
17	105.32	105.29	105.30	105.30	0.02
18	105.33	105.30	105.31	105.31	0.02
19	105.34	105.30	105.31	105.32	0.02
20	105.34	105.31	105.32	105.32	0.02
21	105.34	105.31	105.33	105.33	0.01
22	105.35	105.32	105.33	105.33	0.01
23	105.35	105.32	105.33	105.34	0.01
24	105.36	105.33	105.34	105.34	0.01
25	105.36	105.33	105.34	105.34	0.01
26	105.36	105.33	105.35	105.35	0.01
27	105.36	105.34	105.35	105.35	0.01
28	105.36	105.34	105.35	105.35	0.01
29	105.37	105.35	105.35	105.36	0.01
30	105.37	105.35	105.36	105.36	0.01
31	105.37	105.35	105.36	105.36	0.01
32	105.37	105.36	105.36	105.36	0.01
33	105.37	105.36	105.36	105.37	0.01
34	105.37	105.36	105.37	105.37	0.01
35	105.38	105.36	105.37	105.37	0.01
36	105.38	105.36	105.38	105.37	0.01
37	105.38	105.36	105.38	105.37	0.01
38	105.38	105.36	105.38	105.37	0.01

Table 7-3 Percentage of mass change of EE_36 when exposed to 75% RH at 25 °C using Dynamic Vapour Sorption Apparatus (cont.)

Time (min)	Percentage of mass change				SD
	1	2	3	Average	
39	105.38	105.37	105.38	105.37	0.01
40	105.38	105.37	105.38	105.37	0.01
41	105.38	105.37	105.38	105.38	0.00
42	105.38	105.37	105.38	105.38	0.00
43	N/A	105.37	105.39	105.38	0.01

Table 7-4 Percentage of mass change of GG_36 when exposed to 75% RH at 25 °C using Dynamic Vapour Sorption Apparatus

Time (min)	Percentage of mass change				SD
	1	2	3	Average	
0	100.00	100.00	100.00	100.00	0.00
1	100.55	100.53	100.60	100.56	0.03
2	102.69	102.57	102.72	102.66	0.08
3	104.45	104.28	104.35	104.36	0.09
4	105.22	105.11	105.05	105.13	0.09
5	105.56	105.51	105.38	105.48	0.09
6	105.74	105.71	105.56	105.67	0.09
7	105.84	105.83	105.67	105.78	0.09
8	105.89	105.90	105.74	105.85	0.09
9	105.93	105.94	105.80	105.89	0.08
10	105.96	105.97	105.83	105.92	0.08
11	105.99	105.99	105.86	105.94	0.07
12	106.00	106.00	105.88	105.96	0.07
13	106.02	106.02	105.90	105.98	0.07
14	106.03	106.03	105.91	105.99	0.07
15	106.04	106.04	105.92	106.00	0.07
16	106.06	106.05	105.94	106.01	0.07
17	106.06	106.05	105.94	106.02	0.06
18	106.06	106.06	105.95	106.03	0.06
19	106.07	106.07	105.96	106.03	0.06
20	106.07	106.09	105.97	106.04	0.07
21	106.08	106.09	105.97	106.05	0.06
22	106.08	106.09	105.98	106.05	0.06
23	106.09	106.09	105.98	106.05	0.06
24	106.09	106.10	105.99	106.06	0.06
25	106.09	106.10	105.99	106.06	0.06
26	106.10	106.11	106.00	106.07	0.06
27	106.10	106.11	106.00	106.07	0.06
28	106.10	106.11	106.01	106.07	0.06
29	106.11	106.11	106.01	106.08	0.06
30	106.11	106.12	106.01	106.08	0.06
31	106.11	106.12	106.01	106.08	0.06
32	106.12	106.12	106.02	106.08	0.06
33	106.12	106.12	106.02	106.09	0.06
34	106.12	106.13	106.02	106.09	0.06
35	106.13	106.13	106.02	106.09	0.06
36	106.13	106.14	106.03	106.10	0.06
37	106.13	106.14	106.03	106.10	0.06
38	106.13	106.14	106.03	106.10	0.06

Table 7-4 Percentage of mass change of GG_36 when exposed to 75% RH at 25 °C using Dynamic Vapour Sorption Apparatus (cont.)

Time (min)	Percentage of mass change				SD
	1	2	3	Average	
39	106.13	106.14	106.03	106.10	0.06
40	106.13	106.14	106.04	106.10	0.06
41	106.13	106.14	106.04	106.10	0.06
42	106.13	106.14	106.04	106.10	0.05
43	106.14	106.14	106.05	106.11	0.05
44	106.14	106.14	106.05	106.11	0.05
45	106.14	106.14	106.05	106.11	0.05
46	106.14	106.14	106.05	106.11	0.05
47	N/A	106.14	106.05	106.10	0.07
48	N/A	106.15	106.05	106.10	0.07

Table 7-5 Percentage of mass change of HH_36 when exposed to 75% RH at 25 °C using Dynamic Vapour Sorption Apparatus

Time (min)	Percentage of mass change				SD
	1	2	3	Average	
0	100.00	100.00	100.00	100.00	0.00
1	100.58	100.58	100.56	100.58	0.01
2	102.82	102.88	102.85	102.85	0.03
3	104.80	104.89	104.81	104.84	0.05
4	105.75	105.86	105.75	105.79	0.06
5	106.25	106.33	106.24	106.27	0.05
6	106.54	106.59	106.53	106.55	0.03
7	106.72	106.75	106.72	106.73	0.01
8	106.83	106.85	106.85	106.84	0.01
9	106.91	106.92	106.94	106.92	0.01
10	106.98	106.97	107.00	106.98	0.01
11	107.03	107.02	107.06	107.03	0.02
12	107.06	107.05	107.09	107.07	0.02
13	107.09	107.07	107.12	107.09	0.02
14	107.12	107.09	107.14	107.12	0.03
15	107.13	107.11	107.16	107.13	0.03
16	107.15	107.13	107.18	107.15	0.02
17	107.16	107.14	107.19	107.16	0.03
18	107.18	107.15	107.20	107.18	0.03
19	107.19	107.16	107.21	107.19	0.03
20	107.20	107.17	107.22	107.20	0.03
21	107.22	107.18	107.23	107.21	0.03
22	107.22	107.18	107.24	107.21	0.03
23	107.22	107.19	107.24	107.22	0.03
24	107.23	107.20	107.25	107.23	0.03
25	107.24	107.21	107.25	107.23	0.02
26	107.24	107.21	107.26	107.24	0.03
27	107.25	107.22	107.27	107.24	0.02
28	107.25	107.22	107.27	107.25	0.02
29	107.26	107.23	107.28	107.26	0.03
30	107.26	107.23	107.28	107.26	0.03
31	107.27	107.23	107.29	107.26	0.03
32	107.27	107.24	107.29	107.27	0.03
33	107.27	107.24	107.29	107.27	0.03
34	107.27	107.24	107.30	107.27	0.03
35	107.28	107.24	107.30	107.27	0.03
36	107.28	107.24	107.30	107.28	0.03
37	107.29	107.25	107.31	107.28	0.03
38	107.29	107.25	107.31	107.28	0.03

Table 7-5 Percentage of mass change of HH_36 when exposed to 75% RH at 25 °C using Dynamic Vapour Sorption Apparatus (cont.)

Time (min)	Percentage of mass change				SD
	1	2	3	Average	
39	107.30	107.25	107.31	107.28	0.03
40	107.30	107.25	107.31	107.29	0.03
41	107.30	107.25	107.31	107.29	0.03
42	107.30	107.26	107.32	107.29	0.03
43	107.30	107.26	107.32	107.30	0.03
44	107.31	107.26	107.33	107.30	0.03
45	107.31	107.27	107.33	107.30	0.03
46	107.31	107.27	107.33	107.30	0.03
47	107.31	107.27	107.33	107.30	0.03
48	107.32	107.27	107.33	107.31	0.03
49	107.32	107.27	107.33	107.31	0.03
50	107.32	107.27	107.33	107.31	0.03
51	107.32	107.28	107.33	107.31	0.03
52	107.32	107.28	107.33	107.31	0.03
53	107.32	107.28	107.34	107.31	0.03
54	107.32	107.28	107.34	107.31	0.03
55	107.32	107.29	107.34	107.32	0.03
56	107.32	107.29	107.34	107.32	0.02
57	107.33	107.30	107.35	107.32	0.02
58	107.33	107.30	107.35	107.33	0.02
59	107.33	107.30	107.35	107.33	0.02
60	107.33	107.31	107.35	107.33	0.02
61	107.34	107.31	107.35	107.33	0.02
62	107.34	107.31	107.35	107.33	0.02
63	107.34	107.32	107.35	107.34	0.02
64	107.34	107.32	107.35	107.34	0.01
65	107.35	107.33	107.35	107.34	0.01
66	107.35	107.33	107.35	107.34	0.01
67	107.35	107.34	107.35	107.35	0.01
68	107.35	107.34	107.35	107.35	0.01
69	107.35	N/A	107.35	107.35	0.00
70	N/A	N/A	107.36	107.36	N/A
71	N/A	N/A	107.36	107.36	N/A

Table 7-6 Time of saturation moisture sorption of uncoated corn starch and coated starch after exposed to 75% RH using Dynamic Vapour Sorption Apparatus [Average (SD)]

Sample name	Time (min)			Average (SD)
Corn starch	114.00	110.00	119.00	114.33 (4.51)
EE_36	42.00	43.00	43.00	42.67 (0.58)
GG_36	46.00	48.00	48.00	47.33 (1.15)
HH_36	69.00	68.00	71.00	69.33 (1.53)

Table 7-7 Percentage of total water content of uncoated corn starch and coated starches before and after long exposure to 75% RH for 0, 7, 14, 21, 28, 35 and 42 days at room temperature using Karl Fischer method [Average (SD)]

Time (day)	Sample name			
	Corn starch	**EE_36**	**GG_36**	**HH_36**
0	100.00 (0.00)	100.00 (0.00)	100.00 (0.00)	100.00 (0.00)
7	134.37 (0.11)	105.28 (0.82)	108.98 (1.19)	115.27 (0.48)
14	147.54 (0.09)	105.84 (0.27)	109.04 (1.81)	124.78 (1.46)
21	147.56 (0.03)	105.94 (0.16)	109.07 (0.51)	124.79 (0.11)
28	147.58 (0.39)	106.04 (0.35)	109.11 (0.91)	124.82 (0.54)
35	147.69 (0.05)	106.07 (0.37)	109.14 (0.97)	124.85 (0.36)
42	147.71 (0.42)	106.09 (0.11)	109.17 (0.57)	124.86 (0.13)

Table 7-8 Apparent density of the uncoated corn starch, stearic acid and coated starches [Average (SD)]

Sample name	Volume (ml)	Apparent density (g/cm^3)	Average (SD)
Corn starch	0.7386	1.5028	
	0.7373	1.5039	
	0.7361	1.5024	1.5044 (0.0021**)**
	0.7368	1.5051	
	0.7366	1.5076	
SA_80	0.4716	1.0126	
	0.4728	1.0137	
	0.4693	1.0139	1.0144 (0.0025)
	0.4713	1.0188	
	0.4685	1.0129	
SS_36	0.3823	0.8352	
	0.3815	0.8284	
	0.3841	0.8297	0.8312 (0.0034)
	0.3828	0.8346	
	0.3796	0.8281	
EE_36	0.5355	1.4553	
	0.5312	1.4562	
	0.5277	1.4529	1.4538 (0.0020)
	0.5283	1.4512	
	0.5346	1.4533	
GG_36	0.6262	1.4821	
	0.6187	1.4803	
	0.6196	1.4836	1.4835 (0.0024)
	0.6237	1.4853	
	0.6234	1.4863	
HH_36	0.6326	1.5007	
	0.6282	1.5121	
	0.6349	1.4982	1.5013 (0.0072)
	0.6213	1.5029	
	0.6329	1.4926	

APPENDIX B

Physicochemical characterization of raw materials and coated starches

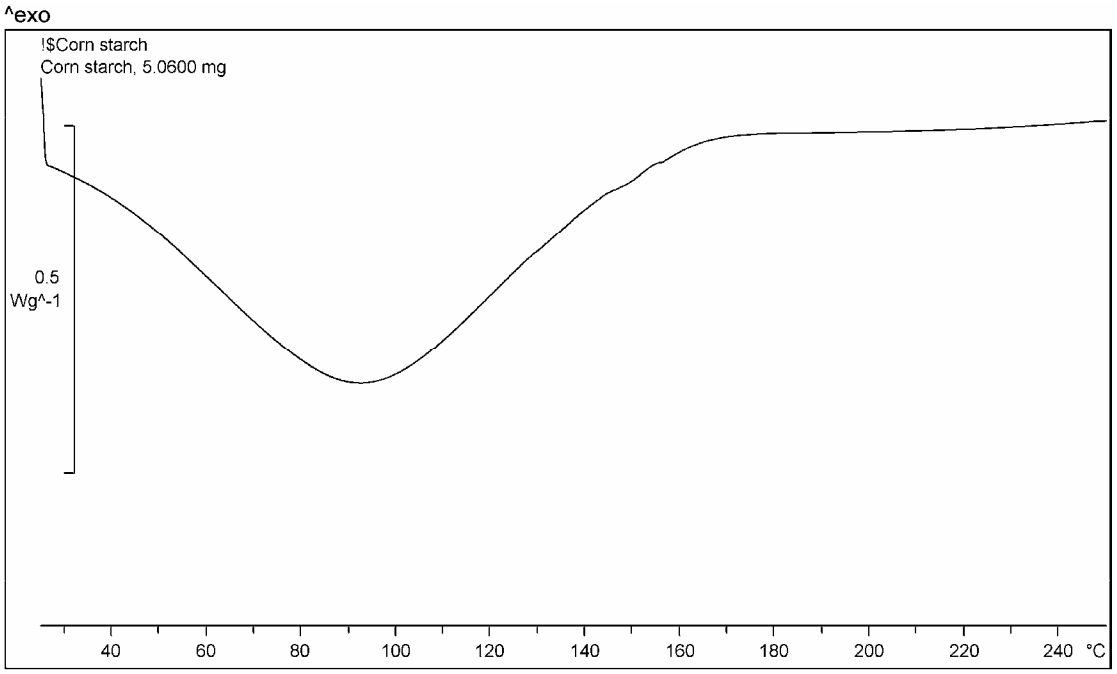

Figure 7-7 DSC thermogram of the uncoated corn starch

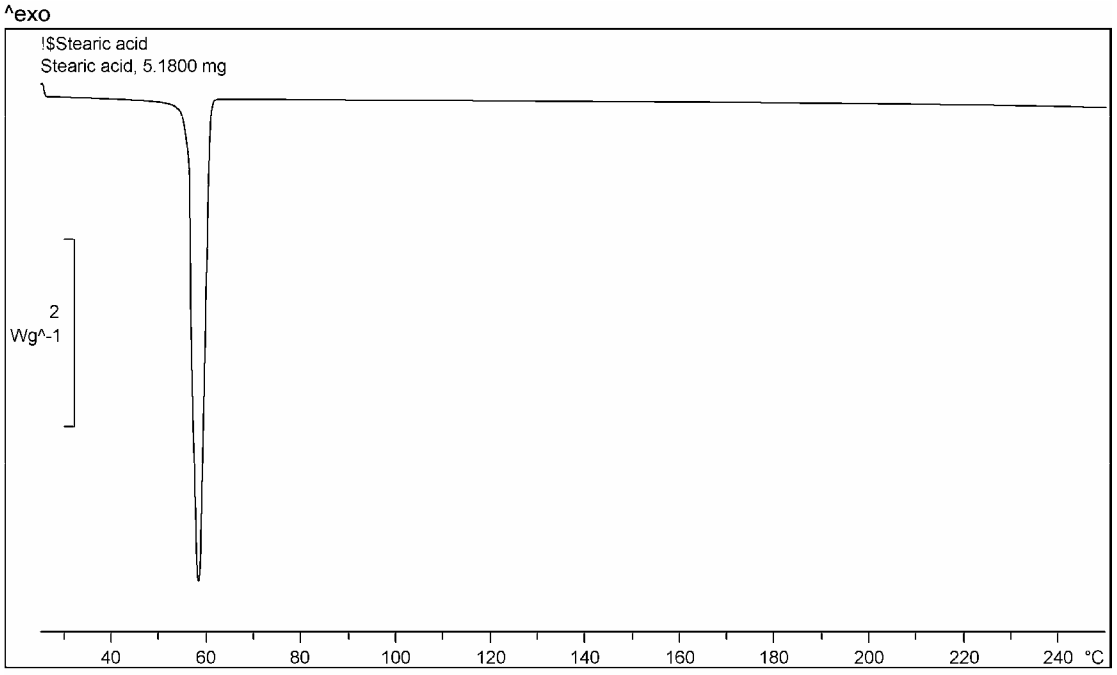

Figure 7-8 DSC thermogram of stearic acid

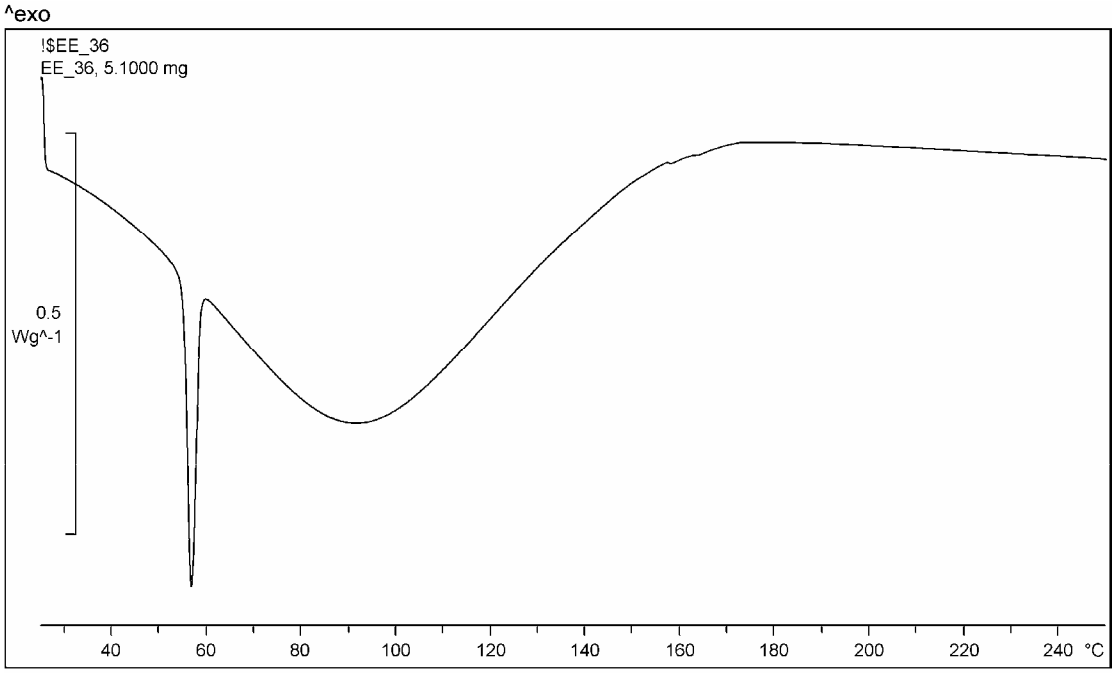

Figure 7-9 DSC thermogram of coated starch at ratio of corn starch and stearic acid of 2.8 : 0.2 grams, pressure 3000 psi and temperature 60 ^{o}C (EE_36)

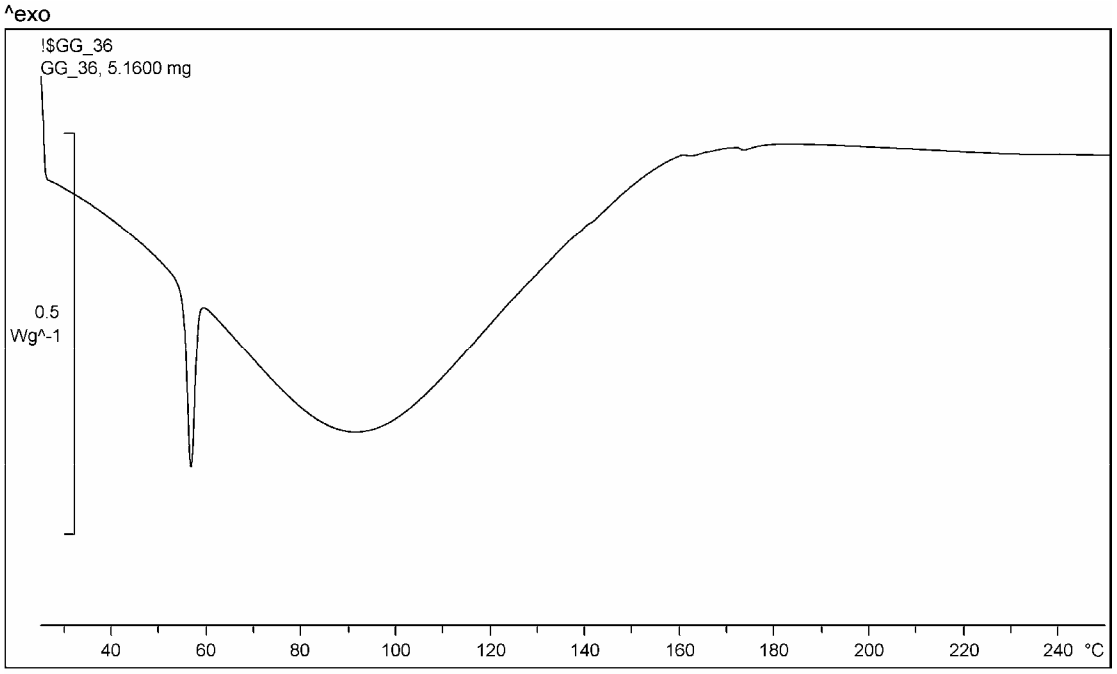

Figure 7-10 DSC thermogram of coated starch at ratio of corn starch and stearic acid of 2.9 : 0.1 grams, pressure 3000 psi and temperature 60 ^{o}C (GG_36)

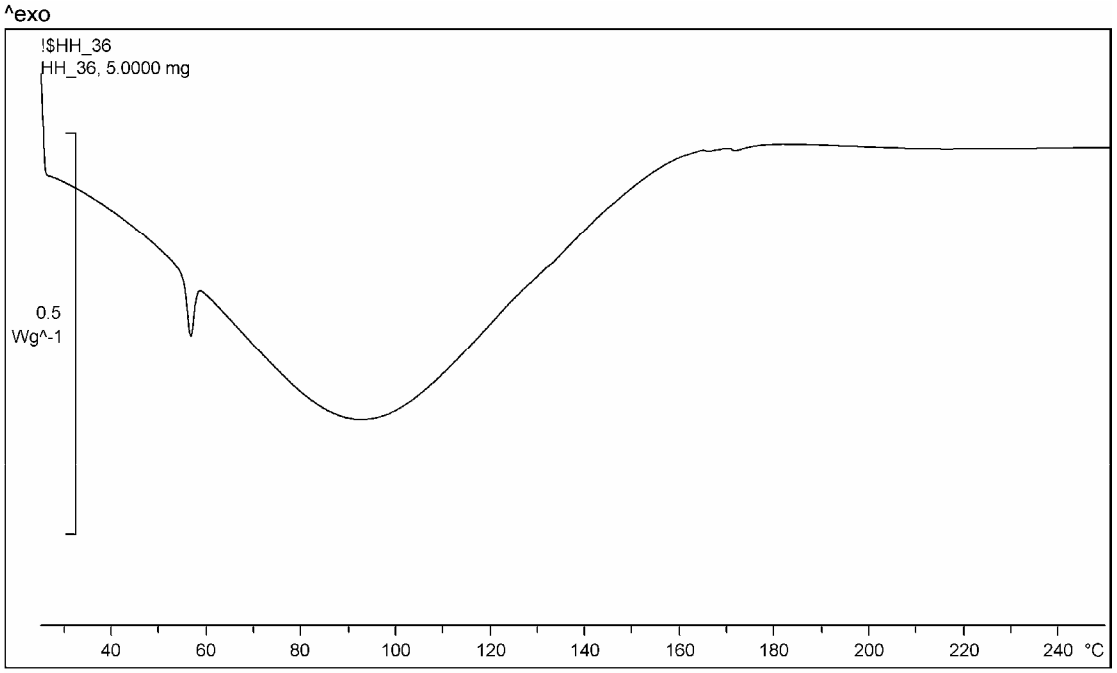

Figure 7-11 DSC thermogram of coated starch at ratio of corn starch and stearic acid of 2.95 : 0.05 grams, pressure 3000 psi and temperature 60 ^{o}C (HH_36)

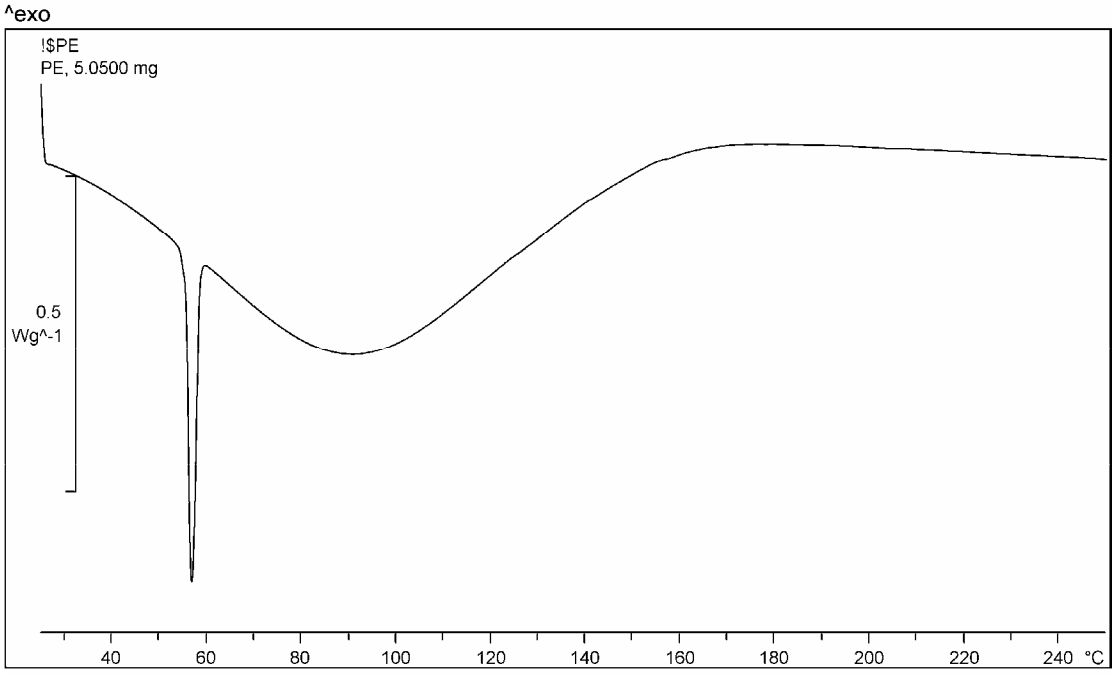

Figure 7-12 DSC thermogram of the physical mixtures of corn starch and stearic acid at ratio of 2.8 : 0.2 grams (PE)

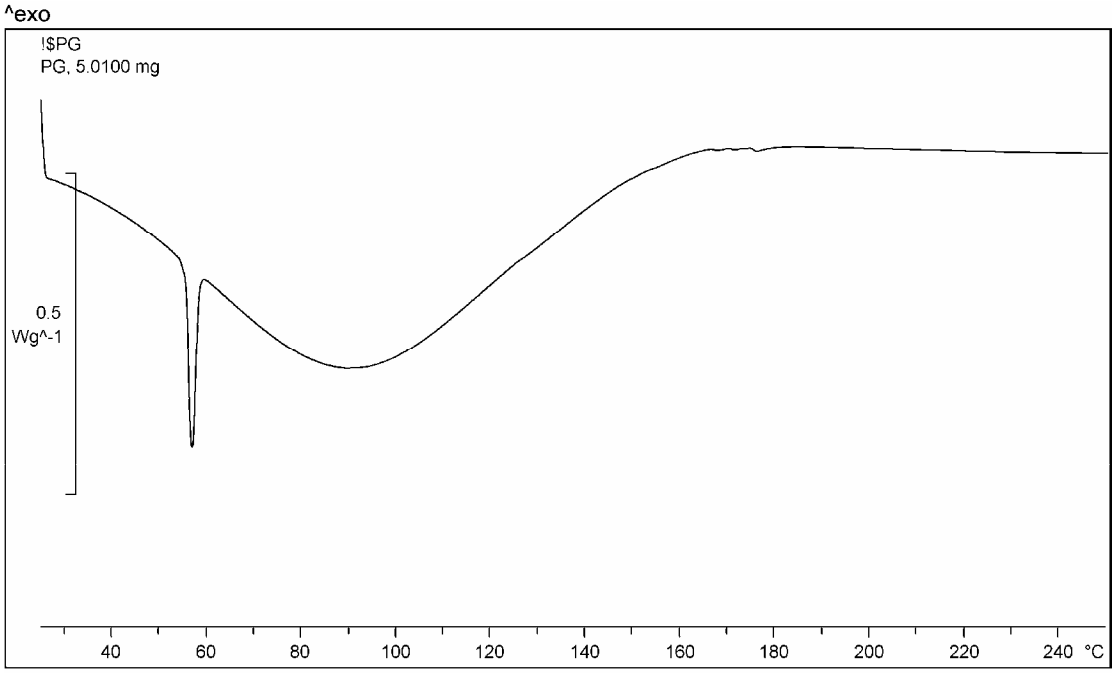

Figure 7-13 DSC thermogram of the physical mixtures of corn starch and stearic acid at ratio of 2.9 : 0.1 grams (PG)

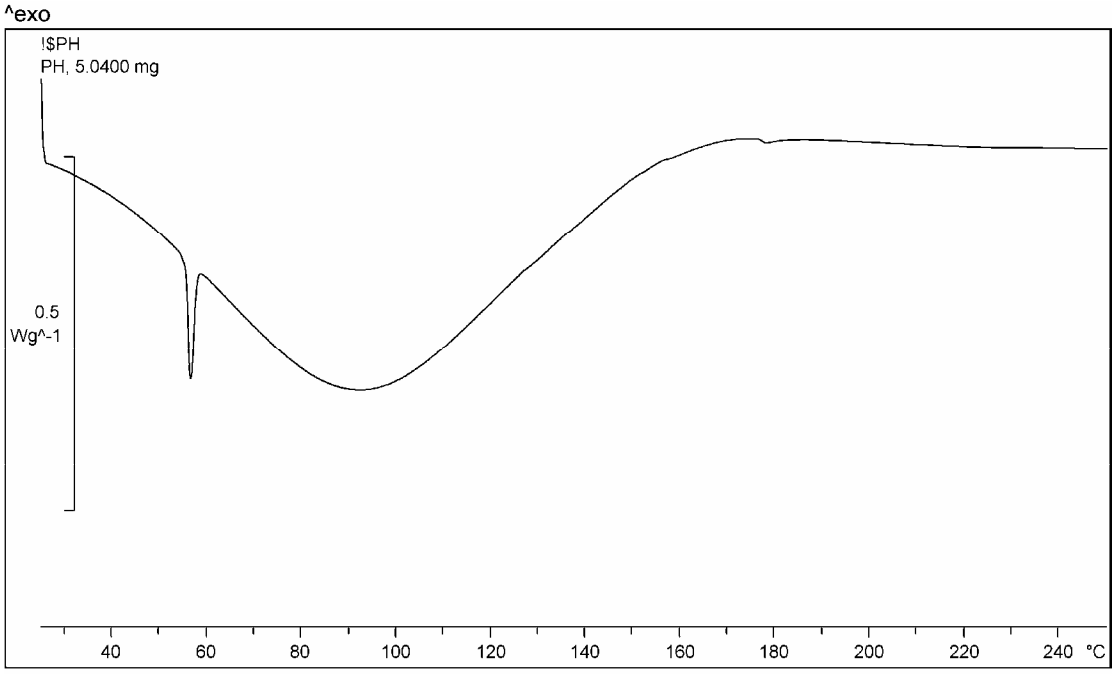

Figure 7-14 DSC thermogram of the physical mixtures of corn starch and stearic acid at ratio of 2.95 : 0.05 grams (PH)

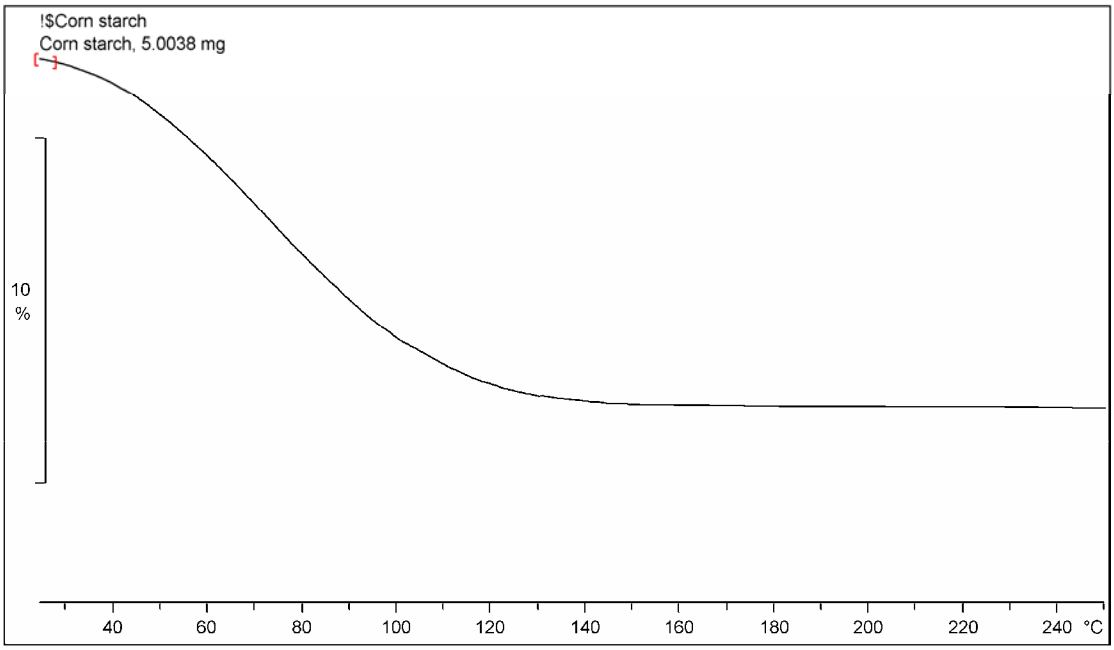

Figure 7-15 TG curve of the uncoated corn starch

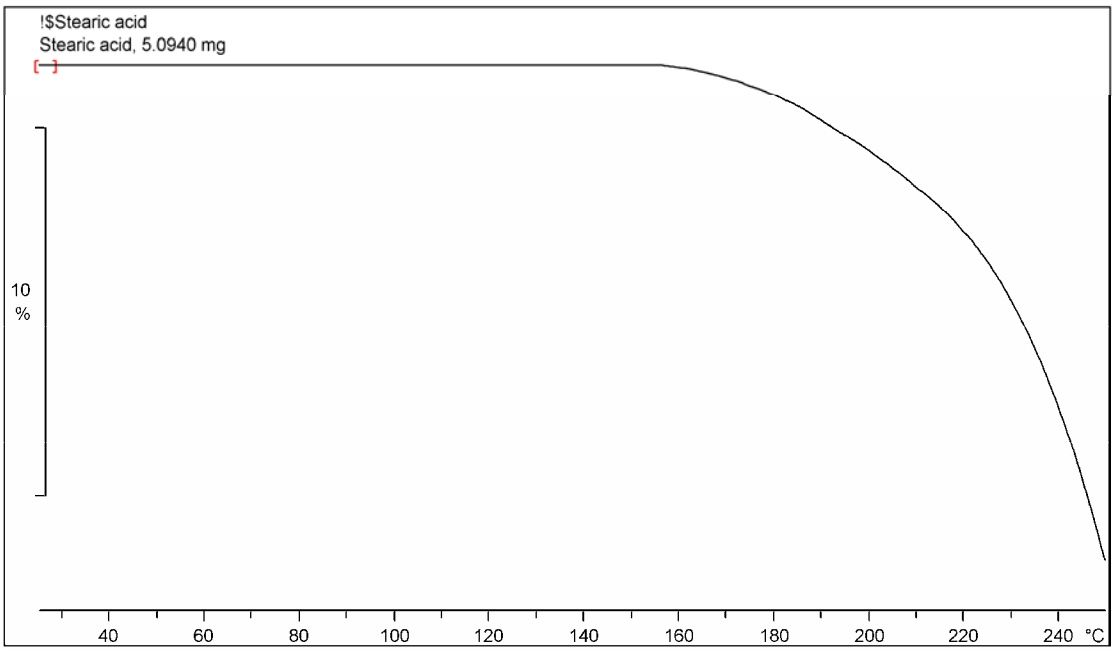

Figure 7-16 TG curve of stearic acid

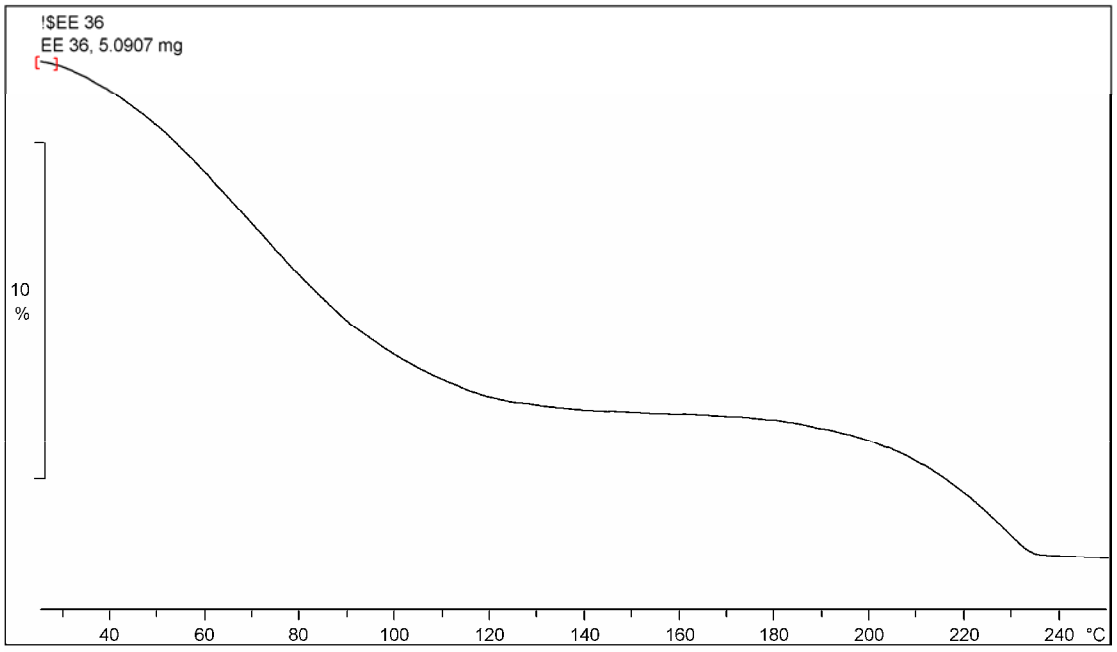

Figure 7-17 TG curve of coated starch at ratio of corn starch and stearic acid of 2.8 : 0.2 grams, pressure 3000 psi and temperature 60 ^{o}C (EE_36)

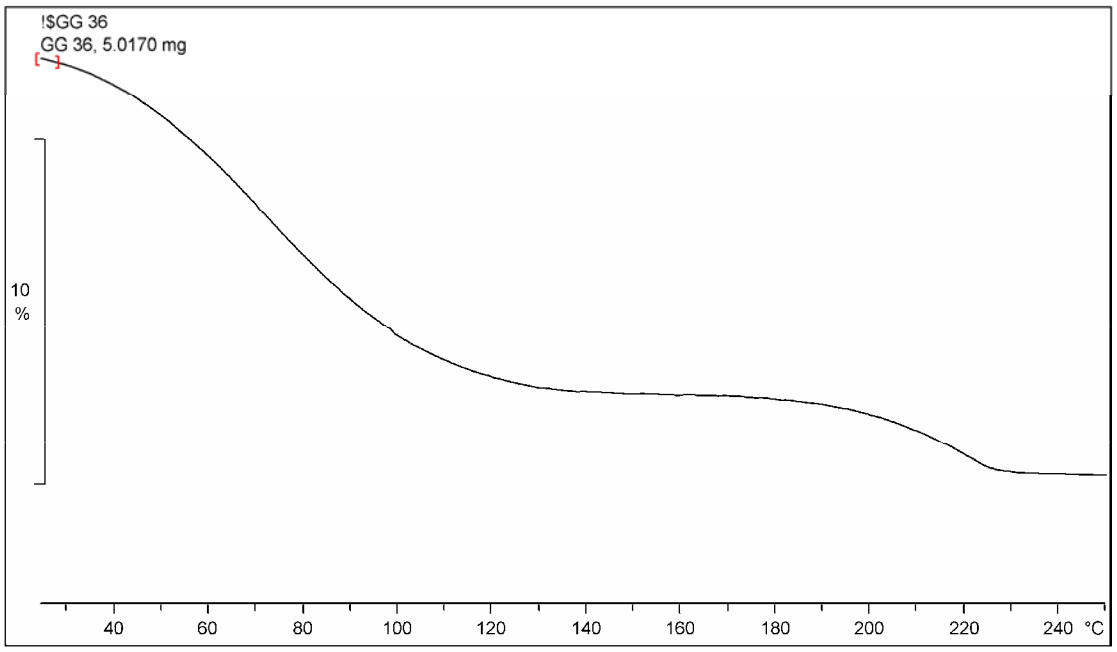

Figure 7-18 TG curve of coated starch at ratio of corn starch and stearic acid of 2.9 : 0.1 grams, pressure 3000 psi and temperature 60 ^{o}C (GG_36)

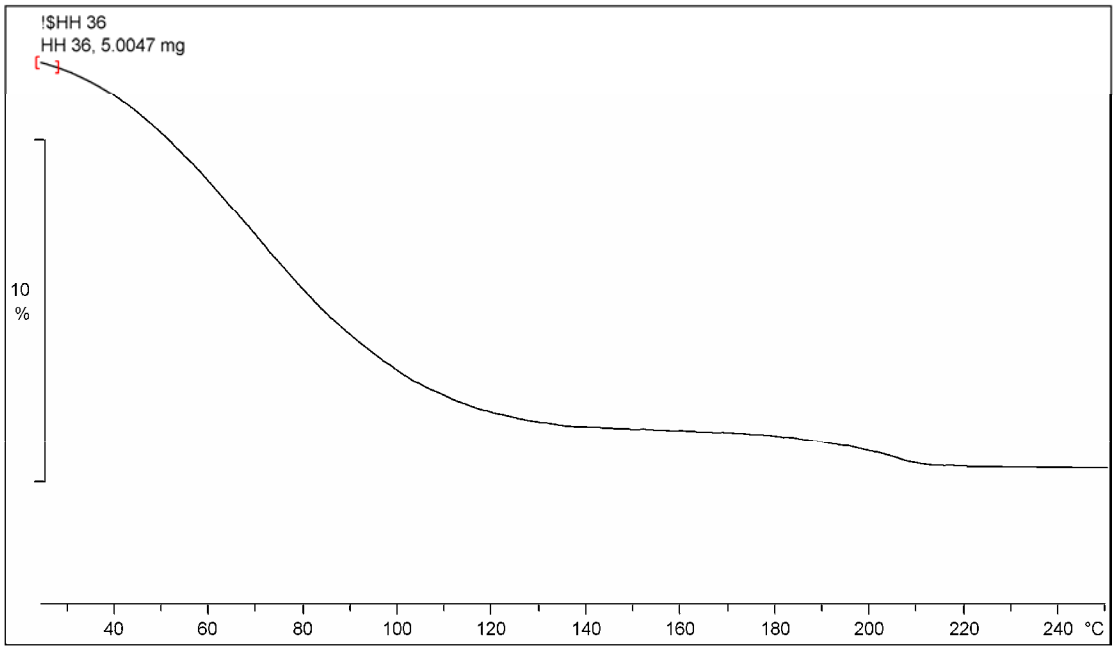

Figure 7-19 TG curve of coated starch at ratio of corn starch and stearic acid of 2.95 : 0.05 grams, pressure 3000 psi and temperature 60 ^{o}C (HH_36)

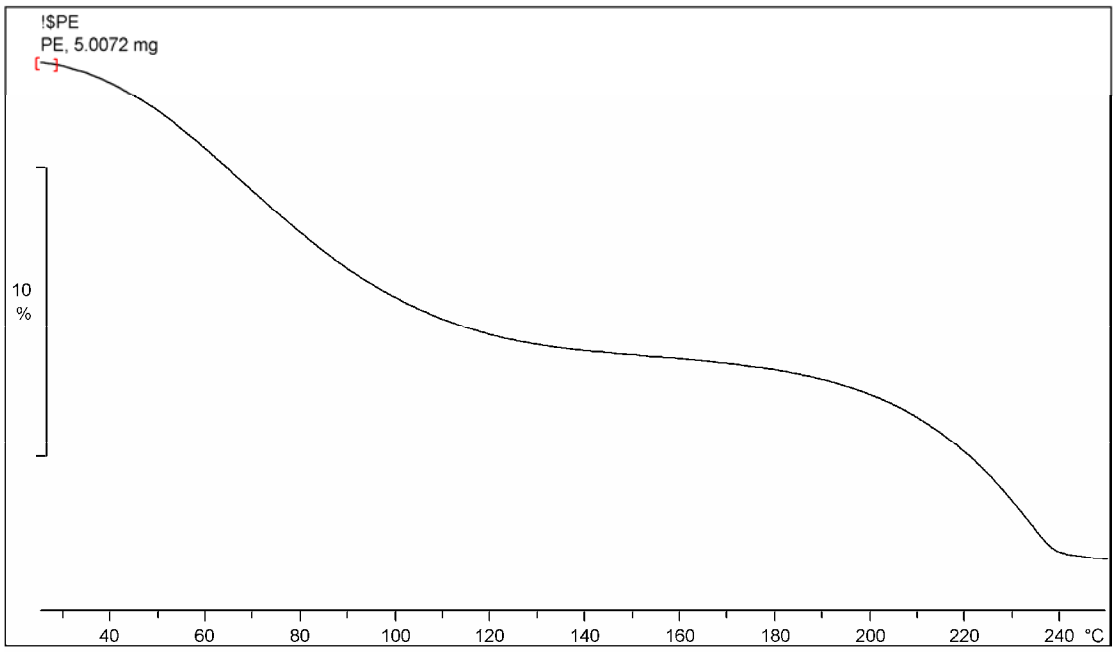

Figure 7-20 TG curve of the physical mixtures of corn starch and stearic acid at ratio of 2.8 : 0.2 grams (PE)

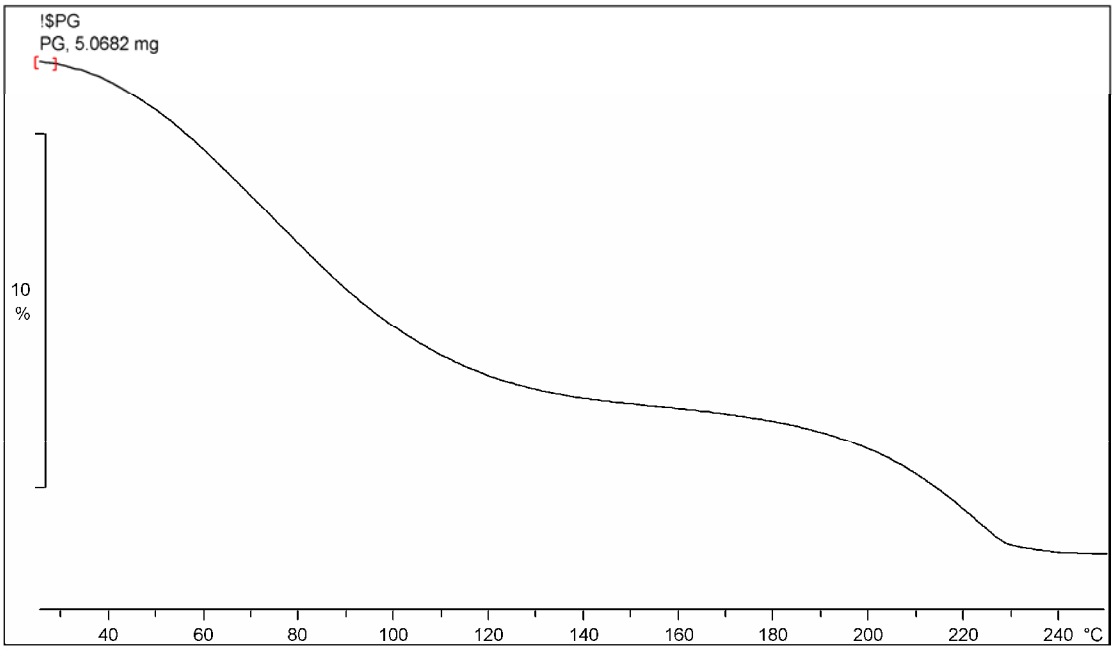

Figure 7-21 TG curve of the physical mixtures of corn starch and stearic acid at ratio of 2.9 : 0.1 grams (PG)

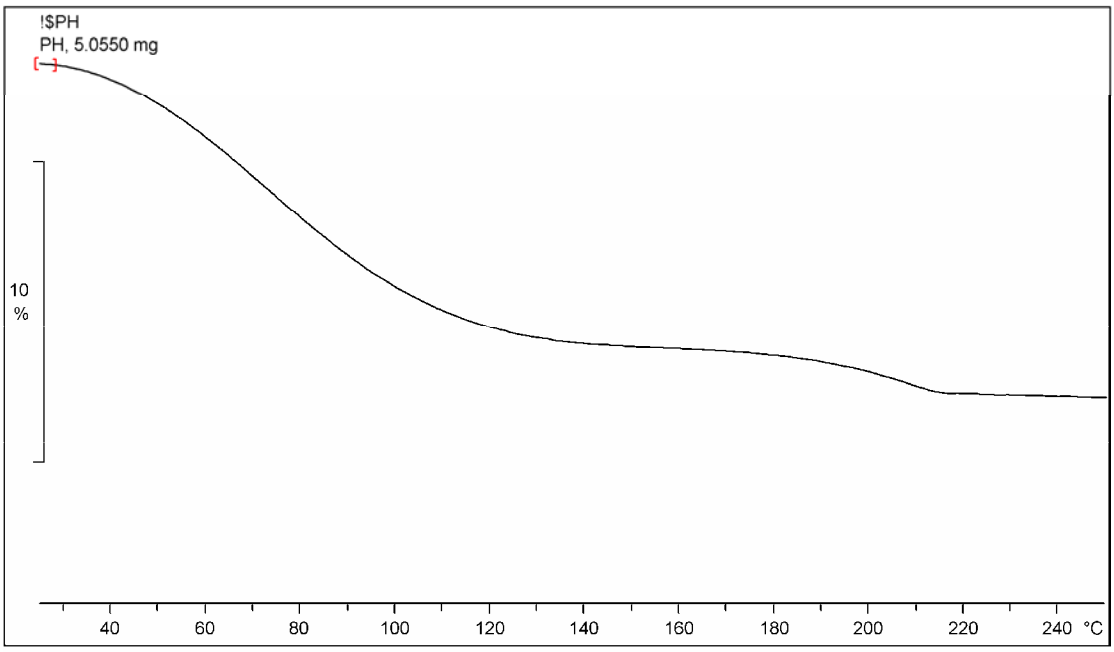

Figure 7-22 TG curve of the physical mixtures of corn starch and stearic acid at ratio of 2.95 : 0.05 grams (PH)

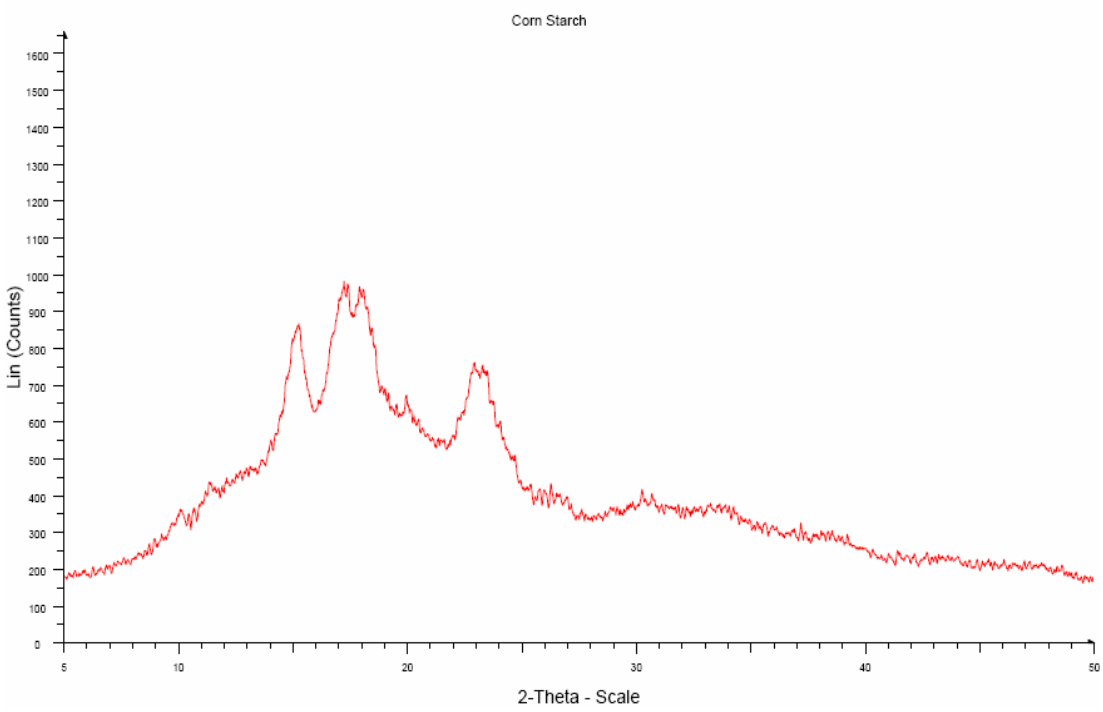

Figure 7-23 XRPD pattern of the uncoated corn starch

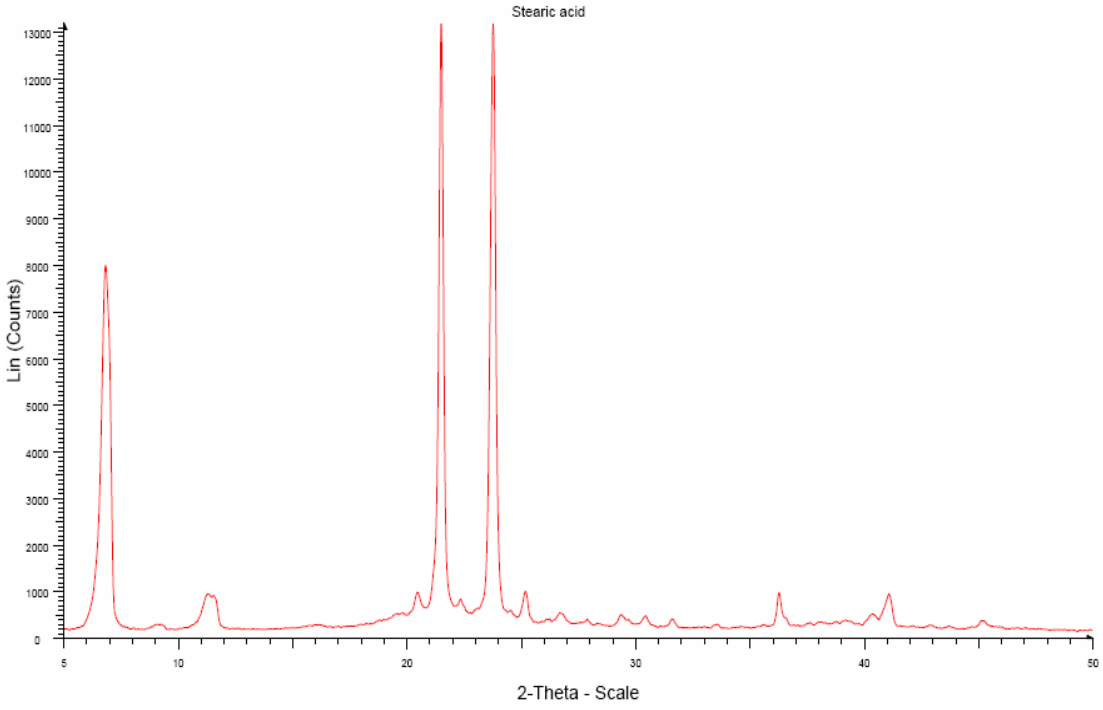

Figure 7-24 XRPD pattern of stearic acid

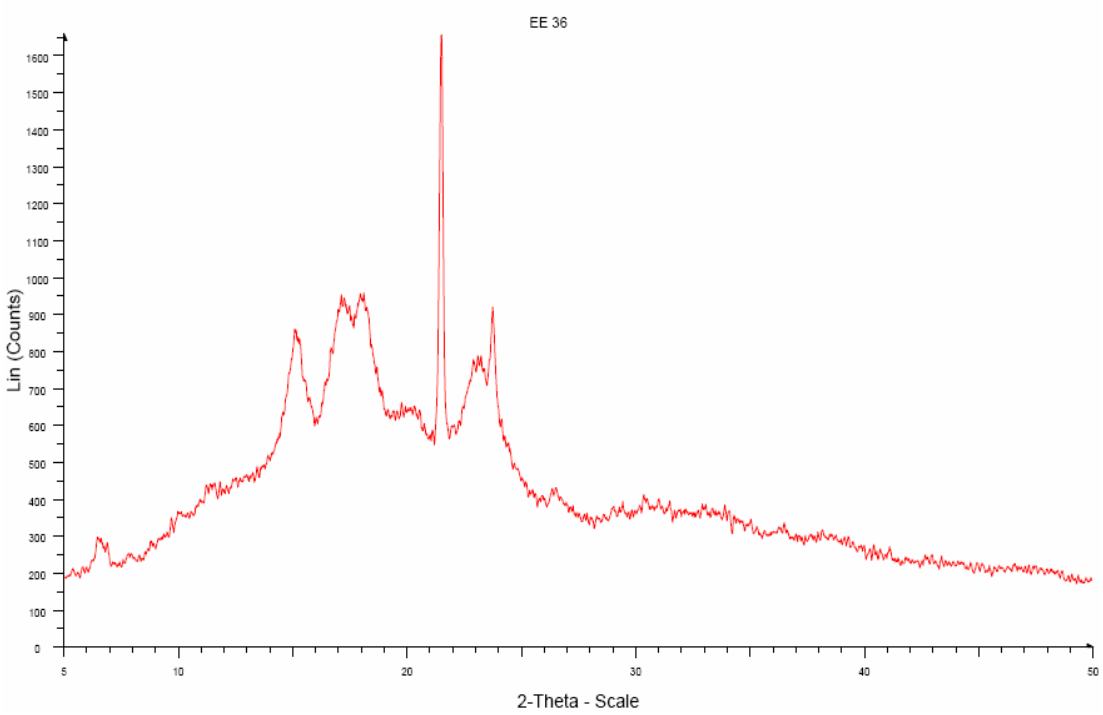

Figure 7-25 XRPD pattern of coated starch at ratio of corn starch and stearic acid of 2.8 : 0.2 grams, pressure 3000 psi and temperature 60 ^{o}C (EE_36)

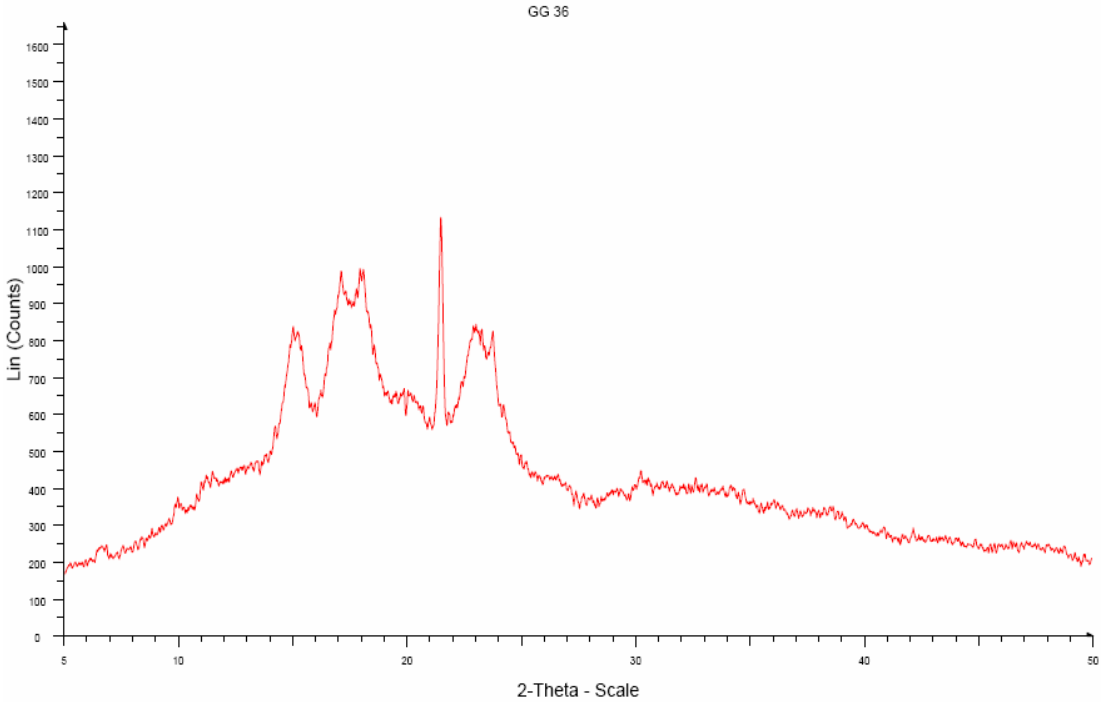

Figure 7-26 XRPD pattern of coated starch at ratio of corn starch and stearic acid of 2.9 : 0.1 grams, pressure 3000 psi and temperature 60 ^{o}C (GG_36)

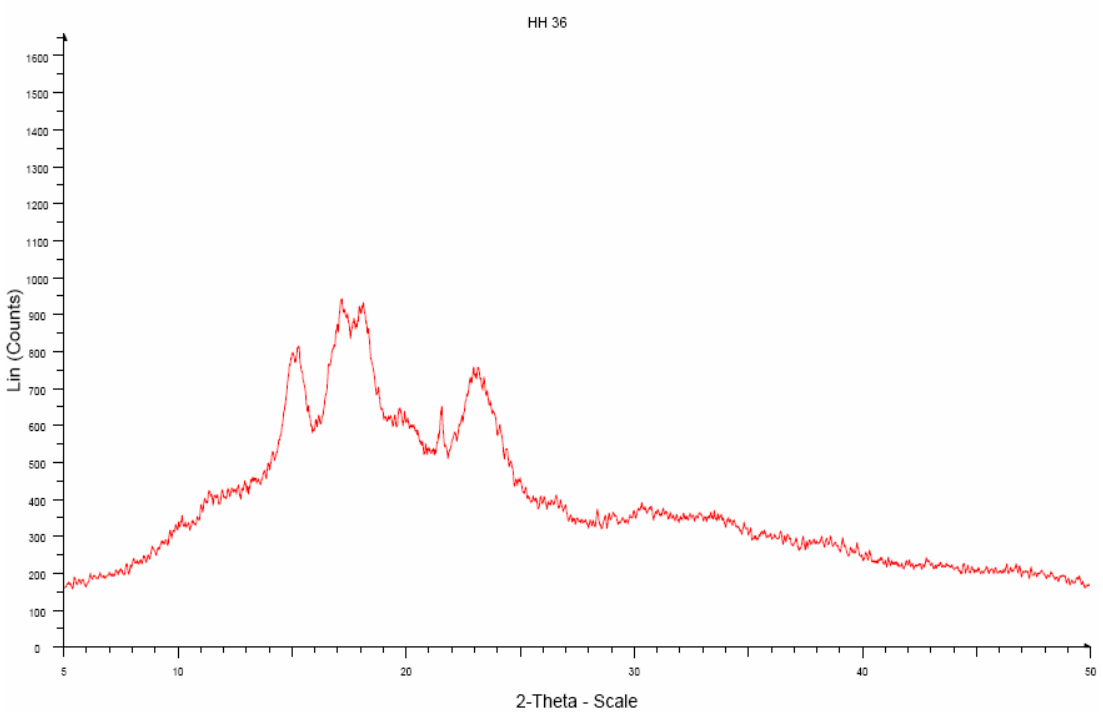

Figure 7-27 XRPD pattern of coated starch at ratio of corn starch and stearic acid of 2.95 : 0.05 grams, pressure 3000 psi and temperature 60 ^{o}C (HH_36)

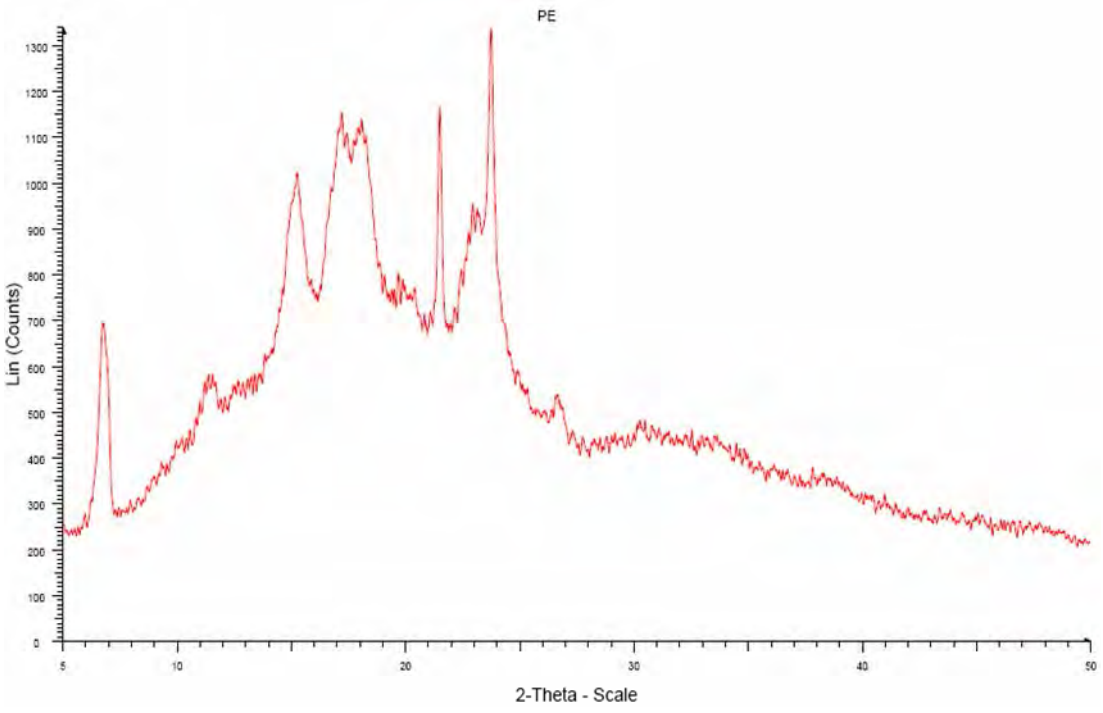

Figure 7-28 XRPD pattern of the physical mixtures of corn starch and stearic acid at ratio of 2.8 : 0.2 grams (PE)

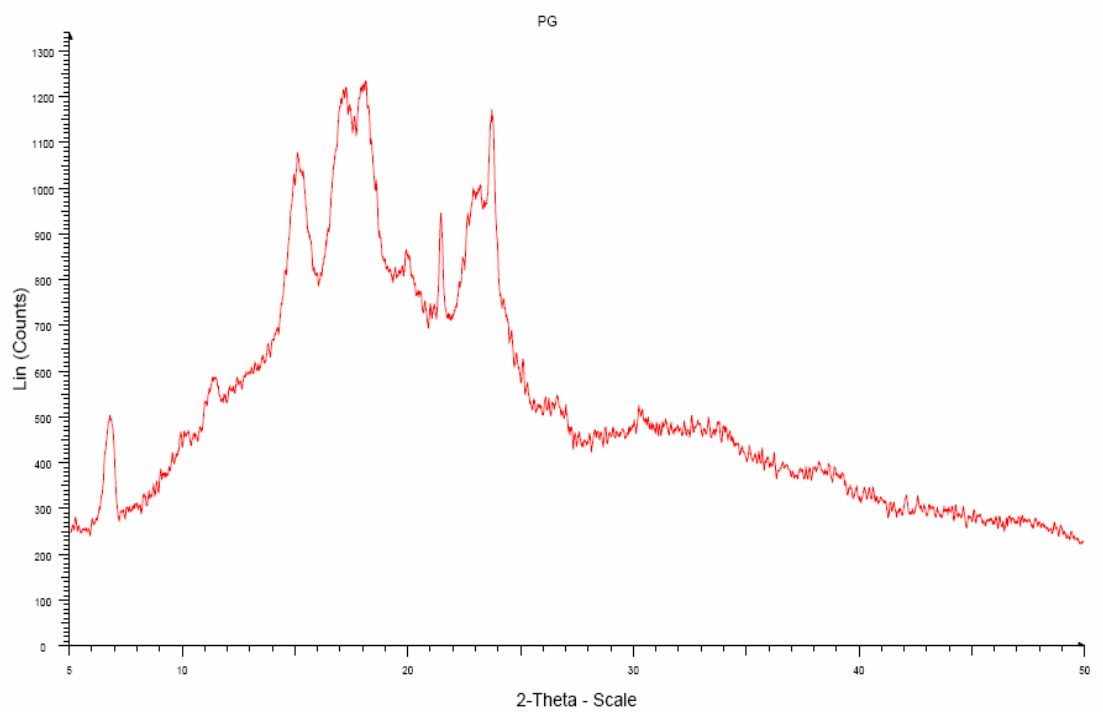

Figure 7-29 XRPD pattern of the physical mixtures of corn starch and stearic acid at ratio of 2.9 : 0.1 grams (PG)

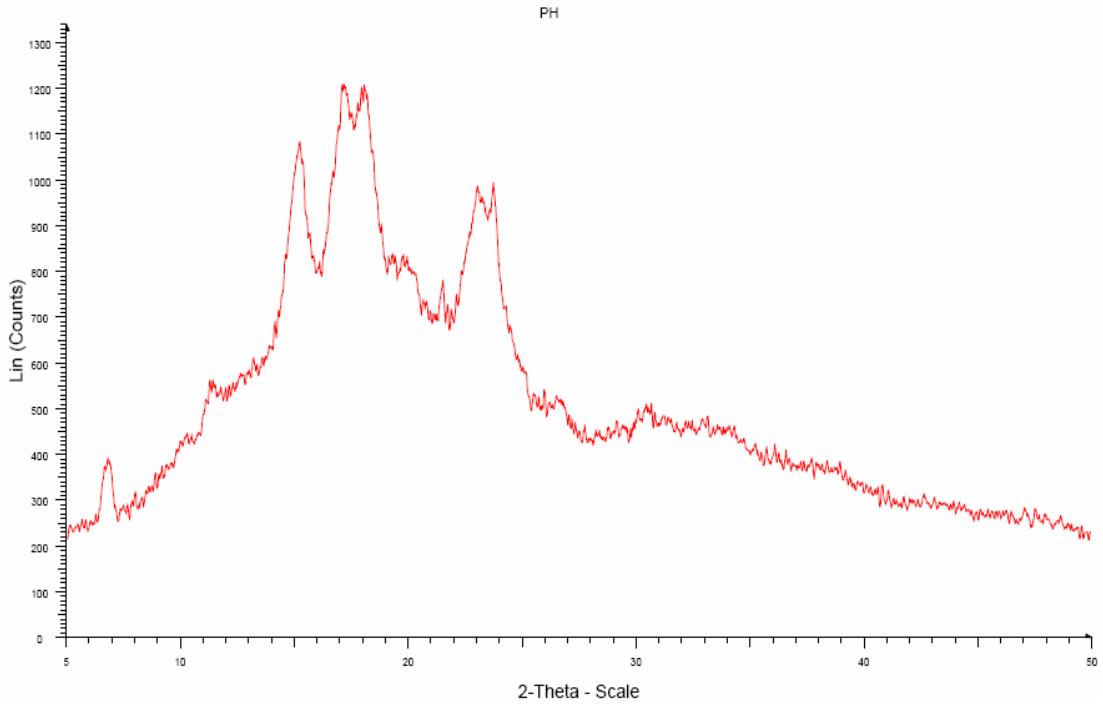

Figure 7-30 XRPD pattern of the physical mixtures of corn starch and stearic acid at ratio of 2.95 : 0.05 grams (PH)

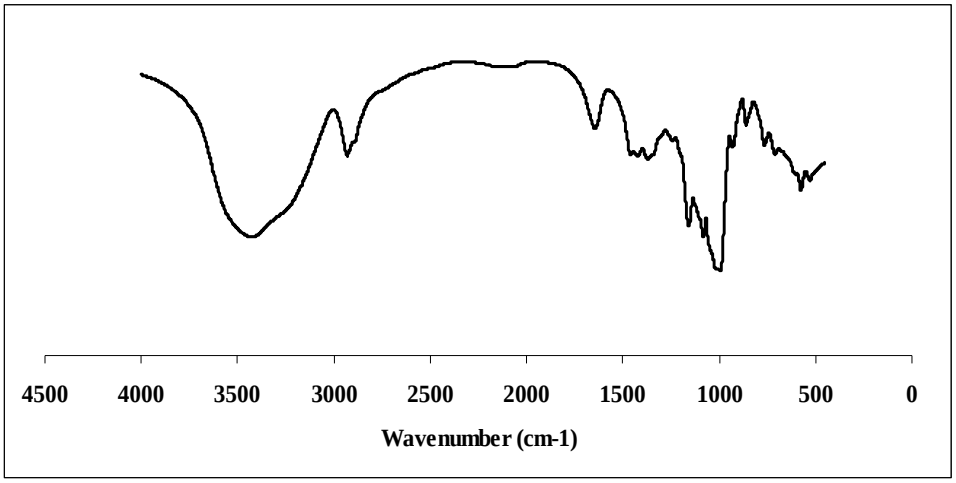

Figure 7-31 FT-IR spectra of the uncoated corn starch

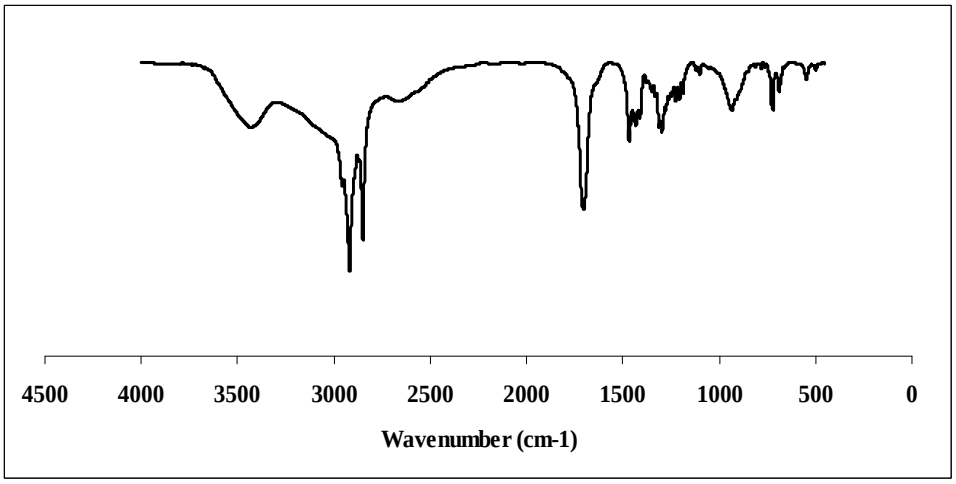

Figure 7-32 FT-IR spectra of stearic acid

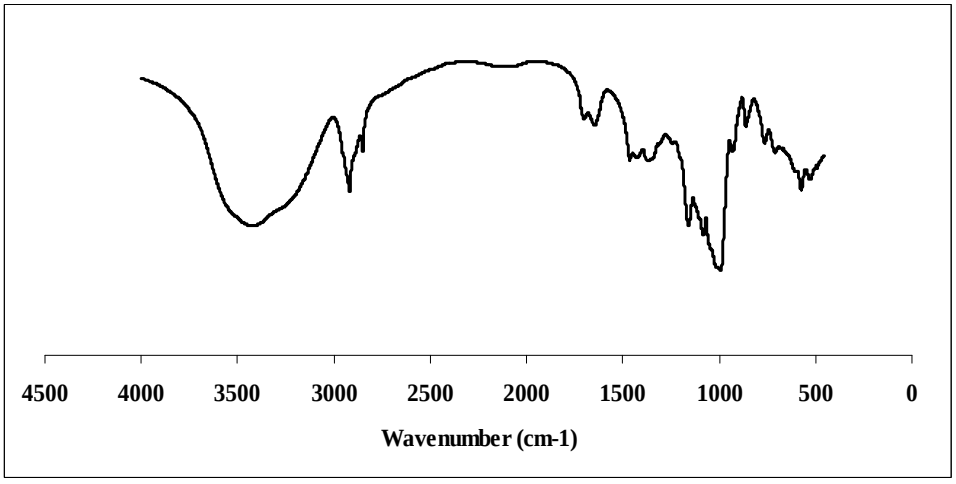

Figure 7-33 FT-IR spectra of coated starch at ratio of corn starch and stearic acid of 2.8 : 0.2 grams, pressure 3000 psi and temperature 60 ^{o}C (EE_36)

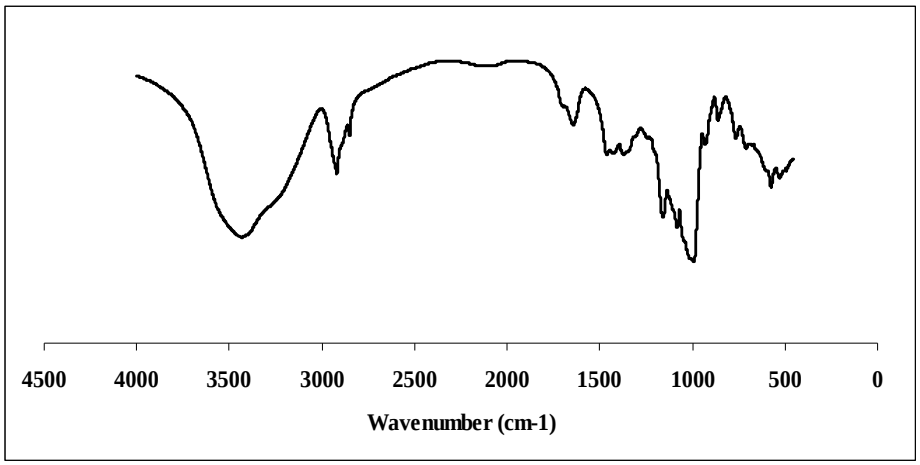

Figure 7-34 FT-IR spectra of coated starch at ratio of corn starch and stearic acid of 2.9 : 0.1 grams, pressure 3000 psi and temperature 60 ^{o}C (GG_36)

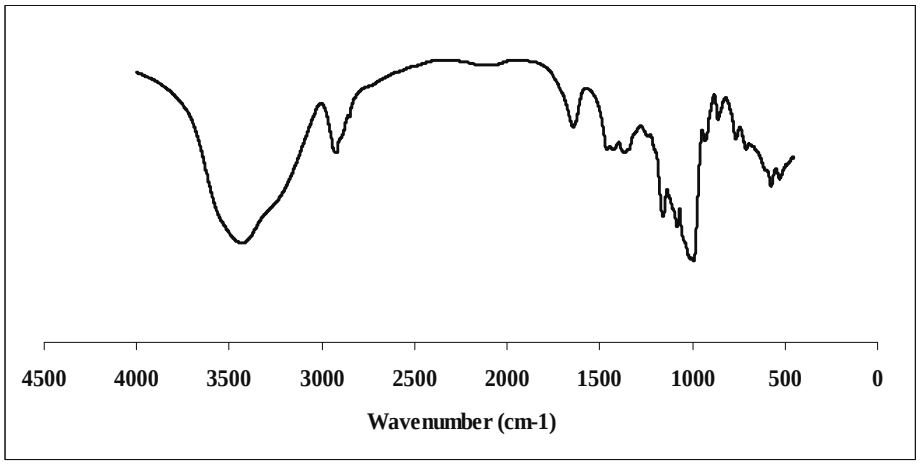

Figure 7-35 FT-IR spectra of coated starch at ratio of corn starch and stearic acid of 2.95 : 0.05 grams, pressure 3000 psi and temperature 60 ^{o}C (HH_36)

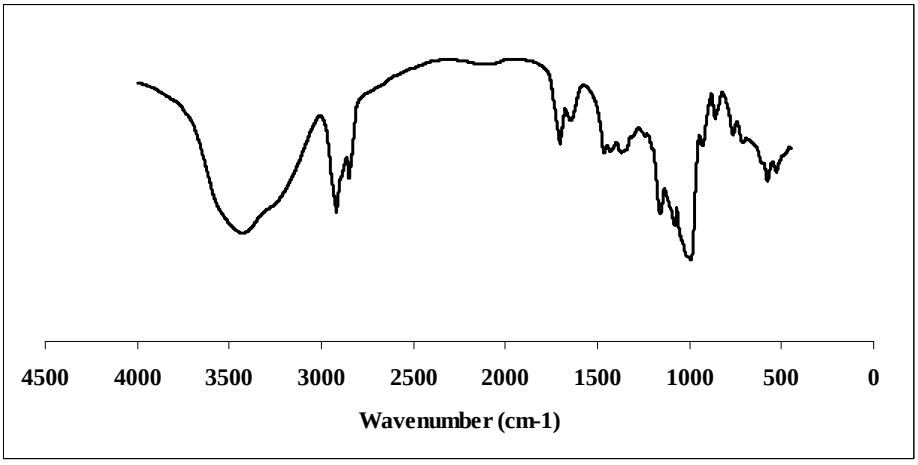

Figure 7-36 FT-IR spectra of the physical mixtures of corn starch and stearic acid at ratio of 2.8 : 0.2 grams (PE)

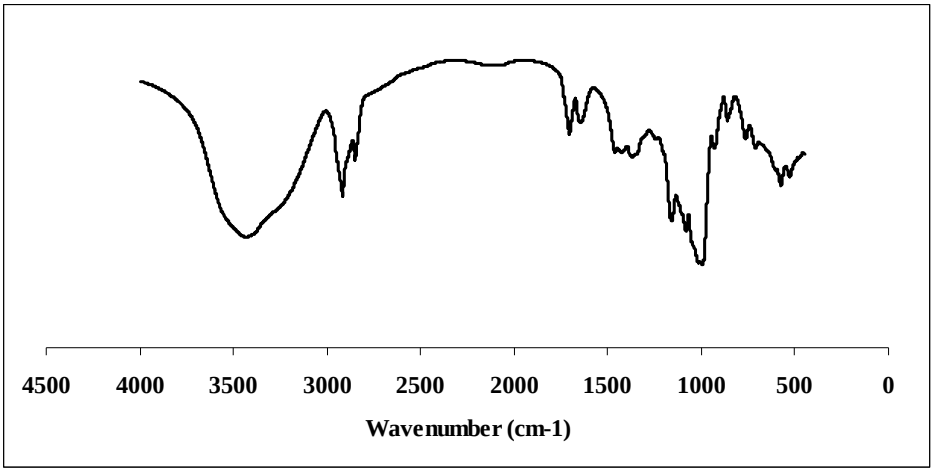

Figure 7-37 FT-IR spectra of the physical mixtures of corn starch and stearic acid at ratio of 2.9 : 0.1 grams (PG)

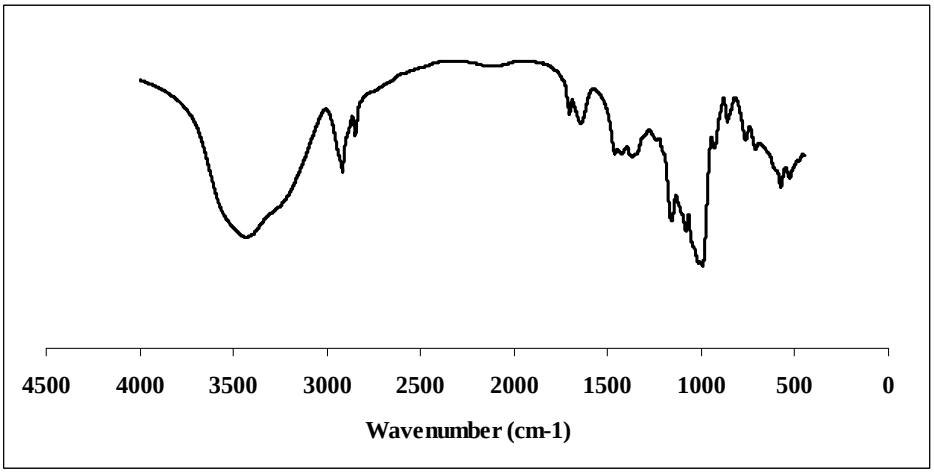

Figure 7-38 FT-IR spectra of the physical mixtures of corn starch and stearic acid at ratio of 2.95 : 0.05 grams (PH)

APPENDIX C

Characterization of powder mixes and tablet properties

Table 7-9 Flow rate and angle of repose of powder mixes

Formulation	Flow rate (g/sec)	Average (SD)	Angle of repose (^{O})	Average (SD)
BL	8.60	**8.58 (0.07)**	26.57	**26.65 (0.14)**
	8.51		26.57	
	8.64		26.82	
CS	8.46	**8.55 (0.11)**	27.07	**26.77 (0.40)**
	8.53		26.92	
	8.68		26.31	
EE	9.37	**9.48 (0.13)**	25.90	**26.00 (0.09)**
	9.62		26.05	
	9.46		26.05	
GG	9.11	**9.12 (0.18)**	26.41	**26.26 (0.41)**
	8.95		25.80	
	9.30		26.57	
HH	8.60	**8.61 (0.08)**	26.31	**26.73 (0.39)**
	8.70		27.07	
	8.53		26.82	
SS	8.87	**8.86 (0.04)**	27.33	**27.28 (0.08)**
	8.81		27.19	
	8.89		27.33	
SA	8.68	**8.75 (0.08)**	27.07	**27.02 (0.09)**
	8.75		27.07	
	8.83		26.92	
MG	8.26	**8.29 (0.03)**	27.57	**27.49 (0.14)**
	8.28		27.57	
	8.32		27.33	

Table 7-10 Tablet thickness, diameter and hardness of each formulation using an upper punch force of 25, 30 and 35 kilonewtons

Formulation	Upper punch force (kN)								
	25			30			35		
	Thickness (kp)	Diameter (mm)	Hardness (mm)	Thickness (kp)	Diameter (mm)	Hardness (mm)	Thickness (kp)	Diameter (mm)	Hardness (mm)
BL	4.13	9.55	9.50	3.89	9.58	15.53	3.75	9.58	21.58
	4.11	9.55	9.78	3.88	9.64	15.38	3.72	9.57	22.22
	4.10	9.55	9.22	3.89	9.56	16.24	3.69	9.63	21.92
	4.12	9.55	9.02	3.87	9.62	14.91	3.69	9.60	22.35
	4.12	9.55	9.15	3.88	9.58	16.54	3.66	9.54	22.00
	4.13	9.55	9.50	3.89	9.58	16.36	3.75	9.58	22.04
	4.11	9.55	9.78	3.88	9.64	15.79	3.72	9.57	20.81
	4.10	9.55	9.22	3.89	9.56	15.32	3.69	9.63	20.74
	4.12	9.55	9.02	3.87	9.62	16.26	3.69	9.60	21.70
	4.12	9.55	9.15	3.88	9.58	15.59	3.66	9.54	21.61
Average (SD)	**4.12 (0.01)**	**9.55 (0.00)**	**9.33 (0.29)**	**3.88 (0.01)**	**9.60 (0.03)**	**15.79 (0.54)**	**3.70 (0.03)**	**9.58 (0.03)**	**21.70 (0.55)**
CS	4.03	9.57	9.35	3.85	9.55	14.74	3.67	9.58	19.35
	3.99	9.59	8.55	3.84	9.58	15.15	3.65	9.56	21.55
	3.98	9.61	7.92	3.84	9.56	16.71	3.65	9.60	20.37
	3.98	9.61	9.53	3.81	9.55	15.04	3.63	9.55	21.06
	3.98	9.54	8.27	3.79	9.57	15.84	3.64	9.60	20.91
	4.03	9.57	8.67	3.85	9.55	15.73	3.61	9.59	19.73
	4.03	9.59	8.85	3.84	9.58	15.15	3.67	9.58	20.74
	3.99	9.61	8.68	3.84	9.56	16.71	3.65	9.56	21.08
	3.98	9.61	8.58	3.81	9.55	15.04	3.65	9.60	19.38
	4.03	9.54	9.14	3.79	9.56	15.84	3.63	9.55	20.30
Average (SD)	**4.00 (0.02)**	**9.58 (0.03)**	**8.75 (0.49)**	**3.83 (0.02)**	**9.56 (0.01)**	**15.60 (0.70)**	**3.65 (0.02)**	**9.58 (0.02)**	**20.45 (0.76)**

Table 7-10 Tablet thickness, diameter and hardness of each formulation using an upper punch force of 25, 30 and 35 kilonewtons (cont.)

Formulation	Upper punch force (kN)								
	25			30			35		
	Thickness (kp)	Diameter (mm)	Hardness (mm)	Thickness (kp)	Diameter (mm)	Hardness (mm)	Thickness (kp)	Diameter (mm)	Hardness (mm)
EE	4.04	9.63	6.80	3.84	9.63	11.54	3.73	9.59	13.22
	4.03	9.59	6.52	3.84	9.61	11.67	3.71	9.60	14.56
	4.02	9.57	6.37	3.82	9.64	10.34	3.70	9.59	13.45
	4.00	9.63	6.71	3.79	9.61	10.81	3.65	9.60	14.24
	4.00	9.61	6.05	3.77	9.60	10.56	3.68	9.60	12.93
	4.04	9.63	6.03	3.84	9.62	11.75	3.73	9.61	14.22
	4.03	9.59	6.27	3.84	9.64	10.21	3.71	9.58	15.26
	4.02	9.57	6.87	3.82	9.63	11.57	3.70	9.60	13.45
	4.00	9.63	6.61	3.79	9.60	11.74	3.65	9.62	15.24
	4.00	9.61	6.67	3.77	9.63	10.65	3.68	9.62	12.57
Average (SD)	**4.02 (0.02)**	**9.61 (0.02)**	**6.49 (0.30)**	**3.81 (0.03)**	**9.62 (0.02)**	**11.08 (0.63)**	**3.69 (0.03)**	**9.60 (0.01)**	**13.91 (0.94)**
GG	4.02	9.57	5.76	3.85	9.57	10.90	3.73	9.57	14.86
	4.04	9.60	7.23	3.85	9.64	10.72	3.70	9.59	14.93
	4.07	9.59	6.73	3.80	9.59	12.13	3.69	9.58	15.54
	4.06	9.54	6.34	3.82	9.63	10.55	3.66	9.61	14.94
	4.03	9.63	5.87	3.79	9.63	11.10	3.67	9.57	14.29
	4.00	9.61	6.09	3.85	9.56	11.21	3.73	9.57	14.93
	4.03	9.58	6.04	3.85	9.58	11.53	3.70	9.59	14.76
	4.07	9.60	6.10	3.80	9.60	12.12	3.69	9.57	14.81
	4.06	9.62	7.97	3.82	9.64	10.62	3.66	9.60	14.87
	4.03	9.62	7.29	3.81	9.63	12.93	3.67	9.57	14.75
Average (SD)	**4.04 (0.02)**	**9.60 (0.03)**	**6.54 (0.74)**	**3.82 (0.02)**	**9.61 (0.03)**	**11.38 (0.79)**	**3.69 (0.03)**	**9.58 (0.01)**	**14.87 (0.30)**

Table 7-10 Tablet thickness, diameter and hardness of each formulation using an upper punch force of 25, 30 and 35 kilonewtons (cont.)

Formulation	Upper punch force (kN)								
	25			30			35		
	Thickness (kp)	Diameter (mm)	Hardness (mm)	Thickness (kp)	Diameter (mm)	Hardness (mm)	Thickness (kp)	Diameter (mm)	Hardness (mm)
HH	4.03	9.60	8.05	3.86	9.63	12.79	3.75	9.58	17.86
	4.02	9.60	8.05	3.87	9.61	12.54	3.71	9.57	19.09
	4.04	9.59	7.16	3.83	9.64	12.92	3.71	9.63	17.75
	4.07	9.54	7.82	3.82	9.61	13.65	3.68	9.60	18.15
	3.99	9.55	7.79	3.84	9.60	11.72	3.68	9.59	18.67
	4.06	9.54	7.24	3.86	9.62	11.61	3.75	9.58	18.61
	4.02	9.58	7.99	3.87	9.64	11.55	3.71	9.57	19.01
	4.04	9.60	7.90	3.83	9.63	12.31	3.71	9.63	17.83
	4.07	9.55	7.44	3.82	9.60	11.47	3.68	9.60	19.03
	3.99	9.59	7.75	3.84	9.63	13.33	3.68	9.59	18.42
Average (SD)	**4.03 (0.03)**	**9.57 (0.03)**	**7.72 (0.33)**	**3.84 (0.02)**	**9.62 (0.02)**	**12.39 (0.79)**	**3.71 (0.03)**	**9.59 (0.02)**	**18.44 (0.52)**
SS	4.02	9.63	8.13	3.81	9.59	13.70	3.70	9.57	18.34
	4.01	9.61	8.01	3.80	9.60	14.32	3.69	9.60	20.27
	3.96	9.59	7.93	3.79	9.59	14.82	3.66	9.59	18.29
	3.96	9.60	8.06	3.77	9.60	14.20	3.64	9.63	19.18
	3.97	9.58	8.17	3.76	9.60	13.33	3.63	9.63	18.68
	4.02	9.62	8.10	3.81	9.61	13.93	3.70	9.57	18.82
	4.01	9.64	8.38	3.80	9.58	13.14	3.69	9.58	19.72
	3.96	9.63	7.92	3.79	9.60	13.63	3.66	9.60	18.94
	3.96	9.60	8.01	3.76	9.62	13.62	3.64	9.63	18.97
	3.97	9.63	7.76	3.77	9.62	12.84	3.63	9.63	19.10
Average (SD)	**3.98 (0.03)**	**9.61 (0.02)**	**8.05 (0.17)**	**3.79 (0.02)**	**9.60 (0.01)**	**13.75 (0.59)**	**3.66 (0.03)**	**9.60 (0.03)**	**19.03 (0.60)**

Table 7-10 Tablet thickness, diameter and hardness of each formulation using an upper punch force of 25, 30 and 35 kilonewtons (cont.)

Formulation	Upper punch force (kN)								
	25			30			35		
	Thickness (kp)	Diameter (mm)	Hardness (mm)	Thickness (kp)	Diameter (mm)	Hardness (mm)	Thickness (kp)	Diameter (mm)	Hardness (mm)
SA	4.03	9.63	6.67	3.84	9.57	11.40	3.71	9.56	16.43
	3.98	9.61	6.72	3.84	9.64	12.72	3.70	9.61	16.19
	4.01	9.64	6.82	3.82	9.59	11.82	3.70	9.59	15.44
	4.01	9.61	7.22	3.79	9.63	11.98	3.65	9.57	15.79
	4.02	9.61	6.92	3.79	9.63	12.14	3.67	9.55	15.83
	4.03	9.62	6.74	3.84	9.56	11.55	3.71	9.57	15.99
	3.98	9.64	7.08	3.84	9.58	11.92	3.70	9.58	16.53
	4.01	9.63	6.96	3.82	9.60	12.10	3.70	9.59	17.33
	4.01	9.60	6.91	3.79	9.64	12.22	3.65	9.59	16.49
	4.00	9.63	7.26	3.79	9.63	12.65	3.67	9.59	15.76
Average (SD)	**4.01 (0.02)**	**9.62 (0.01)**	**6.93 (0.20)**	**3.82 (0.02)**	**9.61 (0.03)**	**12.05 (0.42)**	**3.69 (0.02)**	**9.58 (0.02)**	**16.18 (0.54)**
MG	4.01	9.63	7.18	3.80	9.58	12.31	3.63	9.63	14.71
	4.02	9.61	6.95	3.81	9.57	12.08	3.64	9.59	15.62
	3.99	9.64	6.25	3.74	9.61	12.27	3.65	9.61	15.89
	3.97	9.61	6.31	3.77	9.60	12.24	3.66	9.60	14.36
	3.94	9.60	6.36	3.74	9.59	10.98	3.65	9.61	15.02
	4.01	9.62	6.35	3.80	9.58	11.44	3.63	9.63	16.83
	4.02	9.64	7.21	3.81	9.57	11.79	3.64	9.59	15.16
	3.99	9.63	6.39	3.74	9.61	12.99	3.65	9.61	13.80
	3.97	9.60	7.05	3.77	9.60	12.47	3.66	9.60	13.59
	3.94	9.63	6.73	3.74	9.59	11.12	3.65	9.61	14.78
Average (SD)	**3.99 (0.03)**	**9.62 (0.02)**	**6.68 (0.39)**	**3.77 (0.03)**	**9.59 (0.01)**	**11.97 (0.63)**	**3.65 (0.01)**	**9.61 (0.01)**	**14.98 (0.97)**

Table 7-11 Tablet friability of each formulation using an upper punch force of 25, 30 and 35 kilonewtons

Formulation	Upper punch force (kN)					
	25		30		35	
	Friability (%)	Average (SD)	Friability (%)	Average (SD)	Friability (%)	Average (SD)
BL	0.430	**0.439**	0.346	**0.333**	0.236	**0.236**
	0.471	**(0.029)**	0.332	**(0.014)**	0.223	**(0.013)**
	0.416		0.319		0.250	
CS	0.444	**0.458**	0.375	**0.375**	0.208	**0.277**
	0.486	**(0.024)**	0.375	**(0.000)**	0.278	**(0.069)**
	0.445		0.375		0.347	
EE	0.361	**0.417**	0.306	**0.310**	0.251	**0.236**
	0.419	**(0.055)**	0.320	**()0.008**	0.249	**()0.024**
	0.471		0.305		0.208	
GG	0.418	**0.366**	0.195	**0.278**	0.195	**0.222**
	0.333	**(0.046)**	0.264	**(0.090)**	0.194	**(0.048)**
	0.346		0.373		0.277	
HH	0.376	**0.444**	0.404	**0.352**	0.153	**0.264**
	0.541	**(0.086)**	0.403	**(0.089)**	0.346	**(0.099)**
	0.416		0.249		0.292	
SS	0.334	**0.403**	0.222	**0.306**	0.292	**0.236**
	0.444	**(0.060)**	0.306	**(0.084)**	0.208	**(0.049)**
	0.431		0.390		0.208	
SA	0.487	**0.431**	0.334	**0.315**	0.334	**0.236**
	0.376	**(0.055)**	0.320	**(0.022)**	0.208	**(0.087)**
	0.429		0.291		0.166	
MG	0.388	**0.384**	0.235	**0.297**	0.249	**0.236**
	0.348	**(0.035)**	0.363	**(0.064)**	0.195	**(0.036)**
	0.417		0.291		0.264	

Table 7-12 Disintegration time of tablet for each formulation using an upper punch force of 25, 30 and 35 kilonewtons

Formulation	Upper punch force (kN)					
	25		30		35	
	Time (min)	Average (SD)	Time (min)	Average (SD)	Time (min)	Average (SD)
BL	01:13	**00:56**	05:18	**04:24**	07:45	**06:58**
	00:48	**(0.00)**	03:57	**(0.00)**	06:57	**(0.00)**
	00:45		03:23		05:49	
	00:47		04:49		06:39	
	00:59		05:28		07:38	
	01:05		03:30		07:01	
CS	01:09	**00:45**	04:53	**03:56**	05:53	**06:57**
	00:29	**(0.00)**	03:29	**(0.00)**	06:54	**(0.00)**
	01:07		04:16		06:36	
	00:40		03:57		07:43	
	00:36		02:59		06:46	
	00:31		04:04		07:52	
EE	04:38	**03:50**	07:51	**06:58**	10:06	**09:00**
	02:57	**(0.00)**	06:56	**(0.00)**	08:57	**(0.00)**
	03:41		05:37		09:40	
	02:53		08:01		09:21	
	02:14		05:49		08:03	
	03:07		07:35		07:54	
GG	04:07	**03:15**	07:36	**06:38**	08:46	**07:48**
	02:41	**(0.00)**	05:18	**(0.00)**	07:47	**(0.00)**
	03:02		07:23		07:28	
	02:54		06:58		06:35	
	03:08		05:49		08:13	
	03:36		06:47		07:58	
HH	01:38	**01:01**	05:43	**04:56**	07:43	**07:04**
	00:49	**(0.00)**	03:49	**(0.00)**	06:31	**(0.00)**
	01:01		04:56		06:44	
	00:54		04:04		05:59	
	00:41		05:28		07:36	
	01:05		05:39		07:52	
SS	07:01	**06:24**	10:21	**09:44**	13:00	**12:05**
	06:17	**(0.00)**	08:59	**(0.00)**	12:09	**(0.00)**
	05:59		09:37		12:47	
	06:25		10:04		11:53	
	06:53		09:26		12:12	
	05:48		09:57		10:31	

Table 7-12 Disintegration time of tablet for each formulation using an upper punch force of 25, 30 and 35 kilonewtons (cont.)

Formulation	Upper punch force (kN)					
	25		30		35	
	Time (min)	Average (SD)	Time (min)	Average (SD)	Time (min)	Average (SD)
SA	06:08	**05:11**	08:10	**08:14**	11:22	**10:35**
	04:42	**(0.00)**	09:02	**(0.00)**	09:38	**(0.00)**
	05:04		07:53		10:47	
	05:11		08:35		10:15	
	05:48		07:41		10:23	
	04:13		08:03		11:06	
MG	11:25	**10:38**	10:48	**10:51**	10:54	**12:21**
	10:16	**(0.00)**	11:24	**(0.00)**	12:17	**(0.00)**
	10:37		10:59		13:20	
	10:38		10:41		12:59	
	11:02		11:03		12:41	
	09:53		10:12		11:58	

VITA

Mr. Thanakorn Khroengkhamjornkit was born on October 16, 1982 in Sakaeo, Thailand. He received the degree of Bachelor in Pharmacy program with second class honors in 2005 from Faculty of Pharmacy, Huachiew Chalermprakiet University, Samut Prakarn, Thailand. After graduation from Huachiew Chalermprakiet University, he started to continue studying for the Master's degree of Science in Pharmacy Program in Industrial Pharmacy, Department of Pharmaceutics and Industrial Pharmacy, Faculty of Pharmaceutical Sciences, Chulalongkorn University in May 2006.